UNIVERSITÀ DEGLI STUDI DI PALERMO

Dottorato di Ricerca in Ingegneria Chimica, Gestionale, Informatica, Meccanica
Ingegneria Chimica e dei Materiali
Dipartimento di Ingegneria Chimica, Gestionale, Informatica, Meccanica
ING-IND 27

DEVELOPMENT OF ELECTROCHEMICAL MICROFLUIC DEVICES FOR THE TREATMENT OF WASTEWATERS AND THE SYNTHESIS OF CHEMICAL

LA DOTTORESSA
Simona Sabatino

IL COORDINATORE
Prof. Ing. Salvatore Gaglio

IL TUTOR
Prof. Ing. Onofrio Scialdone

IL CO TUTOR
Prof. Ing. Alessandro Galia

INDEX

INTRODUCTION

In the last years, many research groups have focused their attention on the microfluidic technology. Microsystems technology, coming from information technology and miniaturization of data-processing devices, has been used in various areas such as the food industry through biotechnology to pharmaceutical products, from analytical and laboratory scale equipment through energy conversion to industrial chemistry applications for the production of chemicals. The chemical reactions if performed in microfluidic devices can benefit of enhanced heat and mass transfer, higher yield and selectivity, improved safety, access to new products and easy scale up or modularization of the processes.

The microfluidic devices can be successfully used to perform electrochemical processes, that offer new sustainable routes for both the synthesis of chemicals and the treatment of wastewater contaminated by organic pollutants resistant to biological processes. These methods use a clean reagent, the electron, and very mild operative conditions with limited operative costs. However, electrochemical processes present some important disadvantages when performed in conventional reactors. In particular, to achieve reasonable cell potentials when the medium has not an adequate conductivity, one needs adding to the system a supporting electrolyte. The utilization of microfluidic electrochemical reactors (i.e. cells with a distance between the cathode and the anode of tens or hundreds of micrometers) allow to minimize or even remove some of the above mentioned disadvantages. Thus, very small distances between electrodes lead from one side to a drastic reduction of the ohmic resistances, (allowing to operate with lower cell potentials and without supporting electrolyte), and on the other side to intensify the mass transport of the reagents towards electrodes surfaces.

The objective of my PhD's thesis was the development of microfluidic devices for electrochemical processes and the study of some model applications.

In particular, some model processes for the electrochemical abatement of pollutants and the synthesis of fine chemicals were studied in both conventional and

microfluidic cells in order to highlight advantages and disadvantages given by the utilization of such devices.

In particular, in the first year, the electrochemical treatment of aqueous solutions contaminated by Acid Orange 7 (AO7) was studied with the main objective to evaluate as the electrocatalytic route affects the performances of the degradation process in macro and microfluidic cells. Direct anodic oxidation (EO), electro-Fenton (EF), electro-generation of active chlorine (IOAC) and coupled processes were investigated. The effect of numerous operating parameters (such as the nature of the electrode materials, the flow rate, the current density and the inter-electrode distance) on the performances of the process was studied in detail.

In the first part of the second year a new micro devices was assembled, in collaboration with the Department of Electronic Engineering of the University of Palermo. This device is simple and compact, with major warranty against leaks and it is characterized by easy, cheap and reproducible construction procedures and small interelectrodic distances

In the last part of the second year and in the first part of the third, the possibility to use electrochemical microfluidic devices for the synthesis of chemicals was investigated. The electrochemical conversion of dichloroacetic acid to chloracetic acid was investigated in conventional cells and in microreactors.

Four different micro devices are used: two different type of micro fluidic cell; a microfluidic stack and three micro fluidic cells in series. The electrochemical synthesis of chloracetic acid was performed in the micro reactors under a single-pass mode without supporting electrolyte at low cell potentials.

The utilization of three micro reactors in series and of the stack with two or three electrode chambers in series open interesting new perspectives: the first including the opportunity to modulate the current density among the reactors in order to optimize the process and the second increases the productivity and the final concentration of the target product.

In the last part of third year, the possibility to use more reactors in series for the treatment of wastewater was evaluated, with the aim of optimizing the process in terms of abatements, electrode costs, productivity and energetic consumption. The possibility of operating EF and EO in two different reactors in series was also investigated in order to select the best operating conditions for each process.

CHAPTER 1

1. STATE OF THE ART ON MICROFLUIDIC REACTORS

1.1. Introduction

Microsystems technology, coming from information technology and miniaturization of data processing devices, has entered many fields in our life. In the last years microfluidic technology has been used in various areas such as the food industry through biotechnology to pharmaceutical products, from analytical and laboratory scale equipment through energy conversion to industrial chemistry applications for the production of chemicals [1]. Microfluidic reactors are defined as reactors that have microstructures for chemical reactions. Typical dimensions of microstructures range from 10 to 500 μm. It has been shown that chemical reactions if performed in microfluidic devices can benefit of enhanced heat and kinetic of mass transfer, higher yield and selectivity, improved safety, access to new products and easy scale up or modularization of the processes. The microfluidic technique is a rapidly growing method that has gained wide interest scientifically and technologically. The technique refers to the science and technology of systems that manipulate small amounts of fluids generally in the nanoliter scale and below. [1-4]. Micromachining technologies have recently been applied in manufacturing microfluidic devices for chemical reaction purposes. Microfluidic reactors are expected to bring about revolutionary changes in chemical synthesis from both the academic and industrial viewpoints. The use of microfluidic reactors for the highly efficient screening of functional materials and synthesis of biologically active compounds and efficient catalysts has received significant research interest. It therefore follows that the main feature of these reactors, in comparison to conventional chemical reactors, is the

high surface-area-to-volume ratio. Specific surface areas of microstructures lie between 10 000 and 50 000 m^2m^{-3}, while those of traditional reactors are generally about 100 m^2m^{-3} and in rare cases reach 1000 m^2m^{-3}. Since the heat transfer coefficient is inversely proportional to the channel diameter, a value on the order of 10 $kWm^{-2}K^{-1}$ is obtained, which is significantly higher than for traditional heat exchangers. This high heat-exchanging efficiency allows for fast heating and cooling in reaction mixtures within the microstructures whereby reactions under isothermal conditions with exactly defined residence times can be carried out [3].

The development of hot spots or the accumulation of reaction heat within microstructures is suppressed so that undesirable side reactions and fragmentations are hindered. The outcome in many cases is higher selectivity, yield, and product quality. Thus, microreactors can be used for fast and/or strongly exothermic or endothermic chemical reactions.

In addition to heat transport, mass transport is also considerably improved in microreactors. Mixing times in micromixers (down to several milliseconds) are generally smaller than in conventional systems and due to the small dimensions the diffusion times are very short, thus the influence of mass transport on the speed of a reaction can be considerably reduced.

A third aspect of microreactors is the hydrodynamic flow in the microchannels, which is an important feature of microfluidics. The flows are mostly laminar, directed, and highly symmetric. In addition, the multiphase flows often exhibit high order between the phases. These features are shown to allow the possibility to simulate and model systems to develop microprocess engineering apparatus by rational design. In many cases, basic physical mechanisms or intrinsic kinetics can be directly applied. The prediction and confirmation of residence time distributions are of great value to this procedure. Furthermore, “controlled multiphase flow” is due to the dominance of surface and interface forces, as well as tailor-made active areas. Numerous publications are dedicated to conditions such as capillary flow, slug flow, segmented flow, or hexagon-flow, to name but a few. Process parameters

such as pressure, temperature, residence time, and flow rate are more easily controlled in reactions that take place in small volumes [1-4].
The hazard potential of strongly exothermic or explosive reactions can also be drastically reduced. Higher safety is also achieved in reactions with toxic substances or higher operating pressures. The miniaturization has an immediate effect on the mechanism of explosions, in that radical chains or thermal hold-up are suppressed [3]. This allows a drastic broadening of the safe operating range in previous explosive regimes. Indeed, reactions with toxic substances, or at high pressures, have been carried out more safely.

Due to the properties mentioned above, microreactors can be advantageously used as process engineering tools for acquiring information, which allows, in a short time and with greater safety, a process to be transferred to the pilot and production scale.

In the following paragraphs, the use of micro devices for industrial applications will be described. Moreover the electrochemical microreactors for the abatement of organic pollutants and synthesis of chemicals will be studied in detail.

1.2. Microfluidic devices for industrial processes

The application of microreactors in the chemical process industry has gained significant importance in recent years. Companies that offer not only microreactors, but also entire chemical process plants and services relating to them, are already in existence. In addition, many institutes and universities are active within this field and process engineering oriented reviews and specialized books are available.

The application of microreactors for chemical and biological reactions was discussed at a workshop in 1995 in Mainz (Germany), which can be seen as the starting point for worldwide development.

In 1997, the first International Conference for Microtechnology (IMRET 1) took place, which has since been held annually in Europe and the USA, and in 2001 the Industrial Platform of Modular Micro Chemical Technology (MicroChemTec), highlighting the industrial applications of microprocess engineering, was founded in partnership with DECHEMA. As a consequence of these initiatives, increasing industrial interest, in addition to nationally initiated funding, has led to the publication of approximately 1000 studies on microprocess engineering, albeit mostly in conference proceedings [3].

In spite of all proven advantages, microreactors were found only occasionally in the production in the last years. However, now a number of well known European, American, and Asian chemical and pharmaceutical companies actively introduce the new advanced technology in practice.

Some examples have been published within the past few years showing the potential when an accurate plant designs and development are carried out [6].

The first and up to now most often mentioned example for microreactor process engineering is the DEMiS project in Germany (Degussa, Uhde, TU Chemnitz, TU Darmstadt, MPI Mülheim), in which a microstructured reactor was used for the epoxidation of propylene to propylene oxide using H_2O_2 on a TS-1 zeolite with a production capacity of approximately 5–10 t/year.

Other examples of industrial microreactor applications are the synthesis of azo pigments (Clariant, Frankfurt, Germany, CPC, 80 t/year), the synthesis of

nitroglycerol (Xi'an Chemical Industry Group, China, IMM, 130 t/year), and the radical solution polymerization of acrylate resins (Siemens Axiva, Frankfurt, Germany, 2000 t/year).

DSM Fine Chemicals GmbH (Linz, Austria) installed a microstructured reactor in an existing production plant for the manufacture of a high value intermediate for the polymer industry. The reactor was designed and fabricated at the Institute for Micro Process Engineering (Karlsruhe, Germany) and dimensioned for throughput of 1700 kg/h.

Microinnova KEG (Graz, Austria) also installed a microstructured reactor designed by IMM (Mainz, Germany) in an existing plant for the production of fine chemicals. This installation and the associated speedup of the first reaction step in a running two-step batch process led to a doubling of the throughput.

Evonik Industries together with partners from industry (BASF) and research groups (IMM) developed the ozonolysis reactions in a falling film microreactor in a large scale of 120 t/year in the frame of BMBF-funded project (µPro. Chem).

Lonza has carried out investigations to check whether the innovative microreaction technology could contribute to the process intensification in the production of its products [6]. Recently, in cooperation with the Ehrfeld Mikrotechnik BTS (EMB) and Bayer Technology Services Company, compact microreactors with flexible design for continuous production of fine chemicals and pharmaceuticals were developed.

The microreactor team at Lonza has designed and tested a series of microstructured devices in continuous flow plants, and performed lab studies of pharmaceutical reactions with successful transfer to commercial production [5-6].

Figure 1.1 shows the three micro reactor types that were developed and used at Lonza.

Module A: was developed in collaboration with Corning S.A.S. The microreactor is based on the multi-injection principle to avoid hot spot formation in the mixing zone. Indeed, even a microreactor cannot be considered as an isothermal reactor for fast and exothermic reactions independently of being made out of glass, metal, or

SiC. The multiinjection principle is the most important factor to obtain a good temperature control in the reactor.

Module B: The reactor was initially based on the multi-scale approach, where differently sized plates are used and adapted to the reaction needs. For example a tiny channel may be used at reaction start (when heat evolution is strong) followed by a gradual size increase of the plates to accommodate slower reaction rates (less heat evolution). With such a design, heat transfer is optimized, while pressure drop is minimized coupled with a large gain in volume (up to several mL). In addition, the reactor may be combined with conventional heat exchangers to gain volume of several liters with residence times of several minutes.

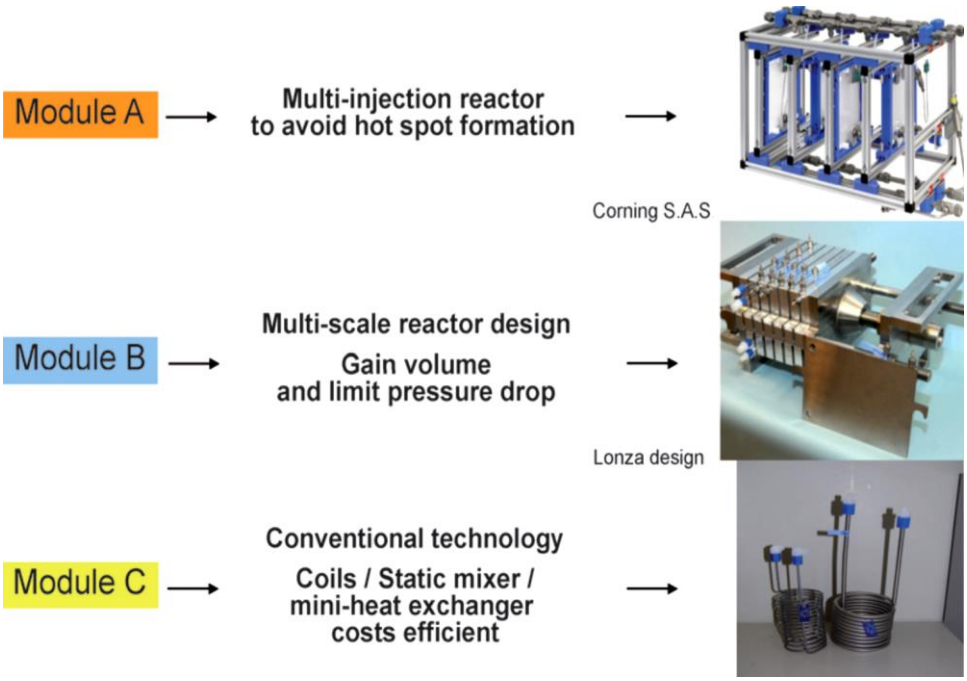

Figure 1.1 *Developed or used reactor technologies at Lonza to address the three reaction classes.*

Module C: the use of conventional technologies such as static mixers and mini-heat/tube in tube exchangers is a pragmatic way to operate flow processes for slow

and non-demanding reactions. The gain in reaction volume with such devices is cost effective and the technology is mature. In many instances it is the technology of choice to operate continuous processes.

Lonza's Universal Reactor Technology is causing a universal buzz of excitement within both process R&D and manufacturing circles at pharmaceutical companies as well as it:

1) illuminates a clear path from laboratory chemistries to large-scale manufacturing processes;
2) completely avoids the parallelization / numbering-up strategies adopted by other technologies in the field that may result in technical problems.

Highlighting these technology as an example, this microreactor platform supports rapid process development and production under continuous flow, using microstructured elements. The developed reactor technology is robust, multipurpose, and scalable and has already been tested for several products processing tons of material within a few weeks of operation.

The reactor technology shows in Figure 1.2 has evolved at Lonza into its Universal Reactor Technology. Indeed, the modularity and versatility of the single plate approach allow the development of plates appropriate to any kind of application. Thus, plates for gas/liquid and multi injection applications were manufactured demonstrating the multipurpose character of this technology. The individual Hastelloymade plates are sandwiched between highly thermal conductive aluminium plates for the thermal fluid passage leading to a very compact reactor. In this way, the thermal fluid layer is not directly bounded on the reactor plates allowing an ease of adaptation and a cost effective manufacture.

FlowPlate MicroReactors (Figure 1.3) is another micro reactors developed by Lonza and exclusively distributed worldwide by Ehrfeld Mikrotechnik BTS. It Has received the prestigious Sandmeyer Prize, which was awarded by the Swiss Chemical Society (SCS) for its outstanding work in the field of applied chemistry. Small and frequently changing product quantities with high quality, a fast time-to-

market, these are the major challenges in the pharmaceutical and fine chemical industry. Flow Plate features a series of compelling advantages: the easy and quick scale-up exactly meets the demands of global competition. In fact, campaign based on demand production under cGMP conditions and production up to ton scale are available within a very short time. High pressure resistance up to 100 bar offers new process windows for users.

Figure 1.2 *Lab-Plate reactor Lonza's Universal Reactor Technology for process development and production.*

The compact design can be expanded modularly; plates with different channel design can be replaced easily, even in the case of a built in reactor. The plate design can be flexibly adjusted to specific customer requirements and process tasks. The Cleaning In Place (CIP) process is easy to apply thanks to the process channel, which is free from dead volume with a closed and seal free single channel design. The smallest in the range but superbly equipped: it is optimally suited for feasibility studies in the laboratory, process development and pre clinical research. The exchangeable micro-structured process plate contains up to 10 inlets and outlets along the reaction channel. This ensures high flexibility for a variety of different processes. The flow process in the entire channel can be visually monitored through a sight glass (made of an outstanding Sapphire glass).

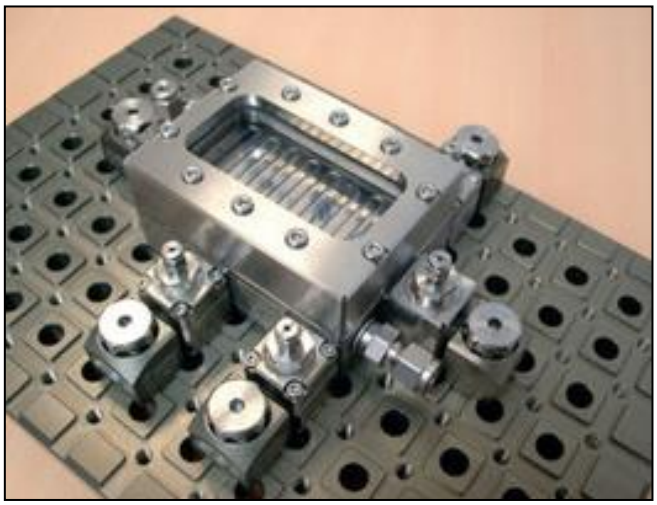

1.3a

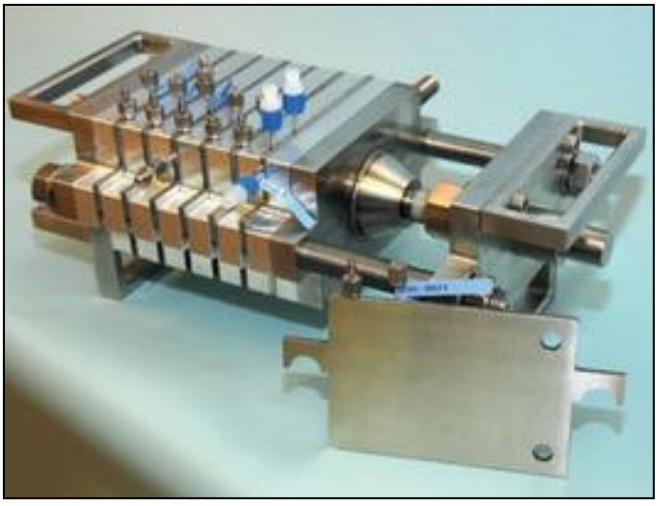

1.3b

Figure 1.3 *Microfluidic reactors for industrial processes. a) The Lonza FlowPlate Lab microfluidic reactor can be used for laboratory-based experimental process development. The reactor incorporates a viewing window to assist in detection and monitoring and was designed for easy scale out and/or scale up to the milliscale for industrial production. b) The Lonza FlowPlate A6 microfluidic reactor can be used for process development in the kilogram range.*

1.3 Electrochemical microfluidic devices

The electrochemical processes for the treatment of wastewater and the synthesis of chemicals have received a great deal of attention from researchers, since it constitutes an alternative synthetic route to traditional chemical processes, which use hazardous or toxic reagents. As above mentioned, chemical reactions if performed in suitable microfluidic devices can benefit of enhanced heat and mass transfer, higher product yield, selectivity and purity, improved safety, access to new products and quite easy scale down, scale up or modularization of the processes [1,2].

Some authors have recently demonstrated that a flow cell with a micrometric distance between the cathode and the anode can be successfully used also to perform the electrochemical processes for the treatment of waters contaminated by organic pollutants and the synthesis of chemicals [7-23].

The utilization of electrochemical micro devices can furthermore offer other important advantages such as:

- Possibility to operate without supporting electrolytes at low cell potentials with a drastic reduction of the ohmic resistances.
- Intensification and better control of mass transport rates of reactant to the electrode surfaces owing to the small inter-electrodes distances and forced laminar hydrodynamic flows.
- Easier scale-up procedure through simple parallelization of many small units.
- A screening of the effect of operative parameters on the performances of the process can be performed in short times by fast changing of the steady state conditions in comparison to conventional macro systems that must operate in batch recycling mode. The small distances between electrodes allow very high conversions for a single passage of the water solution inside the cell, thus allowing continuous operation.
- The possibility to operate in a continuous mode potentially allows the utilization of a multi stage system involving two or more cells operating in series with

different applied current densities in order to maximize the current efficiency and to minimize the treatment times.

Despite the advantages cited above, the microreactors have some disadvantages. Each electrochemical process, consists of two reactions, oxidation and reduction respectively in the anodic and cathodic surface. In conventional cells the reduction reaction and the oxidation could be separated using two compartments or a sacrificial electrode. Here in each case the anodic and cathodic products are in contact. In this case, parasitic reactions with the formation of by-products are possible.

Another disadvantage of the electrochemical microreactors, is the high sensitivity to the purity of the charge [7]. Because of the small size, the device may be subject to an excessive fouling. The cleaning operations is difficult; therefore, fouling, can only be avoided by acting upstream, on the purification of the reagents, with a consequent increase in management costs.

Several kinds of electrochemical microfluidic devices were proposed in literature.

The electrochemical microfluidic devices should be characterized by easy, cheap and reproducible construction procedures, small inter-electrodic distances (thus allowing to operate without the supporting electrolyte with low cell potentials and to increase the mass transport rates of reagents to electrodic surfaces), high productivity and long duration under operative conditions. It is possible to distinguish different types of electrochemical microreactors. They differ from each other in the chemical nature of the materials and for the technical realization.

In the next paragraph, various types of electrochemical microreactor proposed in literature will be described. Then, particular attention will be given to the application of micro electrochemical reactors for the treatment of wastewater and synthesis of chemicals.

1.3.1 Thin layer flow cell (Daisuke-Horii) [7]

The electrochemical microreactor proposed of Daisuke et al. [7] is the most used in the literature, since it is very versatile and usable with any electrode. In this cited case, the thin layer flow cell was made from platinum (Pt) (3 cm width, 3 cm length) and/or glassy carbon (GC) plates (3 cm width, 3 cm length). A spacer (both sides adhesive tape, 80 μm thickness) was used to leave a rectangular channel exposed, and the two electrodes were simply sandwiched together (area of the two electrodes: 1-3 cm^2) (see Fig. 1.4). After connecting Teflon tubing to inlet and outlet, the cell was sealed with epoxy resin.

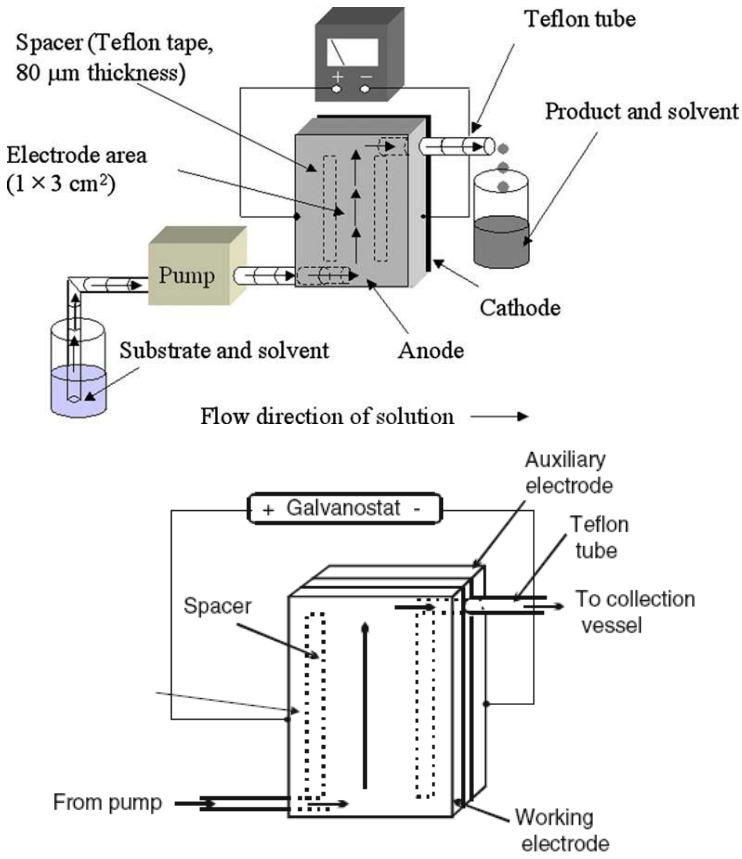

Figure 1.4 *Schematic representation of the thin layer flow cell system.*

1.3.2 Microfluidic electrolytic cells (Pletcher) [8]

The research's group of Pletcher considered that a high conversion in a single pass and a good rate of product formation was the critical performance factors for applicative purposes.

The electrolysis cell was made from two rectangular electrode plates (53 mm × 40 mm× 2 mm thick). The anode was carbon filled polyvinylidene fluoride (PVDF) and the cathode was stainless steel. The perfluoroelastomer (FFKM) spacer had a 'snaking', a microchannel of designed pattern, as shown in Figure 1.5a, cut in order to give an extended channel length and to enhance the convection within the channel.

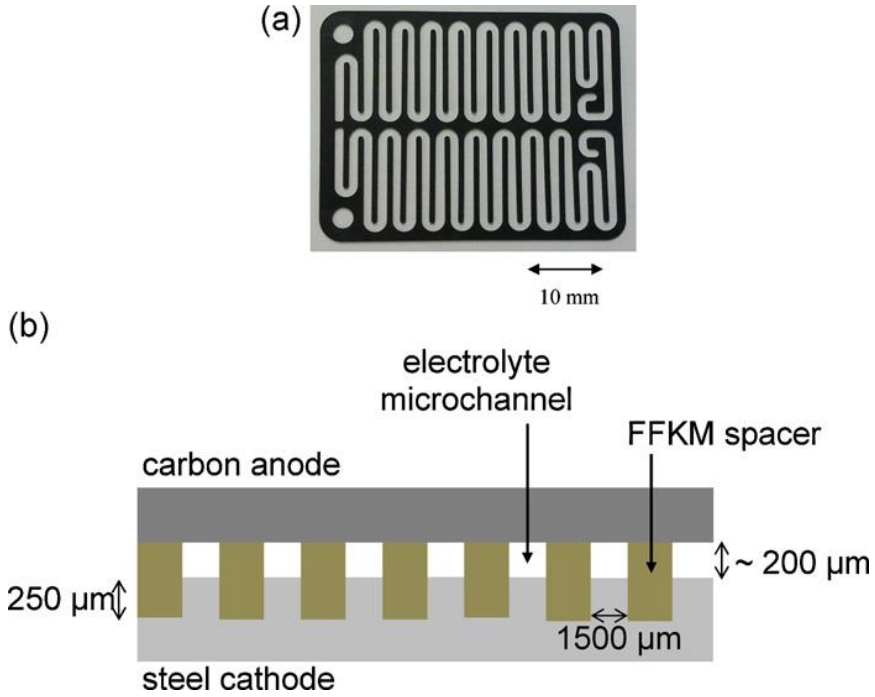

Figure 1.5 *a) Photograph of the FFKM spacer; b) Line diagram to show the structure of the microflow electrolysis cell.*

The steel electrode had a patterned, recessed channel (depth 250µm) machined into it, to allow it to accept the patterned spacer and thereby permit facile alignment of the inter-electrode spacer, as shown in Figure 1.5b; it also incorporated two fluid inlet/outlet holes.

The design provided a channel path-length of 700 mm, combined with a channel depth of 200 µm (with the spacer fitted into recessed channel of the electrode and the cell compressed) and a channel width of 1.5 mm, giving a cell volume of 0.21 cm^3. The total electrode surface area in contact with fluid is 1050 mm^2 per electrode.

1.3.3 A simple and inexpensive microfluidic electrolysis cell (D. Pletcher) [9]

Another electrochemical microreactor has been proposed by the research's group of Pletcher based on inexpensive materials. The round cell design was chosen in order to more evenly distribute pressure across the plates and hence prevent leakage of the cell.

The device consisted of the two flat, circular electrodes (diameter 100 mm) separated by the micro-channelled spacer. The anode was made of a conductive carbon/polyvinylidene fluoride (PVDF) composite (5mm thick). Stainless steel (3mm thick) was chosen as the cathode material. The microchannels within the spacer were cut by laser providing the exact shape required; cells with other dimensions as well as different channel geometries and spacer thicknesses can be easily produced using this technique (Figure 1.6). The inter-electrode distance was approximately 500 µm determined by the thickness and compressibility of the chosen sealant material, the channel width was 1 mm and the total channel length was 600 mm. In order to achieve efficient sealing of the cell and avoid electrolyte leakage, it was compressed between two aluminum plates using ten edge bolts and one central bolt; each bolt was placed in a tubular polymer gasket (6mm outer diameter) to electrically insulate them from the electrodes and to minimize stress distortion of the channel pattern when the bolts were tightened. Finally, two aluminum connectors were attached in the inlet and outlet positions of the flow.

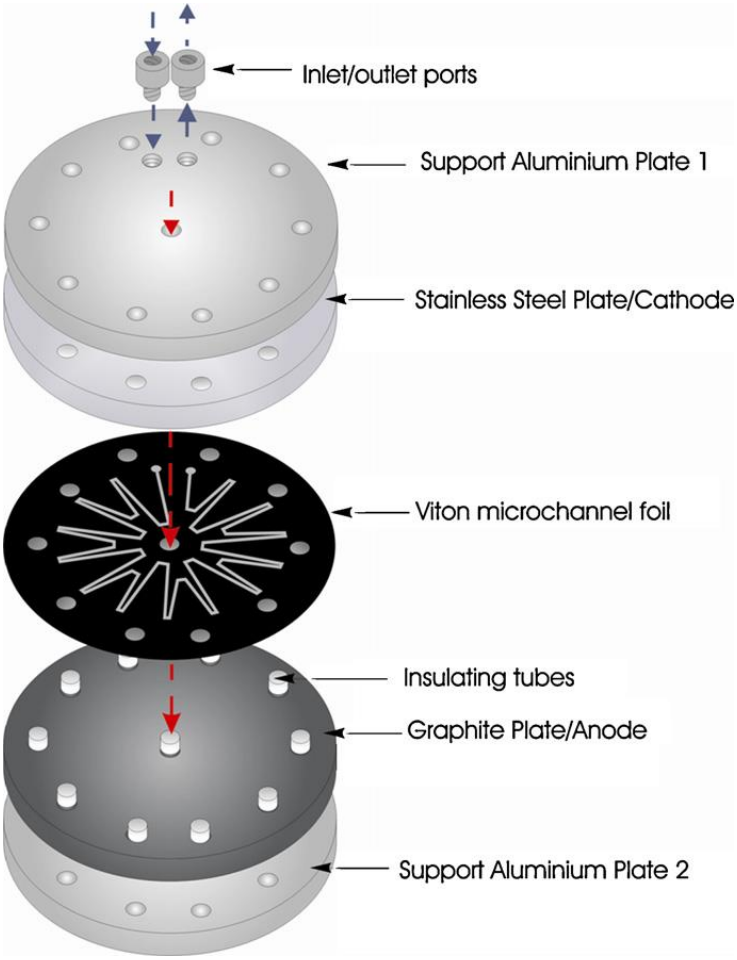

Figure 1.6 *Schematic illustration of the microflow reactor showing the essential components of the electrolysis cell. The diameter of the electrodes was 100mm. The cell was sealed under compression by 11 stainless steel bolts placed in insulating tubes.*

The Figure 1.7 shows a schematic example of the experimental set up. The pump (**2**) was fed from a solvent bottle (**1**). The pump output was then fed either directly into the microreactor (**4**) or through a 5cm^3 sample loop (**3**). This set up enables the introduction of small volumes of material into the solvent flow. The product of the

reaction was collected in a sample vial (**5**) at the outlet of the electrochemical reactor (**4**).

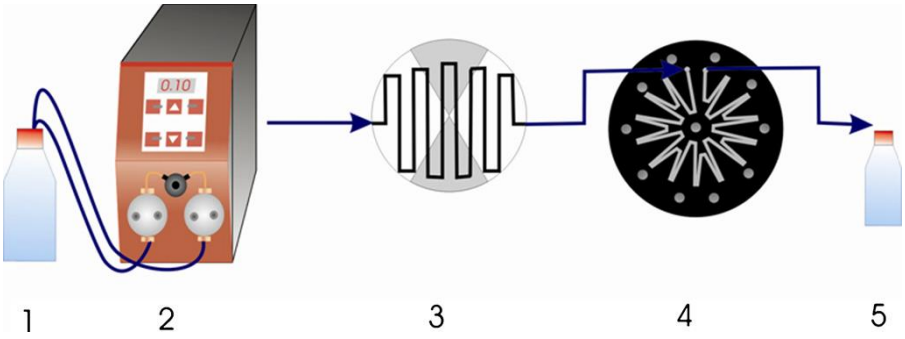

Figure 1.7 *Schematic of the experimental set up, where* ***1*** *the solvent bottle,* ***2*** *pump,* ***3****,* ***4*** *microreactor, and* ***5*** *collection vial.*

1.3.4 Microfluidic electrochemical reactors (R. Simms) [10]

The research's group of Simms reports an efficient method for the fabrication of microfluidic electrochemical reactors. The technique relies on soft lithography and micromolding in capillaries. Intrinsic to the method of fabrication is the capability of controlling the inter-electrode gap between 40 to 200 µm, and the ability to produce microchannels with complex geometries.

The material selected to fabricate the reactor is resistant to most organic solvents, whereas its relative softness eliminates the need for additional sealants required by other methods for the fabrication of microfluidic electrochemical reactors. This device is built with techniques of casting in capillaries and photolithography.

A negative photoresist (SU-8) is deposited in low relief on a support silicone, forming on it a network of routes, with photolithographic techniques (figure 1.8 a).

The height of the SU-8 will also identify the electrode distance. PDMS is cast on this structure, allowing this polymer to fill the spaces evictions (figure 1.8 b).

After the polymerization of the PDMS, it is removed from the base silicone/SU-8 and applied on an electrode of stainless steel. The PDMS is then embossed with a pattern obtained as mold of what was on the layer of silicon. Once in contact with the new support, then the PDMS forms between it and the electrode a network of paths, that in this stage of the preparation, constitutes a vacant volume. The steel plate has the access holes for the insertion of monomer tiolene (NOA 75), which fills the empty spaces by capillary action. It is noteworthy that for all the time necessary to fill the channels of monomer, the PDMS has sufficient adhesion to prevent leakage of NOA 75.

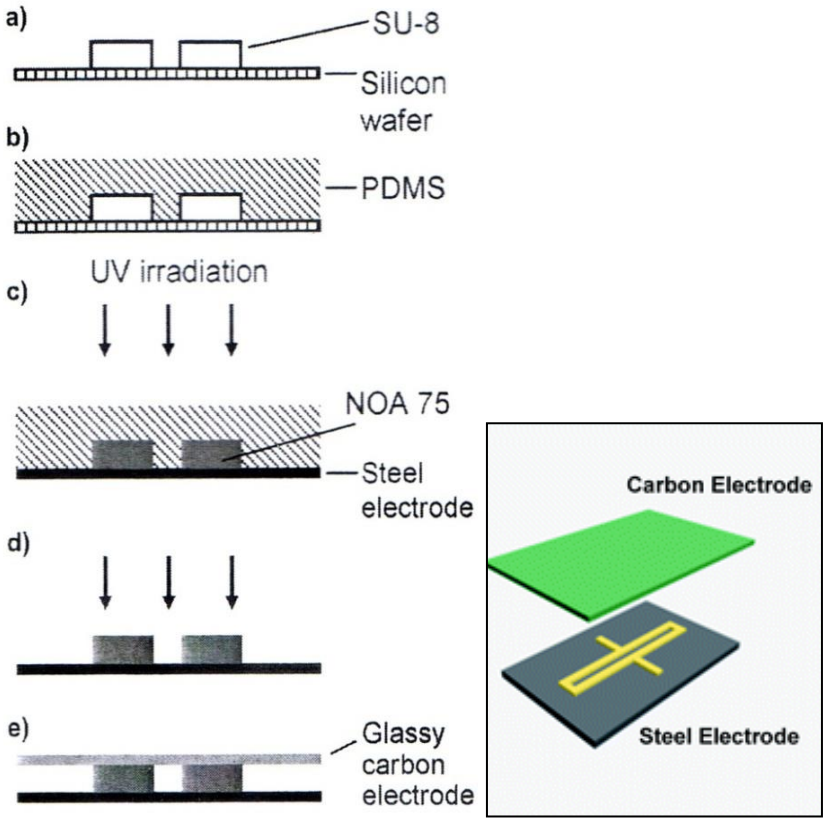

Figure 1.8 *Stages of preparation of the device "Microfluidic Electrochemical Reactor"*

The NOA 75 is finally polymerized by exposure to UV light for about thirty seconds figure 1.8c), the period during which it binds strongly to steel, but not to the PDMS.

At this point, the PDMS is removed and exposed for twenty minutes to UV radiation figure 1.8d) to complete the crosslinking of the NOA 75, and thus to improve the chemical resistance of this polymer.

A second electrode in the vitreous graphite (figure 1.8 e) is placed over this structure and fixed with the aid of two vises. It is not necessary to use sealants or other precautions in order to prevent losses of liquid during operation. The tiolene, in fact, remains relatively soft after curing and this ensures the seal with the electrode closing.

This method allows the construction of channels with complex geometries, well defined distance between the electrode, and a range of inter-electrodic distances ranging fron 40 to 200 µm. All materials used for the fabrications of the reactor (NOA 75, staineless steel and glassy carbon), are compatible with a broad range of organic solvents. NOA 75 remains relatively soft after curing, thereby eliminating the need for additional sealants to produce a leak-proof reactor.

1.3.5 Thin-gap cell (Ziogas)[11]

Ziogas et al. proposes another microreactor denominate thin-gap cell. It was an undivided flat electrode cell in PEEK (Polyetheretherketones) reactor housing. The PEEK housing was chosen for its excellent chemical and mechanical stability as well as good machinability. High-grade stainless steel was chosen as a cathode material. The anode was made of glassy carbon providing suitable electrocatalytic properties and avoiding leakage of the electrolyte. The anode consisted of ten 1 x 1 cm^2 elements, separated from each other by a 1 mm wide insulated section. In order to provide the required functionality, the cathode was first coated with approximately 50 µm Teflon layer. The Teflon layer was later removed by milling

from the electrochemically active area. Special spring contacts were employed and the rear side of the glassy carbon chips forming the anode was gold coated by sputtering in order to provide sufficient electrical contact and thus minimize the contact resistance. The two electrodes, with a 100 µm inter-electrode gap formed a 0.01 cm^2 channel cross sectional.

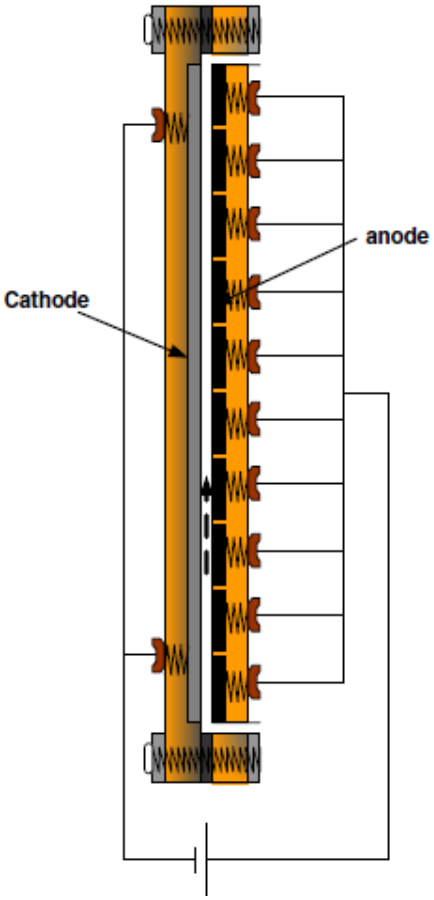

Figure 1.9 *Schematic view of the thin-gap cell*

Construction of the cell was carried out as follows: milling of the PEEK and of the high-grade stainless steel plate by a programmable CNC (Computer Numerically Controlled) machine; the glassy carbon plates as well as the Chemraz sealing were cut by laser in order to provide the exact shape required and avoid any undesirable fracture of the material. A schematic view of the constructed cell is shown in Figure 1.9. Although the anode was segmented, all carbon tiles were connected together, so that the cell potential was uniform in the reactor.

1.3.6 ElectroChemical Micro Fluidic Channels (EC-MFC)[12]

These devices are proposed in literature by many authors. Electrochemical Microfluidic Channels (ECMFC) are constituted by a glass substrate, the electrodes and a block of polydimethylsiloxane (PDMS) containing the microchannels.

The devices fabricated in PDMS can be easily integrated, because the polymer is suitable for many materials. The PDMS is suitable for smooth substrates of plastic or glass, it is possible both reversible to irreversible bonding. The PDMS is also interesting for applications that require a temperature gradient, since it is stable in a wide range of temperature. The PDMS is also compatible with many optical methods of detection because it is transparent in the UV region and the visible. The PDMS channels are suitable for cellular studies because the PDMS is not toxic for protein and for the cells, it is biocompatible and permeable to gases. The chemical structure of the PDMS leads to a hydrophobic surface. This surface can be made hydrophilic by exposing it to a plasma of oxygen or air.

This device is formed by two distinct parts, a glass substrate on which are deposited electrodes and a block of polydimethylsiloxane PDMS that contains the micro-channels, which are then welded together.

The first phase (figure 1.10 a) provides for the placement of a photosensitive polymer on a support matrix, usually glass or silicon. This work is performed by a machine, called spin coating, which can be thought, in first approximation, as a

rotating disk. By means of rotation, this device allows to spread the resist, which initially is placed as a drop of liquid in the central area of the disc. Depending on speed of rotation and the viscosity of the polymeric material, one can obtain the target thickness. The film thickness of the resist depends on the viscosity and the concentration of the resist used, and then also by operating parameters of the spin coating as: speed and time of rotation and acceleration. Once obtained the desired thickness, it passes to a mild heating, from 70 to 130 °C, which has the purpose of removing the solvent by evaporation so as to obtain a solid layer.

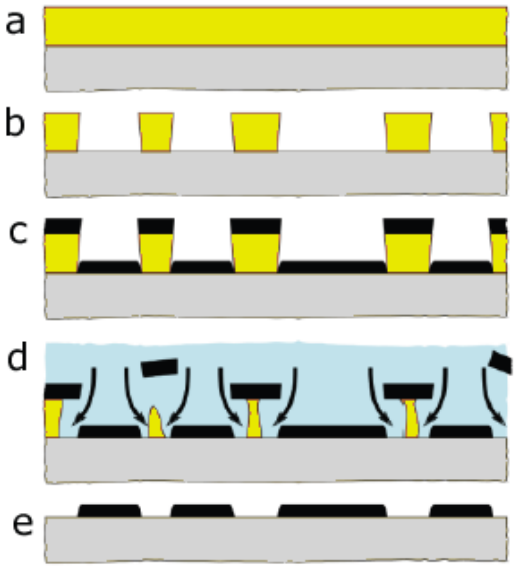

Figure 1.10 *Schematic construction glass blocks with electrodes.*

The second step consists in exposure to UV rays, after application of the photolithographic mask and subsequent dissolution of the irradiated parts (Figure 1.10 b). It is necessary to have conductive channels to use them as electrodes. This is done through a metallization, which consists essentially in a deposition. This can be performed either by physical vapour deposition, or by chemical vapour deposition and represents one of the most important steps of the entire manufacturing process (Figure 1.10 c).Following the metallization, in fact, it is

necessary to obtain a layer resistant to subsequent treatments, of adequate thickness to the intended purposes, and as far as possible, uniform.

The last step involves an operation of lift-off that has the purpose to dissolve completely the resist, initially put in place (Figure 1.10 d). In this way, you get the only parts of the metal film, which are in contact with the silicon substrate glass (Figure 1.10 e). During this process it is necessary not to use aggressive solvents that may detach metal also deposited on the substrate. Usually it is performed by means of a wash under ultrasonic conditions. The block of PDMS has the function of creating channels. These are produced by a molding operation, in which the mold is a substrate worked in the same way as described above. A mixture is prepared, with a rate 10:1 in weight of PDMS, together with a crosslinking agent.

This is placed in the refrigerator for 20 minutes, to prevent the crosslinking of the polymer in the presence of bubbles. The last step sees the insertion in a stove at 80 ° C for about an hour, to allow the cross-linking. The temperature and the time of this process determine the mechanical characteristics the polymer. At this point, the two blocks, one containing the electrodes and the one with the channels, are welded together. The bonding occurs with an oxygen plasma under appropriate conditions of partial pressure of oxygen.

1.3.7 Scaling out of a micro-gap flow cell (P. He)[13]

P. He et al. proposed a scaling out of a micro-gap flow cell. The systems were made with multiple channels and using two distinct cell configurations. A single channel cell consisted of two glass plates (3 cm length, 2 cm width, 6 mm thickness) in which two holes are drilled in the top plate to enable PEEK tubes (id 0.24 mm) to be connected in order to allow inlet and outlet flow. Two equally sized Pt foils (4 mm width and 15 mm length, 50 mm thickness) were used as the working and counter electrodes, and two PTFE spacers (120 mm thick) with a rectangular flow reaction zone (3 mm width and 15 mm length) were used to produce the single channel cell with a working area of 45 mm^2 and inter-electrode distance of 160 µm.

Scaling out systems were made with multiple channels and using two distinct cell configurations. In the first configuration, a single set of electrodes was used in conjunction with a multiple flow manifold to give two (Figure 1.11 a) and four separate flow channels. In the second configuration, independent electrodes were used within the same flow manifold (Figure 1.11 b). In the first configuration, the electrode width was 8 mm and 16 mm for making two channels and four channels, respectively. In the second configuration, each channel was built by using the same procedures as that for making single cells (see above).

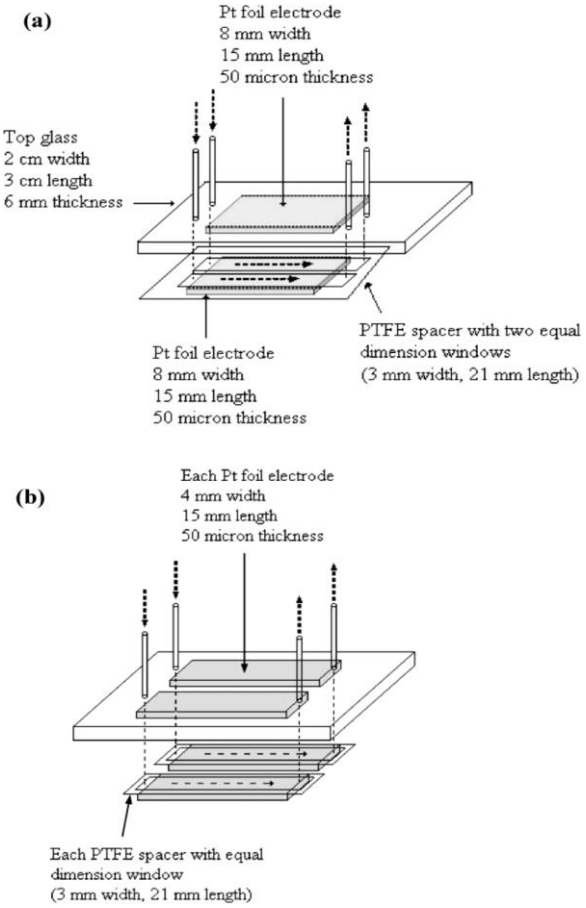

Figure 1.11 *Schematic representation of scale out of micro-gap flow cell showing a) a single pair of electrodes and b) independent electrode configuration for a multiple double flow system. The arrows show reagent flow direction.*

1.4 Electrochemical microreactor for treatment of wastewater

The electrochemical treatment of wastewaters contaminated by organic pollutants can strongly benefit from the utilization of microfluidic electrochemical reactors (e.g. cells with a distance between the cathode and the anode of tens or hundreds of micrometers). Thus, very small distances between electrodes lead from one side to a drastic reduction of the Ohmic resistances, thus allowing electrochemical incineration of organic pollutants with lower cell potientials and without supporting electrolyte, and on the other side to the intensification of mass transport of the pollutants to electrodes surfaces. Please consider that in conventional cells, one needs adding to system a supporting electrolyte to achieve reasonable cell potentials when the medium does not present an adequate conductivity. This is certainly a main obstacle for a wide application of electrochemical abatement. Indeed, adding chemicals to a water stream is often a problematic issue, being opposed to general administrative regulations since this may lead to the formation of secondary pollutants during electrochemical incineration of organics, and anyway increases the operative costs. Mass transfer intensification is also a key point in these processes to increase current efficiencies and to decrease the durations of treatment since mass transfer rates towards electrodes are usually extremely reduced at the low pollutant concentrations required by regulations [15-17].

Despite the many advantages of using micro electrochemical devices in the environment, studies of literature of the electrochemical abatement of organic pollutants in micro reactors are limited. Interesting result were obtained by the research group of Scialdone, as shown in the following paragraphs.

1.4.1 Abatement of 1,1,2,2-tetrachloroethane in micro reactors

Scialdone et al. reported the use of microfluidic cell for the treatment of aqueous solutions of 1,1,2,2-tetrachloroethane [16]. The experiments were performed by

anodic oxidation at boron doped diamond (BDD), cathodic reduction at silver and coupled processes. Experiments were performed in micro reactors with an interelectrode distance lower than 100 μm. Both reduction processes based on the utilization of silver cathodes, oxidation processes at BDD anodes and coupled processes can be carried out in electrochemical micro-gap flow cells in the absence of supporting electrolyte with lower cell potentials and higher abatements with respect to that obtained in conventional laboratory cells, as a result of lower ohmic drops and a more effective mass transport of the pollutant to the electrodes. In the case of 1,1,2,2-tetrachloroethane, the oxidation at BDD gives rise to higher conversions of the pollutant but to the formation of oxidation products of chloride ions and to higher cell potentials with respect to the reduction at silver cathodes. The coupled process gave rise to a drastic increase of the abatements with respect to each single one for two main reasons: (I) the abatement process benefits from the charge passed both at the anode and the cathode surfaces; (II) in the case of the micro reactor, the coupled process gives rise to an acceleration of mass transport kinetics with respect to single routes because of the overlapping of the anode and cathode diffusion layers (Table 1.1). The effect of some operative parameters on the performances of these processes was studied. Higher abatement was often obtained by working with high residence times (e.g., low flow rates) or current densities at the expense of a faradaic yield reduction. An increase of both the abatement and the current efficiency was otherwise achieved by operating with higher initial concentrations of the pollutant or with lower distances between the electrodes (Figure 1.12).

Table 1.1 *Electrochemical abatement of 1,1,2,2-tetrachloroethane in the micro reactor by oxidation at BDD anode and combined process at BDD anode and silver cathode.*[a]

Electrochemical process	Operative conditions	Abatement (%)	Current efficiency (%)
Oxidation	Flow rate: 0.2 ml/min *i*: 15 mA/cm^2	~99.8	4.5
Combined	Flow rate: 0.3 ml/min *i*: 15 mA/cm^2	>99.9	7.3
Combined	Flow rate: 0.1 ml/min *i*: 3 mA/cm^2	~99.8	8.8

[a] Nominal distance between the electrodes of 50 μm. Initial 1,1,2,2-tetrachloroethane: 1 mM.

1.12 a

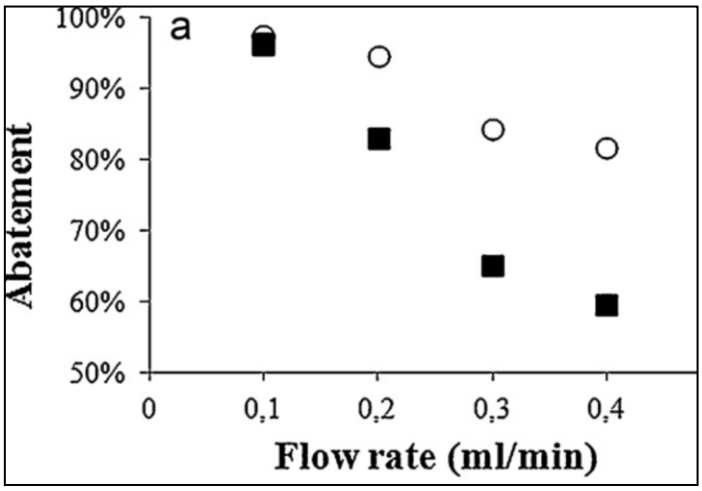

1.12b

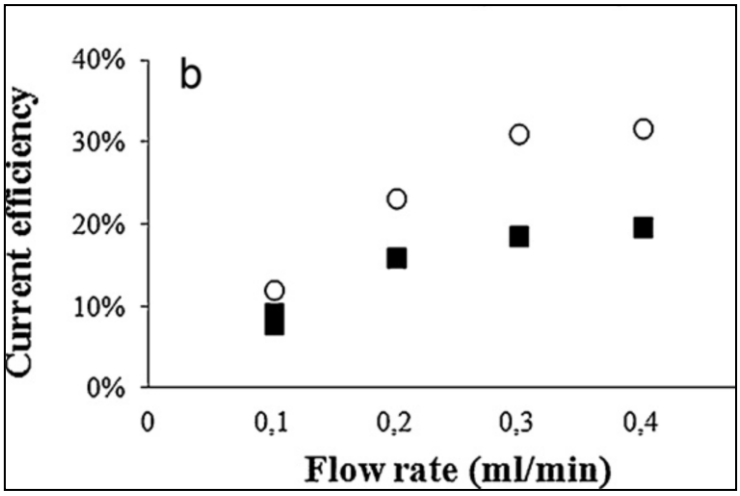

Figure 1.12 *Effect of the nominal distance between the electrodes (50 (o) and 75 µm (■) on the abatement (a) and the current efficiency (b) of the oxidation process of 1,1,2,2-tetrachloroethane performed at a BDD anode in a micro reactor at different flow rates. Current density: 3 mA/cm^2. Initial concentration of 1,1,2,2-tetrachloroethane 0.9 mM. Cathode: nickel.*

1.4.2 Abatement of chloroacetic acid in micro reactors

Scialdone et al. reported also the electrochemical abatement of chloroacetic acid in macro and microfluidic cells [17]. The treatment of aqueous solutions of monochloroacetic acid (CAA) was carried out by different electrochemical approaches including single and combined direct cathodic and anodic processes, as well as mediated oxidation by electro-generated active chlorine and Electro Fenton (EF) in macro and microfluidic cells.

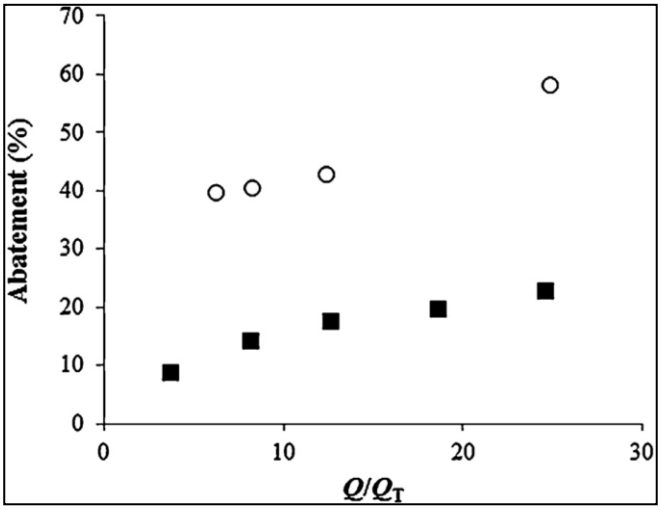

Figure 1.13 *Abatement of CAA using a compact graphite cathode in (■) macro and (o) microreactor vs. dimensionless charge Q/QT(ratio between charge passed and the-oretical charge). The electrolyses of solutions of 5 mM CAA with 0.5 mM $FeSO_4$wereperformed at pH ~ 3 and 8 mA cm^{-2}. The experiments in the microfluidic cell were carried out at 0.1 mL min^{-1} with an interelectrode gap of 100 μm. Theoretical charge(QT): charge required for the total reduction of CAA with 100% CE. Anode: Ti/IrO2-Ta2O5. Electrode surface: 5 cm^2.*

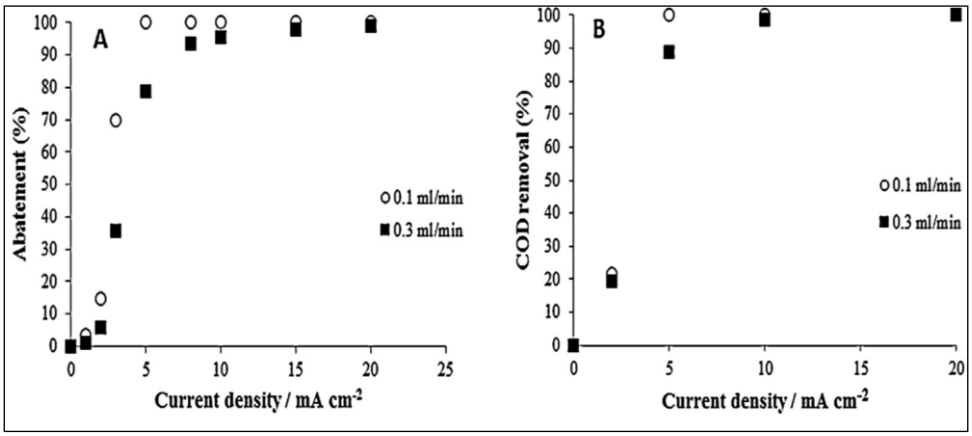

Figure 1.14 *Abatement of (A) CAA and (B) COD using a BDD anode at various current densities and flow rates in the microfluidic cell.*

Entry	Process	System (reactor)	Current density ($A\,m^{-2}$)	Flow rate ($mL\,min^{-1}$)	Time (h)[b]	Abatement (%) and (Current efficiency (%))
1[c]	EF or PEF with an ADE and electro-oxidation on Pt	System I	1000		> 5	Not significant
2	Cathodic reduction on	System II				
	• copper		400		5	< 10 (< 0.5)
	• silver[d]		400		5	27 (1.1)
	• graphite[e]		100		5	28 (4.4)
	(Anode: Ti/IrO_2-Ta_2O_5)					
3	Electro-oxidation on BDD	System II	100		5	89 (42)
	(Cathode: stainless steel)					
4	Electro-oxidation on BDD and cathodic reduction on graphite	System II	100		5	91 (43)[f]
5[c]	Cathodic reduction on graphite	System III (micro)	100	0.4	6.3	40 (5.1)
	(Anode: Ti/IrO_2-Ta_2O_5)		80	0.5	5	36 (7.2)
6[g]	Electro-oxidation on BDD	System III (micro)	200	0.3	8	100 (15)
	(Cathode: stainless steel)		100	0.5	5	87 (42)
			50	0.3	8	75 (44)
7[c]	Electro-oxidation on BDD and cathodic reduction on graphite	System III (micro)	200	0.3	8	100 (15)[f]
			100	0.5	5	95 (46)[f]
			50	0.3	8	86 (50)[f]

[a] Electrolyses of aqueous solutions of 5 mM CAA, using Na_2SO_4 as supporting electrolyte for conventional reactors I and II. Unless stated otherwise, the considered volume was 300 mL.

[b] Normalized time for the treatment of 300 mL of solutions considering a nominal geometric electrode surface of 10 cm^2. Actually, system II has an electrode surface of 10 cm^2. In the case of the microreactor, the calculation is made by considering the utilization of two microreactors (each one with an electrode surface of 5 cm^2) in parallel.

[c] 100 mL of aqueous solution (pH 3.0).

[d] Preliminary activation of the silver cathode by two oxidation ($10\,mA\,cm^{-2}$) and reduction ($-10\,mA\,cm^{-2}$) amperostatic pulses (2 min each).

[e] At pH 2.7, in the presence of 0.5 mM $FeSO_4$. Nominal distance between the electrodes: 100 µm.

[f] Current efficiency conventionally calculated by considering the oxidation of CAA to CO_2.

[g] Nominal distance between the electrodes: 50 µm.

Table 1.2 *Abatement of CAA by various electrochemical routes.*[a]

The reduction on graphite benefited from the utilization of catalytic amounts of iron (II), low pH and intermediate current density values. In the latter two cases, a maximum abatement of about 30% was achieved in a conventional macro cell. When experiments were repeated with graphite cathode in the microfluidic cell in the absence of supporting electrolyte, a drastically increase of the abatements was achieved (see Table 1.2 and Figure 1.13). Quantitative abatements were achieved by direct electro-oxidation on BDD in both macro and microfluidic devices (see Table 1.2 and Figure 1.14). The oxidation of CAA on BDD resulted in the formation of chlorate and of perchlorate. The concentration of perchlorate was drastically reduced by working at low current densities.

1.5 Electrochemical microreactor for synthesis of chemicals

Electrosynthesis can allow the selective production of organic compounds under relatively mild experimental conditions and without the use of toxic/hazardous reagents.

Electrosynthesis is based on adding or removing electrons with defined energy to/from a chemical process and can be employed to make a wide range of clean chemical transformations. The formation of highly reactive intermediates as well as of electrogenerated acids or bases are possible. In several industrial processes large scale electrosynthetic processes (e.g. in the nylon-6,6 synthesis) have been successfully applied and specially designed reactor systems have been developed such as filterpress systems, membrane reactors, fluidised bed reactors, or parallel-plate flow systems with down to 1 mm inter-electrode gaps.

Electrosyntesis conduced in a microfluidic system has following important advantages:

i. precise control of small inter-elctrode gaps. Small inter-electrodic distances allow for self-supported electrochemical synthesis, that is, the synthesis carried out in the absence of added electrolyte. The product is obtained directly by solvent removal and without laborious separation steps, which is of considerable benefit in both laboratory scale and commercial processes;
ii. the stable laminar flow profile enables reactants to be selectively located adjacent to the anode, or cathode, in order to eliminate redox potential constraints, or to facilitate coupled reactions in which the products produced at the anode and cathode are utilized in the synthesis;
iii. minimized exposure to potentially toxic and/or explosive chemicals.

At present, however, the main disadvantage of using micro reactor based methodology is the low quantities of product produced. In order to overcome this problem, whilst maintaining the practical and chemical advantages, the concept of scale-out can be employed. Scale-out systems have included multi-sectioned flow-

through porous electrodes, coplanar electrodes and a miniaturized parallel plate electrochemical cell.

In the next paragraph some significant application of electrochemical microreactor for electro synthesis processes proposed in literature will be described.

1.5.1 Reduction of olefins

Marken and co-workers reported a micro flow cell with thin layer geometry with working and auxiliary electrodes directly facing each other. This arrangement allows electrosynthetic processes to be conducted in flow-through mode [20]. At sufficiently small cell height, the two diffusion layers of working and auxiliary electrode overlap or become 'coupled'. As a result, electro-generated acids or bases are instantaneously neutralised, products from anode and cathode can interact and, more importantly, bulk electrolysis is possible without intentionally added electrolyte. The operation of a microflow cell with coupled diffusion layers is demonstrated for the one electron oxidation of ferrocene and for the two electron–two proton reduction of tetraethyl ethylenetetracarboxylate dissolved in ethanol as shown in Figure 1.15. In proof-of-principle experiments omitting added electrolyte, high yields of the product, tetraethyl ethanetetracarboxylate were obtained at a nickel working electrode . The same author reported the electrolyte free cathodic dimerisation of 4-nitrobenzylbromide in a micro-gap flow cell [21]. The electrochemical reduction of 4-nitrobenzylbromide was studied in N,N-dimethylformamide solution in the presence and absence of intentionally added supporting electrolyte. By conventional voltammetry, it was shown that an ECE-type reaction (E = electrochemical step, C = chemical step) occurs with formation of the dimer 4,4'-dinitrodibenzyl, irrespective of the presence of supporting electrolyte. Subsequently, a micro-gap flow cell was employed for the preparative electro-reduction in the absence of supporting electrolyte. Excellent yields of the dimer were obtained and explained based on a self-propagation mechanism.

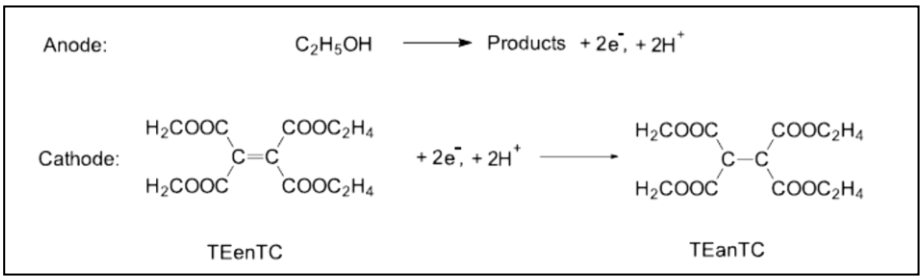

Figure 1.15 *Cathodic reduction of tetraethyl ethylenetetracarboxylate in ethanol [20]*

1.5.2 Direct electrolysis of furan to 2,5-dimethoxy-2,5- dihydrofuran

Atobe and co-workers [19] reported the self-supported paired electrosynthesis of 2,5-dimethoxy-2,5-dihydrofuran using a thin layer flow cell without added supporting electrolyte. The 2,5-dimethoxy-2,5-dihydrofuran, as shown in Fig. 1.16, was prepared by the oxidation of furan and by the reduction of methanol solvent using a thin layer flow cell with anode and cathode directly facing each other and without intentionally added electrolyte. Controlling factors for this kind of self-supported paired electrosynthesis, such as the electrode material, the current density and the flow rate were optimized. The maximum chemical yield of 98% of pure product without work-up could be obtained with a combination of a glassy carbon anode and a platinum cathode in a single pass of furan solution.

The thin layer flow cell was constructed from platinum plates ($3 \cdot 10^{-2}$ m width, $3 \cdot 10^{-2}$ m length) and/or glassy carbon plates ($3 \cdot 10^{-2}$ m width, $3 \cdot 10^{-2}$ m length). A spacer (both sides adhesive tape, 80 µm thickness) was used to leave a rectangular channel exposed, and the two electrodes were simply sandwiched together (Ae= $1 \cdot 10^{-2}$ m width, $3 \cdot 10^{-2}$ m length) as shown in Figure 1.4 paragraph 1.3.1. After connecting Teflon tubing to the inlet and outlet, the cell was sealed with Epoxy resin. In Table 1.3 the performance of chemical and electrochemical processes are compared.

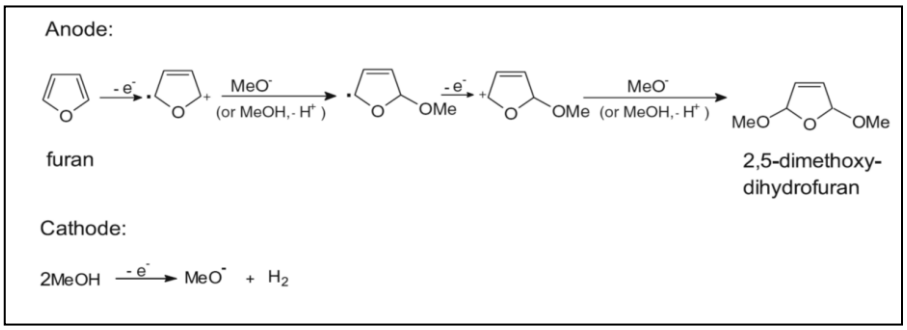

Figure 1.16 *Paired electrolysis of furan to 2,5-dimethoxy-2,5- dihydrofuran without supporting electrolyte [19]*

	Conventional	Electrochemical (conventional)	ECMR directly (i.e. without conductivity salt)
Yield (%)	70–75	80–85	98%
Current efficiency (%)	–	85	10%
Current density ($kA\ m^{-2}$)	–	1.5	0.1
Energy consumption ($kWh\ kg^{-1}$)	–	3	Unknown

Table 1.3 *Comparison of the performance between the chemical and electrochemical operations for the production of 2,5-dimethoxy-2,5- dihydrofurane*

1.5.3 Paired electrolysis of toluene and acetophenone

Horii and co-workers also developed a paired electrosynthetic system using a microflow reactor without intentionally added electrolyte [22]. This system enables paired electrochemical reactions of chloride reduction/alcohol oxidation progressing without added electrolyte. In addition, the use of parallel laminar flow in the microflow reactor resulted in further improvement of the desired product yields (35% toluene and 70% acetophenone) in the paired electrosynthesis as shown in

Figure 1.17. The experiments were conducted in a microreactor composed of a silver cathode and indium-tin oxide (ITO) anode (Figure 1.4 paragraph 1.3.1).

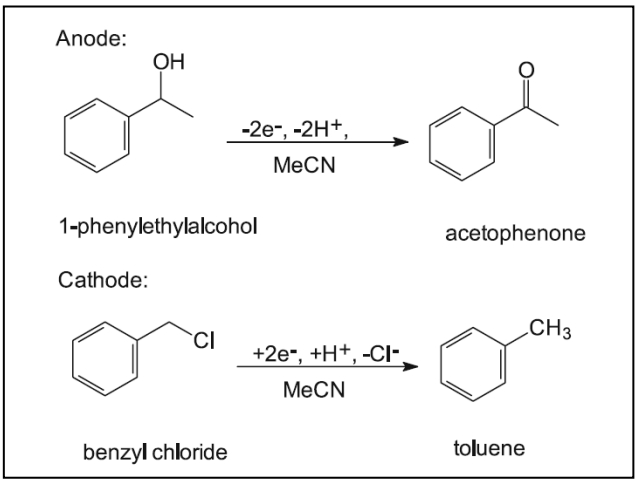

Figure 1.17 *Paired electrolysis of toluene and acetophenone using a micro-flow reactor [22]*

1.5.4 Anodic substitution reaction of cyclic amine with Allyltrimethylsilane

Atobe and co-workers developed a novel electrosynthetic system for anodic substitution reactions by using parallel laminar flow in a microflow reactor. This system enables nucleophilic reactions to overcome the restraint, such as the oxidation potential of nucleophiles and the stability of cationic intermediates, by the combined use of ionic liquids as reaction media and the parallel laminar flow in the microflow reactor [23]. By using this novel electrosynthetic system, the anodic substitution reaction of carbamates, especially of cyclic carbamates, with allyltrimethylsilane, as shown in Fig. 1.18, were carried out to provide the corresponding products in moderate to good yields 80% in a single flow-through operation at ambient temperature (without the need for low temperature conditions).

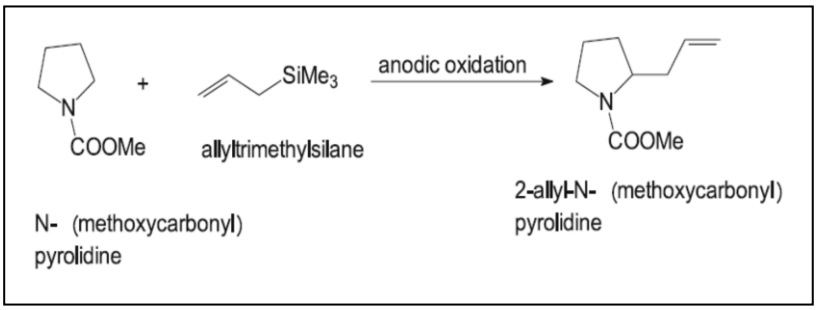

Figure 1.18 *Anodic substitution reaction of N-(methoxycarbonyl)pyrolidine with allyltrimethylsilane*

References

[1] X. Yao , Y. Zhang, L. Du a, J. Liu , J. Yao, Renewable and Sustainable Energy Reviews 47 (2015) 519-539

[2] R.Wohlgemuth1, I. Plazl, et al.,Trends in Biotechnology 33(2015) No. 5

[3] K. Jähnisch, V. Hessel, H. Lowe, M. Baerns, Angew. Chem. Int. Ed. 43(2004) 406-446.

[4] Q.Tu, L.Pang, Y.Zhang, et al. Chin. J. Chem. 31 (2013) 304-316

[5] N. Kockmann, M. Gottsponer, D. M. Roberge, Chemical Engineering Journal 167 (2011) 718-726.

[6] a) Micro Process Engineering A Comprehensive Handbook Vol.1 Edited by Volker Hessel, Albert Renken, Jaap C. Schouten and Jun-Ichi Yoshida; b) D.M. Roberge, M. Gottsponer, M. Eyholzer, N. Kockmann, Chemistry Today 27- 4 (2009) 8-11.

[7] D. Horii, M. Atobe, T. Fuchigami, F. Marken, Electrochenistry Communications 7 (2005) 35-39.

[8] J. Kuleshova, J T. Hill-Cousins, P.R. Birkin, R. Brown, D. Pletcher, T. Underwood, Electrochimica Acta 69 (2012) 197-202.

[9] J. Kuleshova, J T. Hill-Cousins, P.R. Birkin, R. Brown, D. Pletcher, T. Underwood, Electrochimica Acta 56 (2011) 4322-4326.

[10] R. Simms, S. Stubinsky, A. Yudin, E. Kumacheva, Lab Chip, 2009, 9, 2395-2397.

[11] A. Attour, S. Rode, A. Ziogas, M. Matlosz, F. Lapique, J. Appl. Electrochem. 2008, 38, 339-347.

[12] Buyng-Ho Jo et al., J. of Microelectromech. Syst. 9, 2000, 76-81.

[13] P. He, P. Watts, F. Marken, S. J. Haswell, Lab. Chip. 2007, 7, 141-143.

[14] Horii D., Atobe M,, Fuchigami T., Marken F., Electrochem Commun 7 (2005) 35

[15] a)Scialdone, O., Guarisco, C., Galia, A., Sella, C., Thouin, L. Journal of Electroanalytical Chemistry 638-2(2010)293-296; b)Scialdone, O., Guarisco, C., Galia, A. Electrochimica Acta 58-1(2011) 463-473

[16] O. Scialdone, A. Galia, C. Guarisco, S. La Mantia, Chemical Engineering Journal189-190 (2012) 229-236.

[17] Scialdone, O., Corrado, E., Galia, A., Sirés, I. Electrochimica Acta 132 (2014), 15-24.

[18] K. Watts, A. Baker, T. Wirth, J. Flow Chem. 4-1(2014) 2–11

[19] Paddon CA, Atobe M, Fuchigali T, He P, Watts P, Haswell SJ, Prichard GJ, Bull SD, Marken F (2006) J. Appl. Electrochem. 36 (2006) 617-634

[20] Paddon C.A., Pritchard G.J., Thiemann T., Marken F. Electrochem. Commun. 4 (2002) 825

[21] Horii D, Atobe M, Fuchigami T, Marken F J Electrochem Soc 153 (2006) 143.

[22] Amemiya F, Horii D, Fuchigami T, Atobe M J Electrochem Soc 155 (2008) E162.

[23] Horii D, Amemiya F, Fuchigami T, Atobe M Chem Eur J 14 (2008) 10382.

CHAPTER 2

2. ELECTROCHEMICAL PROCESSES FOR THE TREATMENT OF WASTEWATERS AND THE SYNTHESIS OF CHEMICALS

2.1 Introduction

The electrochemical processes for the treatment of wastewater and the synthesis of chemicals have received a great deal of attention from researchers, since they constitute an alternative synthetic route to traditional chemical processes.

Typical methods such as electrocoagulation, electrochemical reduction, electrochemical oxidation and indirect electro-oxidation with active chlorine species are been studied. Recent advances on electrocatalysis related to the nature of anode material to generate strong heterogeneous OH as mediated oxidant of organics in electrochemical oxidation are been extensively examined. Particular attention has been dedicated at the fast destruction of organics, including dyestuffs, mediated with electrogenerated active chlorine, Electro-Fenton and photo-assisted electrochemical methods like photoelectrocatalysis and photoelectro-Fenton, which destroy dyes by heterogeneous OH and/or homogeneous OH produced in the solution bulk.

The electrochemical process offers several advantages over conventional routes and often provides the only viable route, such as, shorter times and milder operating conditions. It also provides the possibility to influence the reaction directly in real-time, offering both more control and the ability to perform the treatment in a continuous fashion.

In the following paragraphs the electrochemical processes for treatment of wastewater containing synthetic organic dyes will be described.

To highlight the advantages of electrochemical processes are also described some important application of electrosyntheis processes.

2.2 Electrochemical processes for treatment of wastewater containing synthetic organic dyes

The environment preservation is a problematic issue of major social alarm also more strict legislation is being imposed on effluent discharge; more effective processes are required for the treatment non-readily biodegradable and toxic pollutants. Synthetic organic dyes in industrial effluents cannot be destroyed in conventional wastewater treatment and consequently, an urgent challenge is the development of new environmentally benign technologies able to mineralize these non biodegradable compounds. The contamination of water by organic chemicals is certainly a crucial question that the recent water framework directives are trying to deal in order to achieve good water quality. Although major attention is currently paid to persistent and emerging pollutants, water pollution by synthetic dyes is also of great concern due to the large worldwide production of dyestuffs [1]. Several studies have reported that there are more than 100.000 commercially available dyes with an estimated annual production of over 7×10^5 tons of dyestuff. Industries such as textile, cosmetic, paper, leather, light harvesting arrays, agricultural research, photo electrochemical cells, pharmaceutical and food produce large volumes of wastewater polluted with high concentration of dyes and other components [2]. These effluents contain organic and inorganic products such as inhibitor compounds, active substances, chlorine compounds, salts, dyeing substances, total phosphate, dissolved solids and total suspended solids. However, dyestuff is the major problem because it creates anesthetic problem and its dye discourages the downstream use of wastewater [3]. According to literature about 280.000 tons of textile dyes are currently discharged in effluents every year because large volumes of wastewaters are generated in various processes of the industry. As a result, dye effluents contain chemicals that are toxic, carcinogenic, mutagenic or teratogenic to various fish species [4-5]. For example, Reactive dyes with good water solubility and easily hydrolyzed into insoluble forms are lost in about 4% during dyeing [2]. Dyes are commonly classified from their chromophore group.

The majority of these compounds consumed at industrial scale are azo (–N=N–) derivatives that represent more than 50% of the all dyes used in textile industries, although antraquinone, indigoide, triphenylmethyl, xanthene, sulphur and phtalocyanine derivatives are frequently utilized. Since dyes usually present high stability under sunlight and resistance to microbial attack and temperature, most of these compounds are not degradable in conventional wastewater treatment plants [6]. The research of treatments to decolorize and degrade dyeing wastewaters to decrease their environmental impact has then attracted increasing interest over the past two decades. For this reason, many studies have been focused mainly on the removal of azo dyes from waters. An extensive literature has reported the characteristics and applications of most important methods for removing dyes from water [1-6].

The Figure 2.1 summarizes the methods classified as physicochemical, chemical, advanced oxidation processes (AOPs), biological and electrochemical for dye removal of the wastewaters.

The mechanisms for dye removal engage physical separation or decolorization by adsorption/biodegradation. The physicochemical processes include coagulation/ flocculation, adsorption and membrane separation. In coagulation, sulfur and disperse dyes are removed from the electrostatic attraction between oppositely charged soluble dye and polymer molecule. However, this method generates large amounts of sludge and high content of dissolved solids remains in the effluent.

Adsorption allows good removal of dyes from the effluent, but the adsorbent regeneration is expensive and involves the loss of adsorbent. The use of apposite membranes is able of removing all types of dyes, being a compact technology without generation of sludge. However, the high cost of membranes and equipment, the lowered productivity with time due to fouling of the membrane and the disposal of concentrates are the principal limitations.

Biological methods are environmentally friendly, produce less sludge than physicochemical systems and are moderately cheap. Many biological treatments

have been studied including anaerobic process, oxidation, trickling filters, activated sludge process and so on [7].

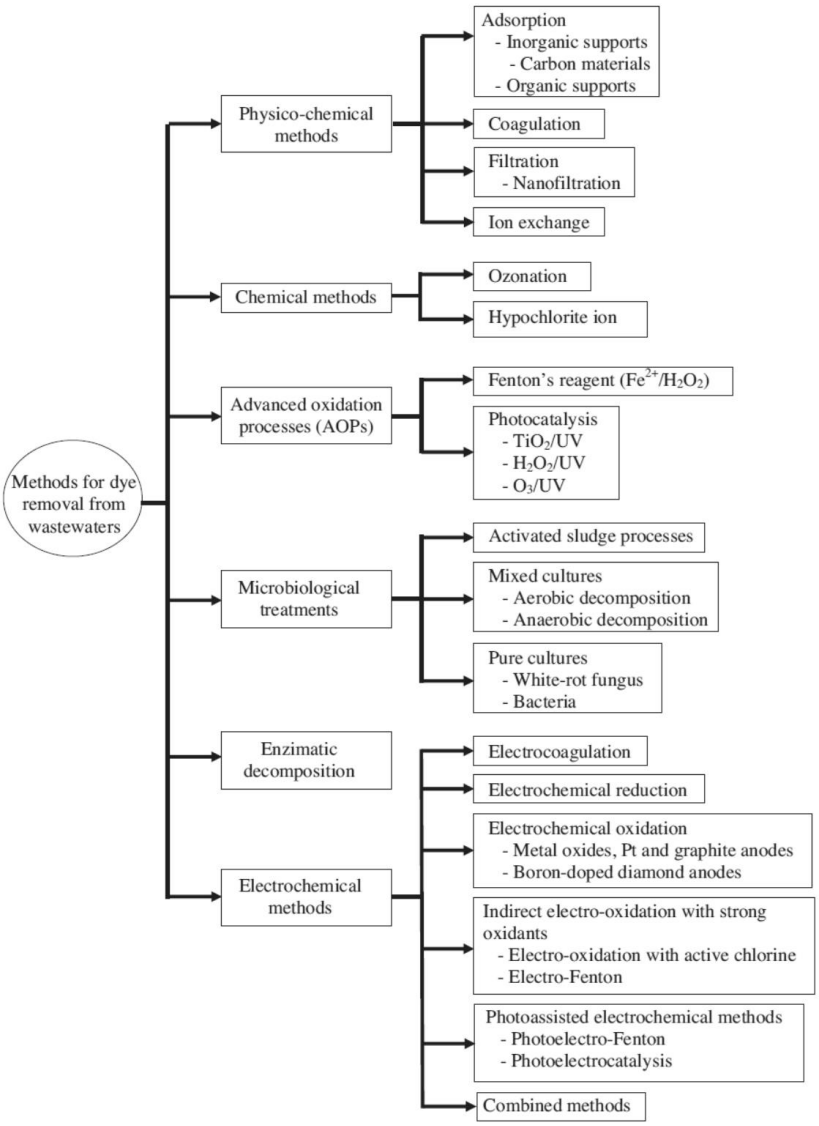

Figure2.1 *Main methods used for the removal of organic dyes from wastewaters (Brillas et.al).*

However, their application is limited because needs a large land area, has sensitivity toward toxicity of certain chemicals and treatment time is very high. Moreover, some dyes are generally toxic and are not biodegradable [1].

More powerful chemical methods such as ozonation and oxidation with hypochlorite ion, as well as AOPs such as Fenton's reagent and photocatalytic systems like TiO_2/UV, H_2O_2/UV and O_3/UV, provide fast decolorization and abatement of dyes. AOPs are environmentally methods involving the on site generation of highly reactive oxygen species such as hydroxyl radicals (•OH) that control the degradation mechanism. Nevertheless, the use of these methods is not currently well accepted because they are expensive and have operational problems [1-2,7].

Electrochemical methods are considered to be among the more efficient Advanced Oxidation Processes (AOPs) for the removal of dyes. The main electrochemical procedures utilized for the abatement of dyestuffs wastewaters are electrocoagulation (EC), direct electrochemical oxidation (EO) with different anodes, indirect electro-oxidation with active chlorine (IOAC) and Electro-Fenton (EF) [6].

Electrochemical methods can offer new sustainable routes for both the treatment of wastewater contaminated by organic pollutants resistant to biological processes. Indeed, these methods use a clean reagent, the electron, and very mild operative conditions with limited operative costs and without the use of toxic/hazardous reactants. Several advantages include high energy efficiency, amenability to automation, easy handling because of the simple equipment required, safety and versatility. The environmental application of electrochemical approaches has been the topic of several books and reviews, summarizing and discussing their use [1-7].

Despite these advantages, electrochemical processes are of a heterogeneous nature, which means that the reactions are taking place at the interface of the electrode and an ion conductivity of the electrolyte. This implies that the performance of electrochemical processes may suffer from limitations of mass transfer and the size of specific electrode area. Another crucial point is the chemical stability of the cell components in contact with an aggressive medium and in particular the long term

stability and activity of the electrode material. Therefore, an efficient, stable and environmentally compatible anode material is required for future technology.

Electrochemical processes have received large interest and many research groups have dedicated a lot of papers to propose electrochemical approaches as potential alternatives for removing dyes from synthetic and industrial effluents. The Figure 2.2 illustrates a general scenario of the papers published in the last 5 years over the treatment of dyes as a function of the electrochemical technology used, including several reviews describing the application of some of such methods [1]. As can be seen, the most popular method is electrochemical oxidation (EO), since heterogeneous •OH is generated at the anode surface. Other typical methods are electrocoagulation (EC) and indirect electro-oxidation with strong oxidants including electro-oxidation with active chlorine and electro-Fenton (EF). This latter method and photo-assisted electrochemical methods such as photoelectrocatalysis (PEC) and photoelectro-Fenton (PEF) are well established electrochemical advanced oxidation processes (EAOPs) where dyes can be destroyed by heterogeneous •OH and/or homogeneous •OH produced in the solution bulk.

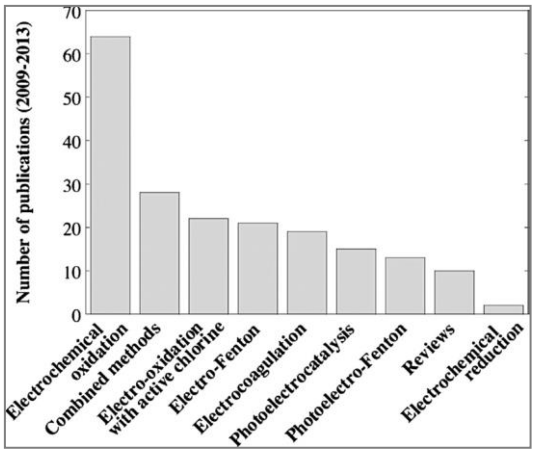

Figure 2.2 *Number of publications devoted to the electrochemical treatment of organic dyes in synthetic and real water effluents in the period 2009–2013.*

– According to the literature, the performances of the electrochemical treatment of dyes are likely to strongly depend on the adopted electrocatalytic route [6].

In the following paragraphs, the electrochemical processes that are used or currently being studied for treatment of wastewaters containing synthetic organic dyes will be described in detail.

2.2.1 Electrocoagulation

Electrocoagulation (EC) is based on dissolution of the electrode material used as an anode that produces metal ions which act as coagulant agents in the aqueous solution *in situ*. EC system consists of an anode and a cathode made of metal plates, both submerged in the aqueous solution being treated [8]. The electrodes are usually made of aluminum, iron, or stainless steel, because these metals are cheap, readily available, proven effective, and non-toxic. Thus they have been adopted as the main electrode materials used in EC systems [8]. During EC, Fe or Al anodes immersed in the polluted water are dissolved by the pass of a current to yield different Fe(II) (and/or Fe(III)) or Al(III)) species with hydroxide ions, respectively, depending on the effluent pH [9]. Aluminum and iron hydrolysis products then destabilize pollutants present in the solution, allowing agglomeration and further separation from the solution by settling or flotation. Moreover, electro flotation also takes place when the bubbles of H_2 gas evolved at the cathode can attach the coagulated particles to transport them to the solution surface where they are separated (Figure 2.3). The advantages of EC include economic aspects (relatively low investment, maintenance, energy, and treatment costs), significantly lower volume of sludge produced, better sludge quality, similar or slightly better efficiency, avoidance of chemical additions, easy of automation, simple equipment and compact size of EC systems greater functional pH range and pH neutralization effect, and the presence of electroflotation (EF) [5]. Fe^{3+} or Al^{3+} ions, usually in the form of sulfate and chlorides salts, are directly added to the wastewater as coagulating agents of dyes.

The displacement of anions and cations under the electric field applied to the electrodes in EC enhances the collision between charged particles, thereby increasing the efficiency of coagulation. However, anode passivation and sludge deposition on the electrodes, inhibiting the electrolytic process, as well as the production of high amount of iron and aluminum ions solved in the effluent, which need to be removed, are the main disadvantages of EC [8].

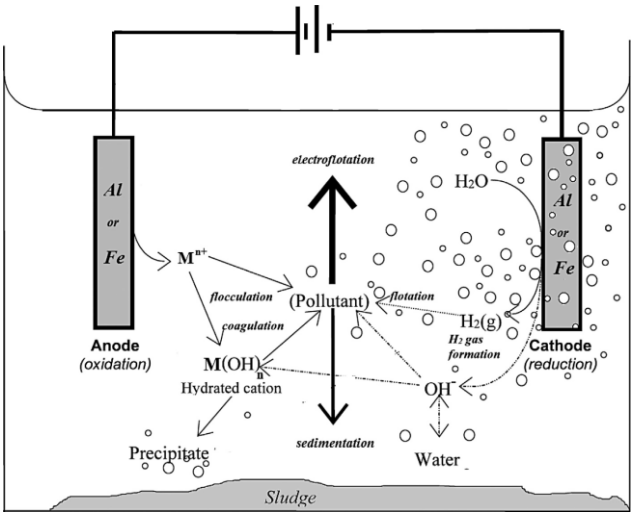

Figure 2.3 *Mechanism for electrocoagulation (EC)[1].*

2.2.2 Electrochemical reduction

A limited number of papers have been published dealing with the direct electroreduction of dyes in aqueous solution on suitable cathodes. The reason of the low interest for this conventional electrochemical technique is that it offers a very poor decontamination of wastewaters compared to other electrochemical treatments. Low decolorization efficiency and TOC removal were found by many authors for the electrochemical reduction of the azoic dyes for example Reactive Blue 4, Acid Yellow 23, Reactofix Golden Yellow 3 with the formation of main by-product.

The azo dye reduction takes place producing hydrazine (in the partial reduction) and its total reduction generates amino compounds (Figure 2.4). However is important the use of a divided cell in the case of the wastewater containing chlorides; this division is important to avoid the formation of chlorine and chlorinated products.

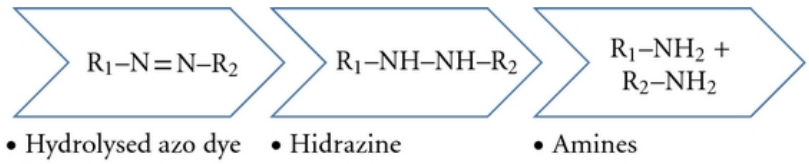

Figure 2.4 *Reduction process for azo dyes.*

2.2.3 Direct electrochemical oxidation

The electrochemical oxidation (EO) has the potential to be a distinct economic and environmental choice for treatment of wastewaters containing synthetic organic dyes. The main results are that this route allows the almost complete mineralization of the organics contained in the wastes with, in some cases, very high current efficiencies.

This process consists in the oxidation of pollutants in an electrolytic cell by:

1. direct anodic oxidation at the electrode surface or direct electron transfer to the anode M, yielding very poor decontamination;
2. chemical reaction with electrogenerated hydroxyl radicals from water discharge at the anode M such as chemisorbed “active oxygen”(oxygen in the lattice of a metal oxide anode MO) or physically adsorbed “active oxygen” (physisorbed M(•OH)).

The existence of different heterogeneous species formed from water discharge has allowed the proposal of two main approaches for EO [10]:

1. electrochemical conversion method, where refractory organics are selectively transformed into biodegradable compounds like carboxylic acids with chemisorbed MO;
2. electrochemical incineration method, in which organics are converted into dehydrogenated or hydroxylated derivatives with physisorbed M(•OH) up to mineralization to CO_2 and inorganic ions.

In both cases, the oxidation of pollutants and production of oxidizing species depend on the potential difference of the electrochemical cell.

The direct anodic oxidation of organic pollutants has been extensively investigated in the last years. The performances of the process in terms of complete mineralization of organic pollutant and current efficiency depends dramatically on the nature of the anode [6]. A high number of electrodes have been tested for the treatment of dyes including metal oxides, carbonaceous materials, Pt and PbO_2. However, synthetic BDD thin films are currently preferred as anodes due to their high performances [10-12].

Electrode	Oxidation potential / V	Overpotential of O_2 evolution / V	Adsorption enthalpy of M-OH	Oxidation power of the anode
RuO_2-TiO_2 (DSA-Cl_2)	1.4-1.7	0.18	Chemisorption of OH radical	
IrO_2-Ta_2O_5 (DSA-O_2)	1.5-1.8	0.25		
Ti/Pt	1.7-1.9	0.3		
Ti/PbO_2	1.8-2.0	0.5		
Ti/SnO_2-Sb_2O_5	1.9-2.2	0.7		
p-Si/BDD	2.2-2.6	1.3	Physisorption of OH radical	

Table 2.1 *Oxidation power of the anode material used in the electrochemical mineralization process in acid media*

The table 2.1 shows that the oxidation potential of the anode (which corresponds to the onset potential of oxygen evolution) is directly related to the over-potential for oxygen evolution and to the adsorption enthalpy of hydroxyl radicals on the anode surface i.e. for a given anode material the higher the O_2 overvoltage the higher its oxidation power. A low oxidation power anode is characterized by a strong electrode-hydroxyl radical interaction resulting in a high electrochemical activity for the oxygen evolution reaction (low overvoltage anode) and to a low chemical reactivity for organic oxidation (low current efficiency for organics oxidation) [10].

2.2.3.1 Boron-doped diamond electrodes

Many research groups have demonstrated that BDD allows total mineralization of a large number of organics [1-2,6,10-12]. In EO, hydroxyl radicals are produced from water oxidation at a high oxygen overpotential anodes such as boron-doped diamond (BDD) electrode (see eq. (1)) where BDD($^{\bullet}$OH) denotes quasi-free or adsorbed hydroxyl radicals).

$$BDD + H_2O \rightarrow BDD(^{\bullet}OH) + H^+ + e^- \quad (1)$$

The BDD allows a total mineralization of organic pollutants, but it is a very expensive electrode and works at high potentials (> 2.3 V vs. SCE), thus leading to high energy consumption [10].

In the presence of low organic concentrations as usually occurs with the treatment of pollutants, the oxidation at BDD occurs under the kinetic control of the mass transfer of the pollutant to the anode surface [6]. According to above considerations, the performances of the process at BDD anode are expected to depend mainly on the flowdynamic conditions. Highly boron-doped diamond exhibits several

technologically important properties that distinguish it from conventional electrodes, such as [13]:

- An extremely wide potential window in aqueous and non-aqueous electrolytes: in the case of high-quality diamond, hydrogen evolution commences at about −1.25V versus SHE and oxygen evolution at +2.3V versus SHE, then the potential window may exceed 3V. The width of the window decreases with the quality of the film and with the incorporation of non-diamond sp^2 carbon impurities its response resembles that obtained from glassy carbon and highly oriented pyrolytic graphite;
- Corrosion stability in very aggressive media: the morphology of diamond electrodes is stable during long-term cycling from hydrogen to oxygen evolution even in acidic fluoride media;
- An inert surface with low adsorption properties and a strong tendency to resist to deactivation: the voltammetric response towards ferri/ferrocyanide is remarkably stable for up to 2 weeks of continuous potential cycling;
- Very low double-layer capacitance and background current: the diamond-electrolyte interface is ideally polarizable and the current between −1000 and +1000mV versus SCE is < 50 A/cm^2. The double-layer capacitance is up to one order of magnitude lower than that of glassy carbon.

Many works have also been focused on the treatment of different dyes and the selection of experimental conditions to improve the performance of this technique. This synthetic material deposited on several supports like Nb, Ti and Si has then been widely applied to dyestuff treatment [1].

Nb/BDD makes unfeasible its large scale utilization in practice for the excessive high cost of this metallic substrate. Ti/BDD anodes with better requirements and small dimension have also been tested for the mineralization of several dyes. However, these electrodes can present problems of cracking and detachment of the diamond film during long term electrolysis.

Si/BDD thin films have been widely used in the EO of dyes in spite of their fragility and relatively low conductivity of the Si substrate [1].

2.2.3.2 DSA-type electrodes Dimensionally stable anodes (DSA) are constituted of a Ti base metal covered by a thin conducting layer of metal oxide or mixed metal-oxides of Ti, Ru, Ir, Sn,Ta and Sb. Many studies have been performed to find new coating layers for electrochemical applications [1-2]. However, these active anodes show a limited oxidation power to incinerate dyestuffs because of their low ability to electrogenerate M(•OH).

The lower abatement achieved at iridium based anodes is due to the fact that the oxidation of water results in the formation of chemisorbed oxygen (Equations (2)-(3)) that have a less oxidation power and that gives rise more easily to the competitive oxygen evolution (Eq. (4)) [14-16].

$$MO_x + H_2O \rightarrow MO_x(^{\bullet}OH) + H^+ + e^- \quad (2)$$

$$MO_x(^{\bullet}OH) \rightarrow MO_{x+1} + H^+ + e^- \quad (3)$$

$$MO_{x+1} \rightarrow MO_x + 0.5\ O_2 \quad (4)$$

Some authors studied the treatment of effluents contained with synthetic dyes by EO with DSA anodes. Ruthenium-based oxide electrodes have received great attention for the abatement of numerous dyes such as Chrome Brown, Reactive Blue 4, Reactive Orange 16, Methyl Orange. A very limited number of papers has reported the use of SnO_2-doped electrodes during the EO of dyes. The different aromatic compounds formed during the degradation of both dyes were identified by GC–MS to understand their oxidation and reduction processes [1].

2.2.4 Indirect electro-oxidation with strong oxidants

2.2.4.1 Electro-oxidation with active chlorine

Aqueous solutions of organic pollutants can be decontaminated by indirect oxidation with electro-generated active chlorine (IOAC), where anodic oxidation of chloride ions leads to the formation of free chlorine, hypochlorous acid and/or hypochlorite, depending on the pH (Eqs. (5-7)), that can oxidize the organics near to the anode or/and in the bulk of the solution (Eq. (8) in alkaline medium) [17].

$$2\ Cl^- = Cl_2 + 2e^- \quad (5)$$

$$Cl_2 + H_2O = HOCl + H^+ + Cl^- \quad (6)$$

$$HOCl = H^+ + OCl^- \quad (7)$$

$$Organics + OCl^- \rightarrow intermediates \rightarrow CO_2 + Cl^- + H_2O \quad (8)$$

These reactions take place in competition with oxygen evolution, chlorate chemical and electrochemical formation and cathode reduction of oxidants in the presence of undivided cells [18]. To account for some experimental results and in particular for the different distribution of by-products observed in the electrochemical treatment in the presence of Cl^- and in the chemical oxidation with NaClO [19], some authors have suggested that an important role can be played also by surface electrochemical reactions. In particular, it has been proposed [19-20] that adsorbed chloro- and oxychloro-radicals could be involved in the oxidation mechanism (see as an example Eqs. (9-10) for the oxychlroradicals).

$$MO_x(OH) + Cl^- \rightarrow MO_x(HOCl) + e^- \quad (9)$$

$$Org.+MO_x(HOCl) \rightarrow interm. \rightarrow MO_x + CO_2 + Cl + H_2O + H^+ \quad (10)$$

This method allows to avoid the transport and storage of dangerous chlorine, gives faster destruction of organic matter and lower costs than in chemical oxidation. On

the other hand, the formation of undesirable toxic chloro-organic derivatives such as chloroform and of chlorine–oxygen by-products such as ClO_2, ClO_3 and ClO_4 can occur. The electrochemical oxidation of numerous dyes with active chlorine in aqueous solutions was studied by various authors [1-2]. BDD anodes are often not used in the presence of high concentrations of chlorides due to their low efficacy for the conversion of chlorides to active chlorine [14] and for the possible generation of chlorates and perchlorates.

In the last years, a limited number of papers have compared the treatment of some dyes with active chlorine produced at DSA-type anodes [1-2]. DSA-type anodes were mainly used due to the high generation of active chlorine expected at these anodes [1-2,6,14]. RuO_2- and IrO_2-based anodes are active anodes with excellent electrocatalytic activity for O_2 and Cl_2 evolutions. IrO_2 is one of the cheapest DSA electrodes with enhanced catalytic activity for such reactions and stability against corrosion compared to RuO_2. Both anodes produce so low amounts of physisorbed M(•OH) that cause poor mineralization of organics. In contrast, their low Cl_2 over potential favors the large formation of active chlorine species. Addition of NaCl to wastewaters improves the oxidation ability of Ti/IrO_2, Ti/RuO_2 and Ti/IrO_2–RuO_2 anode.

2.2.4.2 Electro-Fenton process

The Electro-Fenton (EF) process is based on the electro-generation of hydrogen peroxide in aqueous solution by two-electron reduction of dissolved oxygen (eq. (11)) on a cathode such as mercury pool, compact graphite, carbon felt, activated carbon fiber and carbon-polytetrafluoroethylene-O_2 diffusion cathode (ADE) [2,12,21]. The oxidizing power of H_2O_2 is enhanced in the presence of Fe^{2+} via classical Fenton's reaction (Eq. (12)) which leads to the production of hydroxyl radicals.

$$O_2 + 2H^+ + 2e^- \rightarrow H_2O_2 \quad (11)$$

$$H_2O_2 + Fe^{2+} \rightarrow Fe^{3+} + OH^{\bullet} + OH^- \quad (12)$$

Reaction (12) is propagated through the continuous electro-generation of Fe^{2+} by cathode reduction of Fe^{3+} (Eq. (13)).

$$Fe^{3+} + e^- \rightarrow Fe^{2+} \quad (13)$$

The fast regeneration of Fe^{2+} by reaction (13) accelerates the production of $^{\bullet}OH$ from Fenton's reaction (12).

This enhances the decontamination of organic solutions achieved with these EAOPs, which possess much greater degradation ability than similar anodic oxidation and Fenton processes used separately.

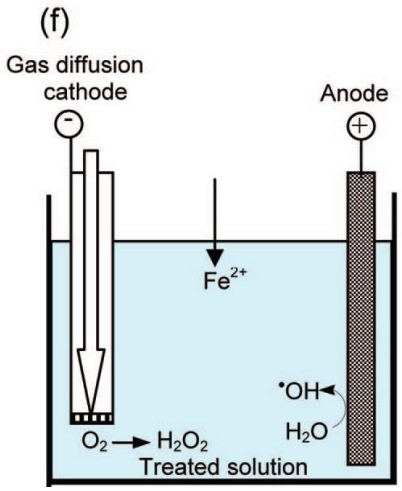

Figure 2.5 *A schematic representation of a bench-scale undivided cell with a gas diffusion cathode used in EF process* (*Brillas et al.*, 2009).

The major advantages of this indirect electro-oxidation method compared with the chemical Fenton process are [22]:

- the on-site production of H_2O_2 that avoids the risks related to its transport, storage, and handling;
- the possibility of controlling degradation kinetics to allow mechanistic studies;
- the higher degradation rate of organic pollutants because of the continuous regeneration of Fe^{2+} at the cathode, which also minimizes sludge production;
- the feasibility of overall mineralization at a relatively low cost if the operation parameters are optimized.

EF process is emerging technologies for wastewater treatment. Over the past decade, they have experienced a significant development showing great effectiveness for the decontamination of wastewater polluted with organic synthetic dyes, pharmaceuticals and personal care products, and a great deal of industrial pollutants. The utilization of cheap graphite electrodes in conventional cells leads to very slow abatements of organic pollutants [6]. Faster abatements are usually achieved using carbon felt or ADE cathodes. The EF process can be considered an economically and environmentally friendly process to remove organic pollutants from water. The abatement of different azo dyes in water by EF processes was studied by different authors. According to the literature, numerous by-products are formed by EF for many organic pollutants [22-23,6]. For example, azo dyestuffs treated by EF process led to the formation of many intermediates and by-products. Several aromatic intermediates such as 1,2-naphthaquinone, 4-aminophenol, 4-hydroxybenzenesulphonic acid, 2-formyl-benzoic acid, salicylic acid, 1,4-benzoquinone and hydroquinone, as well as the some short-chain carboxylic acids (maleic, acetic, malonic, glyoxylic, formic and oxalic) can be formed [22]. Worth mentioning, some of these by-products (such as carboxylic acids) are very resistant to EF method, thus preventing a fast removal of the TOC [6,22].

2.2.5 Photo-assisted electrochemical methods

Photo-assisted electrochemical methods such as PEC (Photoelectrocatalysis) and PEF (Photoelectro-fenton processes) are emerging EAOPs based on the additional destruction of organic pollutants from waters by •OH radicals generated by an incident UV light on the electrolytic system and/or the quick photolysis of intermediates in the treated solution. The incident light can be provided by different artificial lamps supplying UVA (λ = 315–400nm), UVB (λ = 285–315nm) or UVC (λ < 285nm) light. The main drawback of these processes is the high energy cost of the artificial light irradiating the solution and for this reason, direct exposition at natural solar light(λ > 300nm) has been recently utilized as Photo-assisted electrochemical methods such as inexpensive and renewable energy source, giving rise to the derived SPEC and SPEF methods.

2.2.5.1 Photoelectrocatalysis

Photocatalysis consists in the illumination of a stable semiconductor anode with an UV light to induce the oxidation of organics in wastewaters. These processes make use of a semiconductor metal oxide as catalyst and of oxygen as oxidizing agent. Many catalysts have been so far tested for their application to the destruction of environmental toxic pollutants, although only TiO_2 in the anatase form seems to have the most interesting attributes such as high stability, in terms of resistance to photo-corrosion, good performance, namely high oxidative power and non-toxicity, and low cost. The strong oxidizing ability of TiO_2 photocatalysts has been ascribed to highly oxidative holes of the valence band and various oxygen-containing radical species. Among these species, holes and $^{\bullet}OH$ radicals play the most important roles in the photodegradation of organic pollutants. The primary event occurring on the UV-illuminated TiO_2 is the generation of photo-induced electron/hole (e^-/h^+) pairs by promotion of an electron from the valence band (VB) to the conduction band (CB). The oxidizing nature of the holes (h^+) in the valence band means they generate •OH radicals by the oxidation of H_2O molecules or OH^- ions adsorbed on the

semiconductor surface. Organic pollutants can then be oxidized by heterogeneous •OH formed from reaction (15) between the hole and adsorbed water. Moreover, other radicals like $O_2•^-$, $HO_2•$ and H_2O_2, reactions (16)-(19) [24-25].

$$TiO_2 + h\nu \rightarrow e_{CB}^- + h_{VB}^+ \quad (14)$$

$$h_{VB}^+ + H_2O \rightarrow •OH + H^+ \quad (15)$$

$$e^- + O_2 \rightarrow O_2•^- \quad (16)$$

$$O_2•^- + H^+ \rightarrow HO_2• \quad (17)$$

$$2HO_2• \rightarrow H_2O_2 + O_2 \quad (18)$$

$$H_2O_2 + O_2•^- \rightarrow •OH + OH^- + O_2 \quad (19)$$

However, a significant part of electron-hole pairs recombine thus reducing the quantum yield, this represents the major loss in efficiency of photocatalysis.

This problem is solved by using an electrolytic system with a thin film active photo anode subjected to UV illumination in which a constant potential to the anode or a constant current density is applied to promote the extraction of photoinduced electrons by the external electrical circuit, thus yielding an efficient separation of the e^-/ h^+ pairs. This inhibits reactions (16) (19) and enhances the generation of higher quantity of holes by reaction (14) and heterogeneous •OH by reaction (15) with acceleration of organics oxidation compared to classical photo catalysis.

The electrochemical systems for PEC are stirred tank or flow reactors constituted of two- or three-electrode cells equipped with an immersed UV lamp or a quartz window to permit the UV irradiation to the anode surface (Fig 2.6). Recent research on removing dyes by photoelectrocatalysis has demonstrated their better performance than the corresponding EF and EO treatments, respectively.

Moreover, the presence of Cl^- ions accelerated dye removal by the additional oxidative action of active chlorine species (Cl_2/HClO/ClO^-) formed from •Cl radical, previously produced as follows:

$TiO_2\,(_{h+VB}) + Cl^- \longrightarrow TiO_2 + \bullet Cl$ (20)

$Cl^- + \bullet OH \rightarrow \bullet Cl + OH^-$ (21)

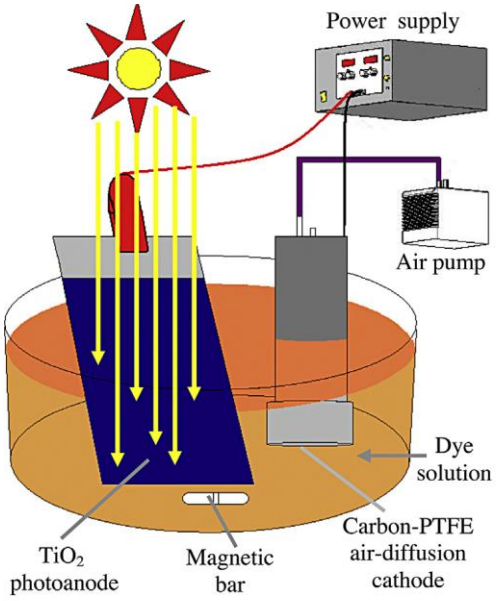

Figure 2.6 *Experimental set-up used for the degradation by solar photoelectrocatalysis of Acid Orange 7 solutions.*

2.2.5.2 Photoelectro-fenton processes

The Photoelectro-fenton consists in the simultaneous use of electrogenerated H_2O_2 in the presence of Fe^{2+} (EF conditions) and UV illumination of the solution to mineralize dyes. The photocatalytic action of this irradiation is complex and its main effects can be related to:

- the photolysis of $Fe(OH)^{2+}$, which is the predominant Fe(III) species at pH 3.0, regenerating greater amount of Fe^{2+} and producing more quantity of $^{\bullet}OH$ via photo-Fenton reaction, according Eq. 21:
- $Fe(OH)^{2+} + h\nu \rightarrow Fe^{2+} + {}^{\bullet}OH$ (21)
- the photolysis of complexes of Fe(III) with generated carboxylic acids.

Nevertheless, some authors have used sunlight irradiation as alternative treatment, since it represents an inexpensive and potent source of UV light, giving rise to the so-called solar photoelectro-Fenton method [26].

Hence, both these combined processes are an extension of Fenton process which takes advantages from UV-VIS light irradiation. Finally, to our knowledge, it is important to consider another kind of electro-oxidation process, known as mediated electro-oxidation, concerning the oxidation on an anode of metal ions, usually called mediators, from a stable, low valence state to a reactive, high valence state. Then, the oxidized mediators, typically Ag^{2+}, Co^{3+}, Fe^{3+}, Ce^{4+} and Ni^{2+}, attack organic pollutants directly, and may also produce hydroxyl free radicals that promote destruction of the organic pollutants. Subsequently, these species are regenerated on the cathode, forming a closed cycle. This process was proposed for treating mixed and hazardous pollutant.

On the other hand, mediated electro-oxidation as well as electro-Fenton usually need to operate in acidic media to avoid precipitation of metal hydroxides and, in addition, there exists the secondary pollution from the heavy metals added. These disadvantages limit the application of these processes. Several authors have emphasized the superiority of PEF over EF for dye removal [1-2].

2.2.6 Combined methods

Many coupled and hybrid electrochemical processes have been proposed aiming developing more powerful processes for dyes removal. They include combined EC, EO, EF and photo-assisted electrochemical methods, as well as the use of microbial fuel cells, which are detailed below. The combination of different techniques has been found frequently very useful to improve the performances in organics degradation processes. Many different solutions are reported in the literature. Among these, the coupling of UV irradiation with chemical oxidation with ozone or/and hydrogen peroxide has to be considered convenient and seems to have already industrial application in water treatment. Interestingly, according to Gimeno et al. (2005), the coupling of ozonation with photochemical and/or photocatalytic oxidation are the most attractive technologies.

Furthermore, some authors have noted that the Fenton-type oxidation is made more efficient by coupling with sonication and hydrodynamic cavitation. Additionally, the coupling of adsorption on alumina with electrical discharges as well as of adsorption on polymeric materials with sonication have been reported as very efficient methods to remove phenol [1-2].

Nevertheless, the most famous coupled processes are the electro-Fenton (EF) and photoelectro-Fenton (PEF), H_2O_2/UV and O_3/UV. In this frame, it is also important to consider the possibility of the degradation of organic pollutants by the contemporary effectiveness of electrochemical anodic and cathodic processes. AOPs involving electrochemical process are also known as EAOPs, i.e. electrochemical advanced oxidation processes [1] Finally, apart from the combination of AOPs, it is important to enunciate the possibility of put in sequence some degradation processes in order to improve the treating of wastewaters. In particular, whereas oxidation processes could transform refractory pollutants in more innocuous products and thus biodegradable, it was considered that AOPs could be optimal pre-treatments for a successive biological degradation step, to limit toxicity of the solution with respect to the microbial cultures.

2.3 Electrochemical processes for synthesis of chemicals

Electrosynthesis in chemistry is the synthesis of chemical compounds in an electrochemical cell. The main advantage of electrosynthesis over an ordinary redox reaction is avoidance of the potential wasteful other half-reaction and the ability to precisely tune the required potential.

Electrosynthesis has many industrial applications. The electron is "environmentally friendly" reagent, this means that in some electrochemical processes less by-product waste compared to chemical processes can generally be expected. For example, catalytic quantities of electrochemically regenerable redox couples can be used for oxidation or reduction reactions instead of stechiometric quantities of redox reagents (so called, indirect electrolysis). If, however, electron transfer is direct, from substrate to electrode (anodic oxidation) or electrode to substrate (cathodic reduction), pollutant levels can be even further decreased.

Still, other important reasons for industrial interest include: possible overall higher energy efficiency of electrochemical compared to thermally based processes; use of less expensive starting materials; less aggressive process conditions, e.g. lower temperatures with less degradation of feed and/or product; fewer processing steps (for example, electrochemical synthesis and product separation may be combined in one reactor); precise control of oxidation or reduction level by control of electrode potential; discovery of unique processing routes to establish or re-establish control of the market position. In any worthwhile comparison of the advantages of chemical vs. electrochemical alternatives, it is obvious that the relative economics, the market, product selectivity and other factors must be considered.

Product quality is also important, and typically an electrochemical process originates products more pure than those synthesised by the chemical route. Although, as strange as it may seem, in very special cases failure of an electrochemical process can occur precisely because the product is too pure when compared to the one obtained chemically. For example, certain anthraquinone dyes produced by chemical means contain coloured by-products in addition to the major

product, and the mixture of a particular colour may have been accepted for decades by a very conservative industry.
In following paragraphs the electro synthesis of chloroacetic acid will be described, an interesting example of electrosynthesis whose aim is to contribute to the diffusion of the interest of the electrochemistry applied to the chemical industry.

2.3.1 Electro synthesis of chloroacetic acid

The monochloroacetic acid (MCAA) is an important reagent for several chemical reactions in industry. It is used in the production of a wide variety of useful compounds; e.g., drugs, dyes, pesticides. Most reactions take advantage of the high reactivity of the C–Cl bond. It is the precursor to the herbicide glyphosate, and the herbicides MCPA (2-methyl-4-chlorophenoxyacetic acid) and dimethoate are prepared by alkylation with chloroacetic acid. MCAA is converted to chloroacetyl chloride, a precursor to adrenaline (epinephrine). Displacement of chloride by sulfide gives thioglycolic acid, which is used as a stabilizer in PVC and as component in some cosmetics. In its largest-scale application, MCAA is used to prepare the thickening agent carboxymethyl cellulose and carboxymethyl starch [27].

MCAA is prepared industrially via two routes. The predominant method involves chlorination of acetic acid, with acetic anhydride as a catalyst (Eq. 22)

$$CH_3CO_2H + Cl_2 \rightarrow ClCH_2CO_2H + HCl \quad (21)$$

Another main industrial route to chloroacetic acid is hydrolysis of trichloroethylene using sulfuric acid as a catalyst.

$$CCl_2CHCl + 2\ H_2O \rightarrow ClCH_2CO_2H + 2\ HCl \quad (22)$$

The production of MCAA by chlorination of acetic acid, the prevalent route, is accompanied by the formation of relevant amounts of dichloroacetic acid (DCAA) and to a small extent of trichloroacetic acid (TCAA) difficult to separate by distillation. Approximately, 420 000 000 kg/y are produced globally [27-28] (Figure 2.7). For this reason, the electrochemical reduction of DCAA to MCAA acid was, in particular, investigated in detail both in bench and pilot scale with promising results [29-30].

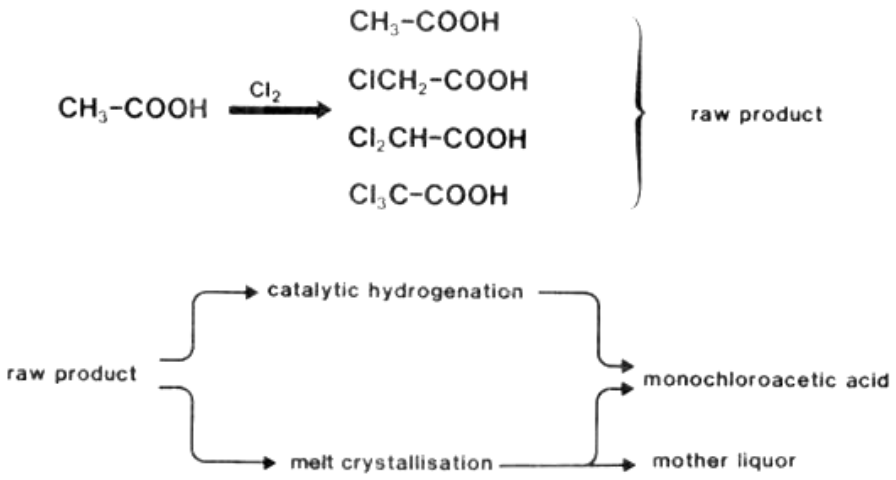

Figure 2.7 *Method for the production of monochloroacetic acid*

The purification of the raw product is carried out either by catalytic hydrogenation or by melt crystallization. The mother liquor resulting from the melt crystallization process contains monoclhoroacetic acid, dichloroacetic acid (DCAA) and thrichloroacetic acid (TCAA) and unreacted acetic acid as main components.

The recycling of these products is of potential industrial interest. One of the most promising routes in electrochemical reduction which has been known for about 100 years. DCAA and TCAA have been reduced to MCAA in concentrated aqueous solution using lead and graphite or magnetite cathodes. Generally a divided cell was

used (Eq. 23-25). The anolyte consisted of concentrated hydrochloric acid giving chlorine at the anode. The overall reactions is the reverse of the undesired over chlorination of MCAA.

Cathode reaction: $CHCl_2COOH + 2e^- + 2H^+ \rightarrow CH_2ClCOOH + HCl$ (23)

Anode reaction: $2HCl \rightarrow Cl_2 + 2H^+ + 2e^-$ (24)

Global reaction $CHCl_2COOH + HCl \rightarrow CH_2ClCOOH + Cl_2$ (25)

This process was not developed to a commercial scale. The main problem for the scale up of this process stems from the behaviour of the electrode material. Metal cathodes, e.g. lead, which have sufficiently high hydrogen overpotential are subject to severe corrosion in the strongly acidic medium. Although in this experiment the electrode has, for the whole time, been carefully under cathodic protection, a thick spongy layer of lead was deposited onto the surface as a result of corrosion of those parts of the electrode which were not sufficiently protected.

Graphite cathodes exhibit excellent stability but are readily contaminated by impurities which give rise to side reactions. In addition, because previously know cathode materials allow applications of only low current densities, the commercial viability of this process was lowered by the high investment cost needed.

The general problems relating to previously known cathode materials are:

- Corrosion and contamination of the electrodes
- Low current density: -low space-time yield
  - high investment costs
- Low selectivity
- $2\ H^+ + 2e^- \rightarrow H_2$
- $CCl_2CHCl + 2e^- + H^+ \rightarrow CH_3CO_2H + HCl$

The solution to these problems was initiating by a surprising discovery. In order to combine the good stability of graphite and the good electroactivity of lead, a lead was deposited on a carbon cathode. However, tha addiction of about 40 ppm of lead sals to a concentrated solutions of DCAA in water, followed by electrolysis did not result in deposition of a layer of lead in the graphite surface but instead, produced a strong catalytic effect. The cyclic voltammogram clearly demostrates an increase of the cathodic surrent by a factor four (Figure 2.8).

This effect was not restricted to lead salt, The increase of cathodic current was even higher in the presence of 8 pp, gold or 22 ppm copper salts (Figure 2.9).

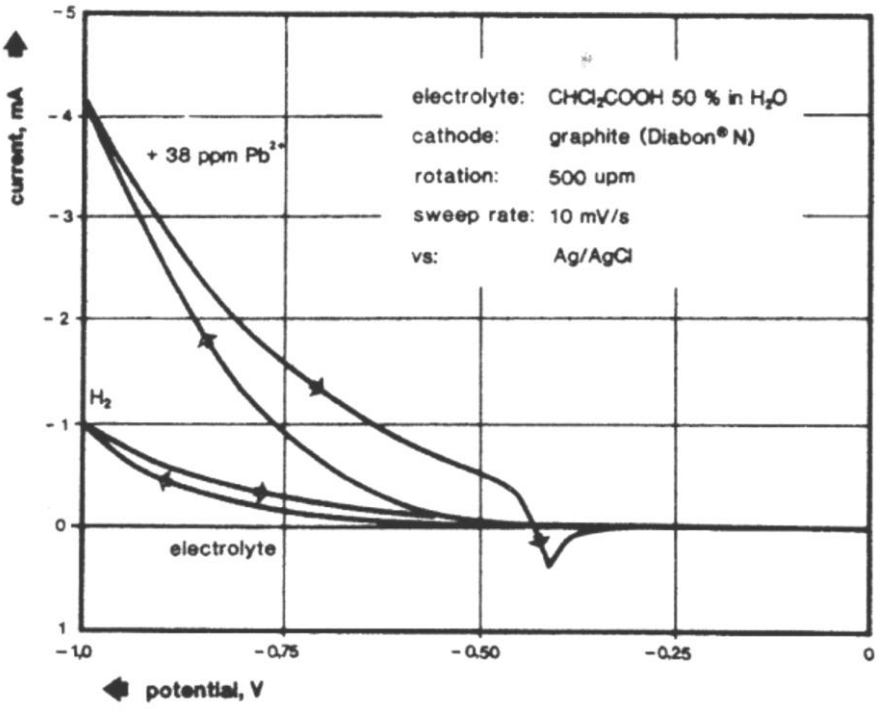

Figure 2.8 *Cyclic voltammograms before and after the addition of 38 ppm Pb^{2+} to the solution of DCAA.*

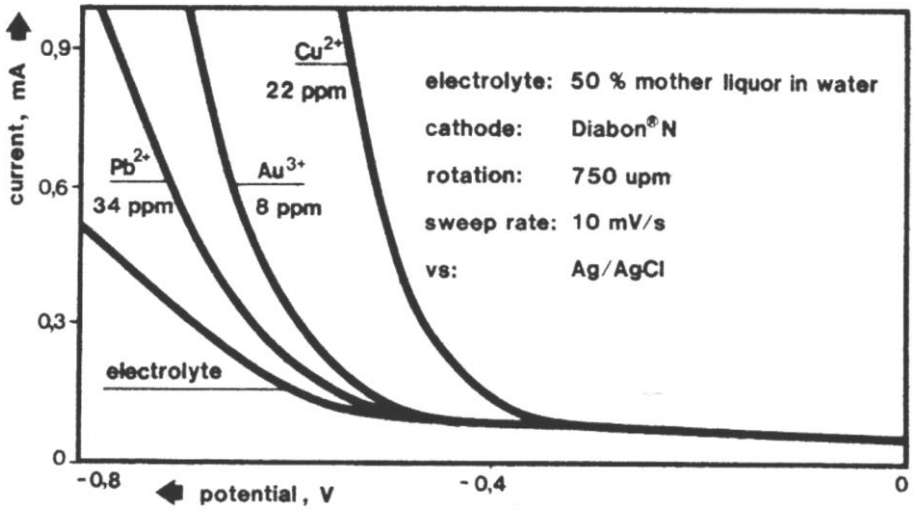

Figure 2.9 *Electrochemical reduction of DCAA. Current voltage curves, in the present of different metal ions.*

The electrolysis was performed in the presence of Pb^{2+} in a cell by laboratory with a working surface 0.02 m^2 and using a current density of 5000 A m^{-2} at 80 °C to a cell potential of about 5V.

The two electrodes were spaced using a Nafion® 324 membrane. The anodic reaction sees the disappearance of one mole of hydrochloric acid per mole of acid MCAA formed, and then, in order to maintain in the anode compartment a HCl concentration of 20% was appropriate to enter that acid throughout the process. In the cathode compartment, instead, it was sent initially a solution 80:20 respectively of the mixture to be treated (MCAA, DCAA and TCAA) and water. For the reasons we mentioned before it was decided to use a cathode with a surface deposit of lead on graphite, which worked for more than 1000 hours continuously without deactivation; it has been shown to be immune to impurities in the mixture of MCAA, DCAA and TCAA arising from the chlorination process.

Under these conditions, acid DCAA and TCAA were reduced by getting conversions higher than 99% with a yield in acid MCAA greater than 97%. Furthermore the efficiency of current reached is 90%.

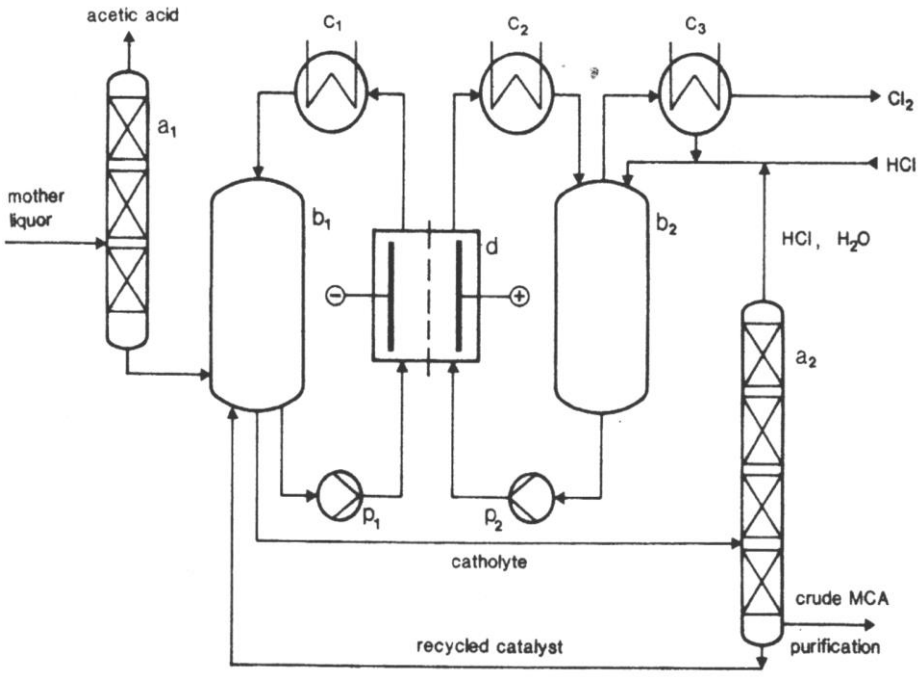

Figure 2.10 *Flow diagram of the production of MCAA for chlorination of DCAA and TCAA. In figure distinguish distillation columns (a1) and (a2), the containers of the solutions and cathodic respectively anodic (b1) and (b2), and the electrochemical reactor (d).*

The final catholyte mixture composition of the solution was so redistributed: 56:33:11 as a percentage respectively of monochloroacetic acid, water and hydrochloric acid. Consistent with the operational parameters described above, a plant pilot has been built with a total cathode area of 1.6 m^2 and a capacity of 80 ton/year of MCAA.

The scheme of this system is shown in figure 2.10, which shows all the stages of production of MCAA from DCAA and TCAA. The diagram shows that the process is fully integrated in the MCAA production plant. All loops are closed. No wastes and no air pollution occur except for small amount of Hydrogen occur.

References

[1] E. Brillas, C. A. Martınez-Huitle, Appl. Catal. B: Environ. 166-167 (2015) 603-643.

[2] C.A. Martínez-Huitle, E. Brillas, Appl. Catal. B: Environ. 87 (2009) 105-145.

[3] D. Brown, Ecotoxicol. Environ. Saf. 13 (1987) 139-147.

[4] X.C. Jin, G.Q. Liu, Z.H. Xu, W.Y. Tao, Appl. Microbiol. Biotechnol. 74 (2007) 239-243.

[5] M. Solís, A. Solís, H.I. Pérez, N. Manjarrez, M. Flores, Process Biochem. 47 (2012) 1723-1748.

[6] O. Scialdone, A. Galia, S. Sabatino, Appl. Catal. B: Environ. 148-149 (2014) 473-483.

[7] T. Robinson, G. McMullan, R. Marchant, P. Nigam, Bioresour. Technol. 77 (2001) 247-255.

[8] G. Chen, Separation and Purification Technol. 38(2004) 11-41.

[9] V. Kuokkanen, T.Kuokkanen1, J. Rämö, U. Lassi, Green and Sustainable Chemistry 3 (2013) 89-121.

[10] a) A.Kapałka, G. Fóti, C.Comninellis, J. Appl. Electrochem. 38 (2008) 7–16; b) A. Kapałka,G. Fóti, C. Comninellis, Electrochimica Acta 54 (2009) 2018-2023

[11] M. Panizza, G. Cerisola, Chem. Rev. 109-12 (2009) 6541-6569

[12] C. A. Martinez-Huitle, S. Ferro, Chem. Soc. Rev. 35 (2006) 1324-1340;

[13] Panizza M., G. Cerisola, Electrochimica Acta, 51 (2005) 191–199.

[14] O. Scialdone, A. Galia, C. Guarisco, Electrochimica Acta 58 (2011) 463– 473.

[15] O. Scialdone, Electrochim. Acta 54 (2009) 6140–6147; O. Scialdone, A. Galia, S. Randazzo, Chemical Engineering Journal 183 (2012) 124-134.

[16] C. Comninellis, Electrochim. Acta 39 (1994) 1857-1862.

[17] O. Scialdone, S. Randazzo, A. Galia, G. Silvestri, Wat. Res. 43 (2009) 2260-2272.

[18] Ch. Comninellis, A. Nerini, Journal of Applied Electrochemistry 25 (1995) 23-28.

[19] F. Bonfatti, S. Ferro, F. Lavezzo, M. Malacarne, G. Lodi, A. De Battisti, Journal of the Electrochemical Society 147 (2000) 592-596.

[20] C. A. Martinez-Huitle, S. Ferro, A. De Battisti, Electrochemical and Solid-State Letters 11 (2005) D35-D39.

[21] A. Özcan, M. A. Oturan, N.Oturan, Y. Sahin, J. of Hazard. Materials 163 (2009) 1213-1220.

[22] E. Brillas, I. Sires, M. A. Oturan, Chem. Rev. 109 (2009) 6570.

[23] A. Özcan, M. A. Oturan, N.Oturan, Y. Sahin, J. of Hazard. Materials 163 (2009) 1213-1220.

[24] I. Sirés, E. Brillas, M.A. Oturan, M.A. Rodrigo, M. Panizza, Environ. Sci. Pollut. Res. 21 (2014) 8336–8367.

[25] M.A. Oturan, J.-J. Aaron, Crit. Rev. Environ. Sci. Technol. 44 (2014) 2577–2641.

[26] a)Skoumal M.et al., Electrochimica Acta, 54 (2009) 2077–2085; b) Skoumal M. et al., Applied Catalysis B: Environmental, 66 (2006) 228–240.

[27] G. Koenig, E. Lohmar, N. Rupprich in *Ullmann's Encyclopedia of Industrial Chemistry*, Weinheim, Wiley-VCH, 2005, electronic release.

[28] *Electrosynthesis from laboratory, to pilot, to production* (Eds.: J. D.Genders, D. Pletcher), The electrosynthesis company Inc., New York, 1990, Chapter 5.

[29] E. Steckan "Electrochemistry, 3. Organic Electrochemistry" in Ullmann's Encyclopedia of Industrial Chemistry, Weinheim, Wiley-VCH, 2005, electronic release.

[30] Jap. Pat. 54-076251; Chlorine Engineers 1979.

CHAPTER 3

3. EXPERIMENTAL

3.1 Introduction

In order to pursue the objectives of my thesis, the following kinds of study were performed:

I. Electrochemical abatement of azo dye Acid Orange 7

Uncoupled processes

- Direct anodic oxidation with Ti/IrO_2-Ta_2O_5 (DSA) and boron doped diamond (BDD);
- Electro-generation of active chlorine (IOAC) with DSA electrode;
- Elettro-Fenton (EF).

Coupled processes

II. Electrochemical conversion of dichloroacetic acid to chloracetic acid

Both electrochemical processes were performed in different systems that will be described in detail in the next paragraphs:

1. Conventional macro reactor
2. Micro reactors: system I and system II
3. Micro reactors in series
4. Stack of micro reactors
5. High-pressure reactor.

3.2 Chemicals

3.2.1 Chemicals for electrochemical abatement of azo dye Acid Orange 7

Bi-distilled water and Acid Orange 7 (Sigma Aldrich) were used as solvent and model pollutant, respectively. Na_2SO_4 35 mM (Janssen Chimica) was used as supporting electrolyte for experiments in macro cell and $FeSO_4$ (Fluka) 0.25 - 1 mM as catalyst for EF. Main by-products were determined by HPLC analyses by comparison of their retention times with that of pure standards. Oxalic (Sigma Aldrich), formic (Sigma Aldrich), tartaric (Merck), malonic (Alfa Aesar), acetic (Sigma Aldrich), salicylic (Merck), maleic (Merck), succinic (Fluka), fumaric (Fluka), lactic (Sigma Aldrich), and phtalic (Fluka) acids, hydroquinone (Sigma Aldrich), 1,2-naphthaquinone (Sigma Aldrich), and 4-amminophenol (Sigma Aldrich), were used as standards for HPLC analyses. Different electrodic materials were used during the electrolyses in dependence of the process and organic substrate studied. Compact graphite (Carbon Lorraine), carbon felt (The Electosynthesis Co.), a carbon-PTFE ADE from E-TEK, which was fed with 0.35 L min^{-1} of compressed air to electrogenerate H_2O_2, or Ni were used as cathodes while Ti/IrO_2-Ta_2O_5, (ElectroCell AB) Ti/RuO_2-IrO_2 (ElecroCell AB) and BDD-Nb, supplied by Condias or ElecroCell AB were used as anodes with a geometric surface of 5-6 cm^2. Prior to each experiment, diamond electrodes were polarized at 3.0 V vs. SCE for 5 minutes. The thickness of the stagnant layer in the adopted conditions was estimated trough a typical limiting-current essay using the redox couple hexacyanoferrate(II)/hexacyanoferrate(III) focusing on the oxidation reaction and using the value 6.631 10^{-10} m^2 s^{-1} for the diffusivity of ferry-cyanide ion [1]. The mass transfer coefficient of AO7 k_m was estimated as the ratio between its diffusivity D (assumed to be about 10^{-9} m^2 s^{-1}) and the thickness of the stagnant layer.

3.2.2 Chemicals for electro synthesis of chloroacetic acid

Electrolyses were performed using a Bi-distilled water solution of 0.1 M DCAA (Acros Organics). 0.1 M Na_2SO_4 (Janssen Chimica) was used as supporting electrolyte for experiments in macro cell. NaOH (AppliChem) was used to adjust the pH of the solution when necessary and MCAA (Alfa Aesar) and acetic acids (Sigma) as standards for HPLC analyses. Compact graphite (Carbone Lorraine), Cu, Ag were used as cathodes and a Ti/IrO_2-Ta_2O_5 (from Electrocell) as anode. Cathodes were polished with sand paper.

3.3 Experimental settings

3.3.1 Conventional macro reactor

Electrolyses in macro scale were performed in batch mode in a cylindrical, undivided tank glass cell under vigorous stirring performed by a magnetic stirrer with 50 mL of solution (Fig.3.1). The inter-electrode gap was about 2 cm. Electrolyses were driven by an Amel 2053 operated in galvanostatic mode.

Different electrodes were used dependently of the electrochemical processes.

I. Electrochemical abatement of azo dye Acid Orange 7

Electrochemical direct oxidation

- Anode: Ti/IrO_2-Ta_2O_5, Ti/RuO_2-IrO_2 and BDD-Nb, with a geometric surface of 5-6 cm^2;
- Cathode: Nickel with a working area of 3.75 cm^2.

Electro-generation of active chlorine

- Anode: DSA-O_2 (Ti/IrO_2-Ta_2O_5 and DSA-Cl_2 (Ti/RuO_2-IrO_2) with a working area of 3.75 cm^2;
- Cathode: Nickel with a working area of 3.75 cm^2.

Figure 3.1 *Electrochemical conventional cell*

Elettro-Fenton

For the electro-Fenton process the configuration of the head of the cell was slightly varied and compressed air was fed (0.35 L min^{-1}) to the solution Fig.3.2. DSA-O_2 (3.75 cm^2) and compact graphite or carbon felt (6.75 cm^2) were used as anode and cathode, respectively. Some experiments were carried out with a gas diffusion Carbon-PTFE (polytetrafluoroethylene) Air Diffusion Electrode (AED) from E-TEK (Sommerset, Nj, USA) (Fig.3.3). The volume of the electrolytic solution was of about 130 ml and it was stirred by magnetic stir bar. The carbon-PTFE cathode was fed with an oxygen flow rate of 0.35 l/min, from an oxygen generator KNF LAB LABPORT, to continuously electrogenerate hydrogen peroxide by oxygen electrochemical reduction. In particular, the carbon-PTFE electrodic material was placed at the bottom of a cylindrical holder of polypropylene with an inner nickel screen of 125 mesh as current collector in contact with a nichel wire as electrical connection.

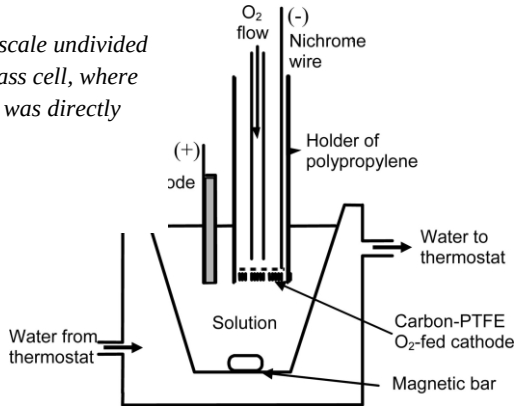

Figure 3.2. *Scheme of a bench-scale undivided and thermostated cylindrical glass cell, where the carbon-PTFE ADE cathode was directly fed with pure O_2*

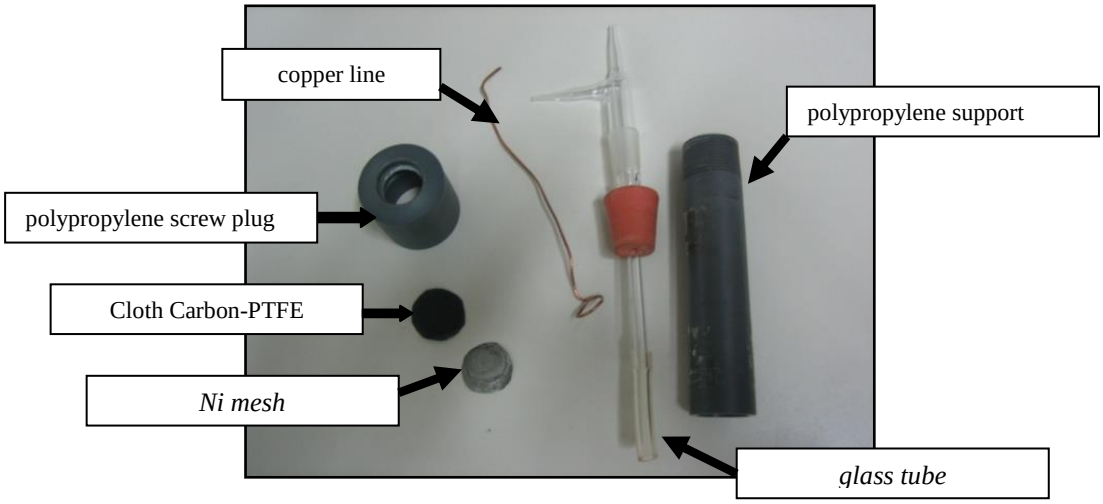

Figure 3.3. *The components of Oxygen-diffusion cathode*

II. Electrochemical conversion of dichloroacetic acid to chloracetic acid

For this process the electrolyses were performed also in batch mode in the undivided tank glass cell (Fig.3.1) equipped with Pb, compact graphite, Ag and Cu cathodes (working area A = 3-4 cm^2) and a Ti/IrO_2-Ta_2O_5 anode and containing 50 mL of solution under vigorous stirring performed by a magnetic stirrer. The inter-electrode gap was about 2 cm.

3.3.2 Micro reactors

3.3.2.1 Micro reactor: system I

The micro reactor consists in a commercial undivided filter press flow cell ElectroCell AB, equipped with one or more polytetrafluoroethylene (PTFE) spacers with the following nominal distances between electrodes: 50 (using one spacer), 75 (using two spacers of 50 and 25 μm), 120 (with a single spacer) and 240 μm (using two spacers of 120 μm) Fig.3.4 .

The microreactor is constituted by:

- Two steel plates provided with two holes, to impart mechanical stability to the cell;
- Two plates of teflon equally provided with holes one for inlet and one for the outlet of the fluid;
- Two neoprene gaskets, each of which is interposed between the plate of Teflon containment and the electrode, which ensure the sealing and prevent any loss of solution from the cell;
- Two electrodes consisting of two flat plates with the same dimensions;
- One or more spacers (made of PTFE by Bohlender Gmbh) which allow to define the working area.

In particular, the work area on the electrode has been realized by creating on the standoffs of the windows of the optimized geometry for the purpose of sealing of the cell. Spacers were cut to define the working area (A = 4-6 cm^2).
The geometry used for most of the experiments is shown in figure 3.4b.
The whole was tightened through twelve bit, in order to distribute a uniform load, to avoid any loss of solution or deformation of the electrodes. For each tested operative condition at least 3 samples of 1 mL were analyzed to be sure that steady state

conditions were achieved. Different electrodic materials were used during the electrolyses dependently of the electrochemical process.

Experiments in the micro reactor were performed in a continuous mode with a single passage of the solution inside the cell using a syringe pump (New Era Pump Systems, Inc.) to feed the solutions with flow rate between 0.05 and 0.4 mL/min and without addition of a gaseous stream to the solution.

3.4a

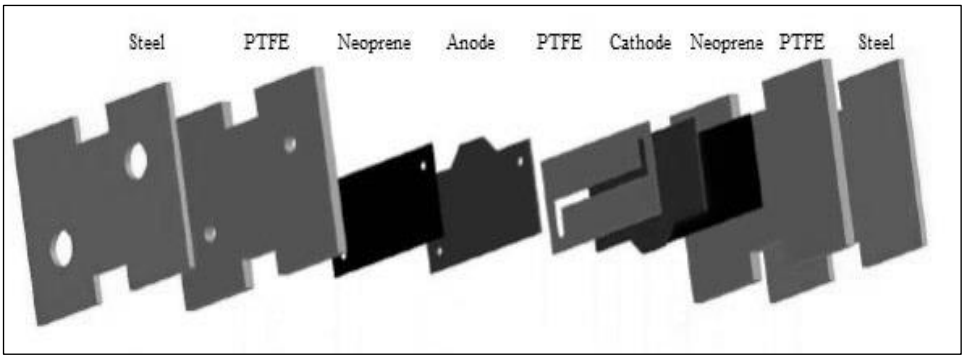

3.4b

Figure 3.4. *Photo and scheme of adopted micro-reactor based reaction systems: a) reports a photo for one micro reactor and b) a scheme of one micro reactor.*

3.3.2.2 Micro reactor: system II

The second micro reactor (micro-reactor II) consisted of two flat, rectangular electrodes (a compact graphite or a Cu cathode and a Ti/IrO_2-Ta_2O_5 anode) separated by two micro-channelled spacers (DuPont Pyralux LF sheet adhesive with a nominal thickness of 50 µm) (Fig. 3.5). The device was assembled by the following steps:

(i) adhesion of one electrode with one or two spacers at T ≥ 120 °C for at least 5 min at 400 psi (using a Carver bench heated Press);

(ii) creation of microchannels within the spacer (width = 0.5 cm, length = 7 cm, A = 3.5 cm^2) by LPKF PROTOMAT S42 milling machine (NITZ Engineering Srl) (Fig.3.6);

(iii) adhesion of the other electrode with suitable holes by press at T ≥ 120 °C for 1.5 h at 400 psi;

(iv) inlet/outlet ports insertion. A working area of 3-4 cm^2 was used.

For each tested condition, at least five samples, taken with 10 minutes time interval from the outlet stream from the microreactors, were analysed after a single pass to be sure that steady state conditions were achieved.

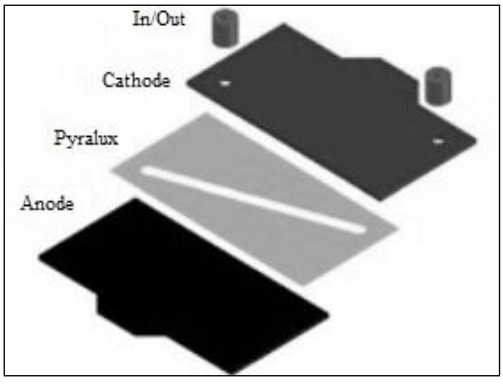

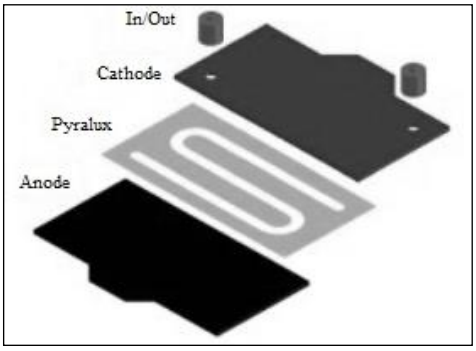

Figure 3.5. *Schemes of the micro-reactor II*

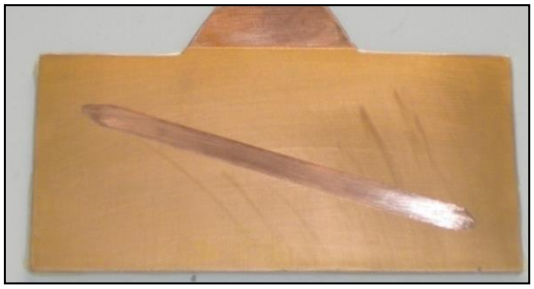

Figure 3.6. *Microchannels created in the electrode*

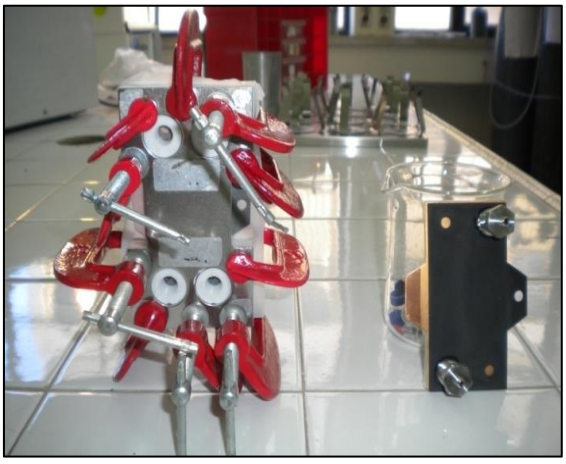

Figure 3.7. *Comparison of two different micro reactors: system I and system II*

3.3.2.3 Micro reactors in series

The possibility given by micro cells of operating in continuous opens to the possibility of using more electrochemical microfluidic reactors in series making also possible an independent choice of the electrodic processes confined in each of them. The adoption of micro reactors in series can allow, from one hand, to increase the productivity of the process (as a result of higher electrode surfaces) and, from the other hand, to work with different operating conditions in the reactors, thus allowing to improve the figures of merit of the process in terms of productivity for both electrochemical processes treatment of wastewater and synthesis of fine chemicals. This system consists in two or three micro reactor in series with an overall area of 8 or 12 cm^2 (fig. 3.8a and 3.8b). The electrodes of the micro reactors were changed dependently of the electrochemical processes.

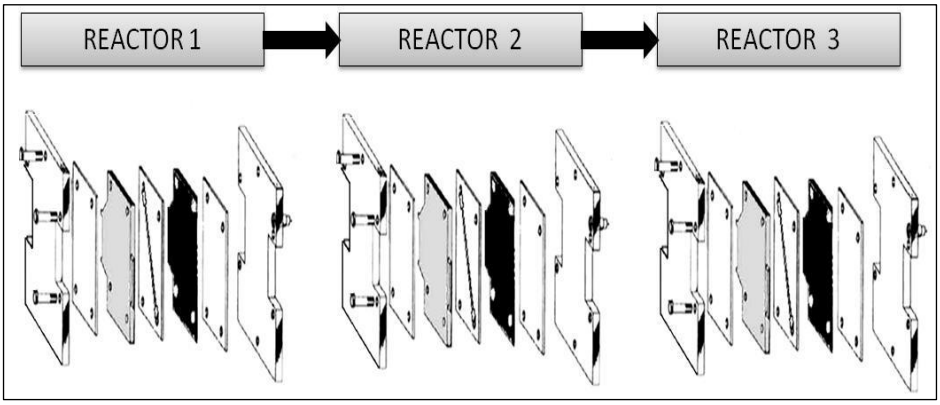

3.8a

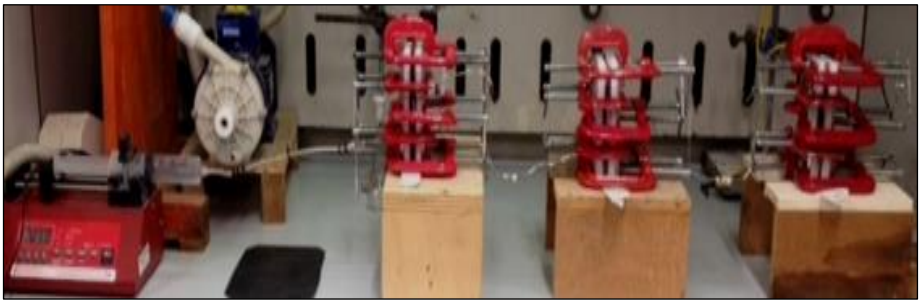

3.8b

Figure3.8 *Schemes and photos of adopted micro-reactors. Fig. 3.8a and 3.8b report a scheme and a photo, respectively, for the utilization of three micro-reactors in series.*

3.3.2.4 Stack of micro reactors

The stack was equipped with two or three electrolytic chambers (electrode area for each chamber 6 cm^2). It was assembled as described in fig. 3.9a and 3.9b and consisted in a commercial undivided filter press flow cell ElectroCell AB with three or four electrodes, dependently on the number of electrolytic chambers. The solutions were passed in series through all the electrolytic chambers. Bi-layer electrodes (ie, both sides are coated with the electrocatalytic material) are used for the central chambers. Different electrodic materials were used in dependence of the process.

3.9a

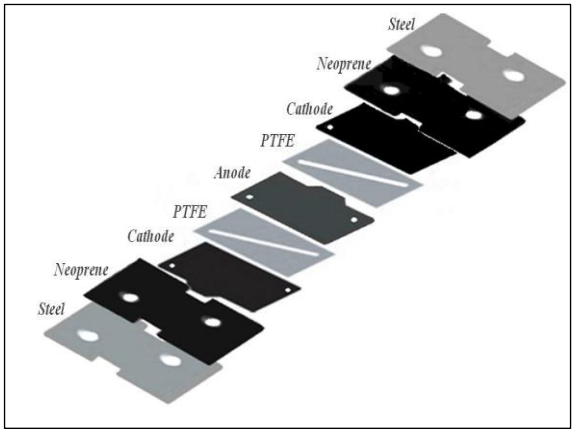

3.9b

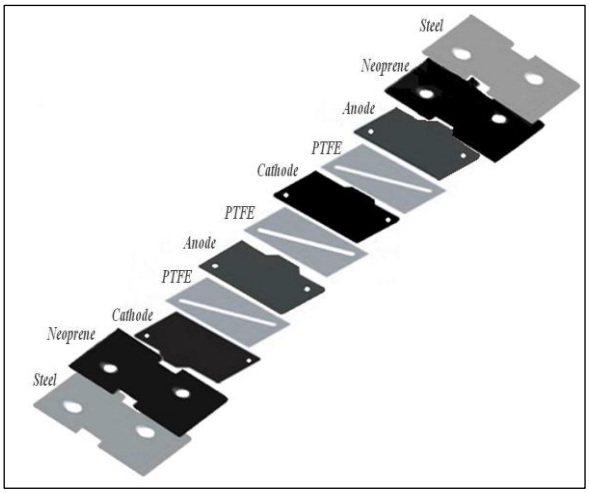

Figure 3.9 *Scheme of the stack a) two chamber (12cm^2); b)three chamber (18cm^2)*

3.3.3 High-pressure reactor

The electro-generation of H_2O_2 and the abatement of the model organic pollutant Acid Orange 7 (AO7) in water by an electro-Fenton process were performed under moderate air pressures. Electrolyses were performed in an undivided high-pressure AISI 316 stainless steel cell (Fig.3.10) with a coaxial cylindrical geometry, equipped with a gas inlet, a $Ti/IrO_2Ta_2O_5$ anode (1.6 cm width, 1cm length and 0.2 cm thickness) from ElectroCell AB, a graphite cathode from Carbon Lorraine (inter electrode gap 3.7 cm) and a magnetic stir bar. Stirring of the electrolytic solution was performed with a magnetic stirrer centering the autoclave in a fixed position and keeping constant the nominal stirring speed at 600 rpm.

Reproducibility of the stirring regime was verified by visual observation of the solution with the open vessel. The cathode was a hollow cylinder (4.9 cm inner

diameter, 0.55 cm thickness, 0.51 cm height, with a lateral wet surface of 40 cm^2) closed at its bottom that was also employed as container of the electrolytic solution. The cathode external diameter was equal to the internal diameter of the steel cell. The cathode was polished with emery paper of decreasing grain size and by ultrasound bath. The high pressure vessel was equipped with a thermocouple for temperature measurement and a pressure gauge. Chromatography grade air was used to pressurize the reactor. A pressure reducer was used to control the operative pressure.

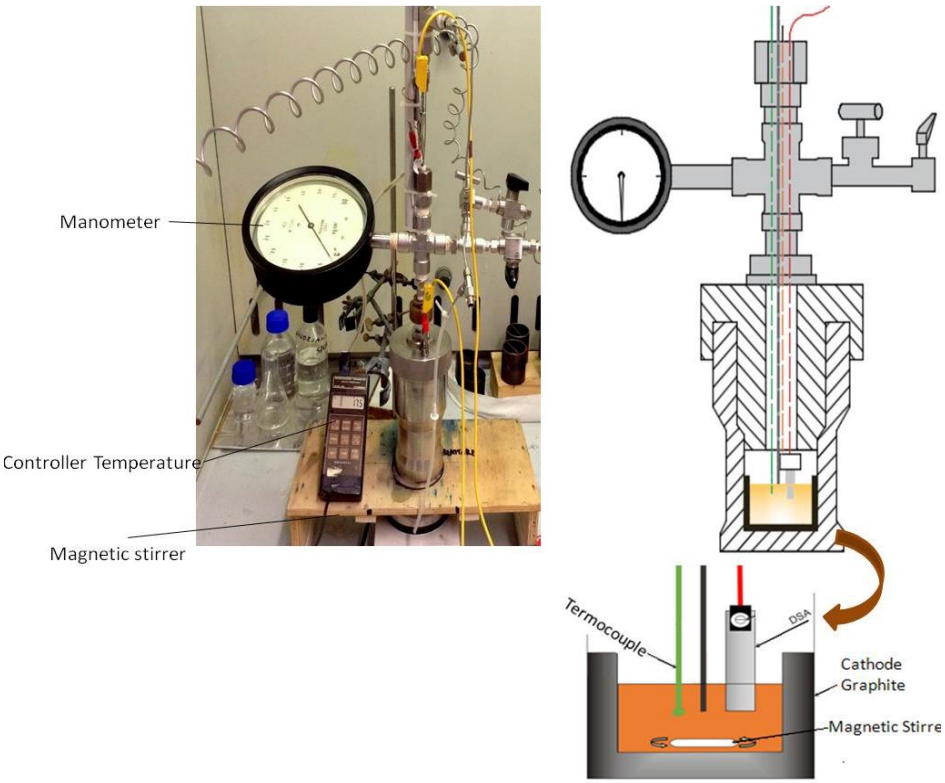

Figure 3.10 *Photo and scheme of high pressure cell.*

The volume of the electrolytic solution was 50 mL. The electrolyses were performed with amperostatic alimentation (Amel 2053 potentiostat/galvanostat) at room temperature. Most of the experiments were repeated at least twice, giving rise to a good reproducibility of results. In most of the experiments, the reactor was opened to collect intermediate samples. After each intermediate sampling, the reactor was closed and brought again to the operative pressure, before activate the electrical current flow.

3.4 Analysis equipments

Samples of the electrolytic solutions were periodically taken and analyzed during the electrolyses, to evaluate the performances of the electrochemical processes, in the different stages of the experiments.

For the electrochemical abatement of AO7 was used different analysis techniques: UV-Vis (Spectrophometric analysis), TOC (Total Organic Carbon) and HPLC (high-performance liquid chromatography) to evaluate the performance of the process.

While for electro synthesis of chloroacetic acid the concentration of the acids was monitored by HPLC.

This section is devoted to give detailed information on the measurement of global parameters well as individual parameters including qualitative and quantitative analysis of the sample of the experiments.

3.4.1 Spectrophometric Analysis

Determination of the concentration of Acid Orange7

The removal of color AO7 was monitored from the decay of the absorbance (A) at λ = 482 nm for AO7 measured by a Cary 60 UV-Vis Agilent Spectrophotometer.

Determination of electrogenerated H_2O_2 by its complex with Ti(IV)

The concentration of H_2O_2 was determined from the light absorption of the Ti(IV)–H_2O_2 colored complex at λ = 409 nm, using $O_5STi•H_2SO_4$ from Fluka.

This method is based on the reaction (1):

$$Ti^{4+} + H_2O_2 + 2\ SO_4^{2-} \rightarrow (TiO_2(SO_4)_2)^{2+} + 2\ H^+ \quad (1)$$

Determination of Fe^{2+}/Fe^{tot} contents by reaction with 1,10-phenantrolin

Ions Fe^{2+} form a red colour complex with 1,10-phenantrolin with λ = 510 nm. The analyses were effectuated by measuring the absorbance for each sample using a Cary 60 UV-Vis Agilent Spectrophotometer. The spectrophotometric calibration curves have been made using ammonium sulfate of iron (II) which is more stable than the respective sulfate.

In order to detect the concentration of iron (II) ions by spectrophotometric analyses, samples were prepared putting 1 mL of phenantrolin + 1 mL of a buffer solution constituted of sodium acetate/ acetic acid + xx mL of H_2O if is necessary to dilute + (4- xx mL) of the sample taken from the electrochemical cell during the experiments or prepared for the calibration curve.

In order to estimate the concentration of total iron (i.e. iron (II) and iron (III)), is necessary to add some ascorbic acid, which by its high reducing power, reduce Fe^{3+} ions to Fe^{2+} and make the ionic form of iron (II) stable. After 30 minutes is possible to analyse these samples.

3.4.2 pH

The pH measurements were carried out with a Crison 2000 pH-meter, calibrated with two buffers of pH 4 and 7 purchased from Panreac for the electro-Fenton experiments and with a HI 8314 membrane pH-meter, calibrated with three buffers of pH 4, 7 and 10 purchased from Hanna for the anodic oxidation experiments.

3.4.3 Chemical oxygen demand (COD)

The trend of some of the oxidative processes was also monitored by measuring the COD. This parameter represents the measurement of the oxygen equivalent to the organic matter contained in a sample that is susceptible to be oxidized by a strong chemical oxidant. The COD value is given in concentration of oxygen (mg O_2 /l) COD has been determined by the potassium dichromate method according to the following reaction (2):

$$C_xH_yO_z + mCr_2O_7^{2-} + 8m\ H^+ \rightarrow xCO_2 + (y+8m)/2\ H_2O + 2m\ Cr^{3+} \quad (2)$$

where $m = (2x/3) + y/6 - z/3$

The oxidation takes place by adding 2 or 3 ml of solution (depending on the range of the concentration of COD) to a Merck vial containing both silver compound as catalyst to oxidize resistant organics and mercuric sulphate to reduce interference from the oxidation of chloride ions by dichromate in sulphuric acid. After reaction of the mixture for 2 h at 148 °C in a thermoreactor (Merck, Spectroquant Thermoreactors TR320) and cooling at room temperature, the COD value was obtained from the spectrophotometric absorbance of Cr^{3+} formed, by a Cary 60 UV-Vis Agilent Spectrophotometer.

3.4.4 Total organic carbon (TOC)

Total Organic Carbon (TOC) analysis of a solution is based on the complete conversion of all carbon atoms present in the sample up to CO_2 and constitutes another global parameter that serves to evaluate the degree of mineralization of a pollutant during its destruction. This technique allows evaluating the degree of mineralization of the starting pollutant during the electrochemical processes. This parameter was monitored on a TOC analyzer Shimadzu VCSN ASI TOC-5000 A.

The TOC value is given in milligrams of carbon per liter (mg l^{-1}), performing the average of three consecutive measurements with a precision of about 2%. The calibration of the equipment was made using potassium hydrogen phtalate standards in the range between 20 and 400 mg l^{-1}.

3.4.5 High-performance liquid chromatography (HPLC)

The degradation of AO7 and of some byproducts was monitored by (HPLC) using a Hewlett Packard 1100 system, equipped with UV-Vis detector, and fitted with a Platinum EPS C18 column 100A 5µ, 4.6mm×250mm, from Alltech, which was thermostated at 25 ◦C. Injection volumes were 30µL. The column was eluted at isocratic mode with a mixture of a buffer solution, containing HK_2PO_4 (99+% ACS reagents, Aldrich) and H_3PO_4 at pH=2.5, methanol (≥99.9% for HPLC, Aldrich), 1-pentanol (ACS reagent, ≥99%, Aldrich), 65:30:5 (v/v) with a flow rate of 1 $mLmin^{-1}$. Detection was performed at 280 nm.

The concentration of carboxylic acids, dichloro acetic acid and monochloro acetic acid were identified and quantified using the same system by a Preavail Organic Acid 5µ column, 4.6mm×250mm, from Grace with a 100% of the same buffer solution. The detection was performed at 210 nm with a flow rate of 1 mL min^{-1}. Calibration curves were obtained by using the pure standards of the related carboxylic acids.

The eventual presence of chlorinated products was evaluated by HPLC/MS thermo TSQ Quantum Access, Type ESI, negative Polarity Q1 MS, fitted with a Zic-Hilic column 5µ, 2.1mm×150mm, from Merck. The column was eluted with a mixture of a buffer solution, containing CH_3CN (99+% ACS reagents, Fluka) and 10 mM of Ammonium Acetate (99+% ACS reagents, Aldrich) at pH=5, 90:10 (v/v).

3.5 Global Electrochemical parameters

3.5.1 Electrochemical Abatement of Acid Orange 7

The color remove the abatement (e.g., the conversion) of the Total Organic Carbon X_{TOC} and the current efficiency CE for a macro and a micro cell were defined by Eqs. (1)(2) (3) and (4), respectively [2-5]:

$$Color\ removal = 100\times (A^0 - A^f)/A^0 \quad (1)$$

$$X_{COD}\,(\%) = 100\times (\Delta COD)_t / COD^0 \quad (2)$$

$$X_{TOC}\,(\%) = 100\times (\Delta TOC)_t / TOC^0 = \quad (3)$$

$$CE = 100\times nFVC^0X_{TOC}/(It) = \quad (4)$$

where A° and A are the absorbance at initial time and time t at λ = 482 nm, $(\Delta COD)_t$ and $(\Delta TOC)_t$ are respectively the decay of the COD and TOC ($mg_{carbon}\ L^{-1}$), COD^0, TOC^0 and C^0 are the initial concentrations of Chemical Oxygen Demand, Total Organic Carbon ($mg_{carbon}\ L^{-1}$) and of the Acid Orange 7 (mol L^{-1}), respectively, inside the electrochemical cell, n is the number of electrons exchanged for the oxidation of the organic pollutant to carbon dioxide, F the Faraday constant (96487 C mol^{-1}), I the applied current intensity, t the average residence time of the solution in the cell (s), V the volume of the cell (L).

The energy consumption EC (KWh g_{TOC}^{-1}) for the abatement of TOC was defined by Eq. (5)

$$EC = E_{cell}\, I\, t\, /(\Delta TOC)_t\, V \quad (5)$$

where E_{cell} is the potential difference of the cell (V), I the current intensity (A) and t the time of electrolysis (h).

3.5.2 Electro synthesis of chloroacetic acid

The conversion of dichloroacetic acid to monochloroacetic X_{DCAA}, the yield Y, the current efficiency CE and the productivity P (mmol h^{-1}) were defined by Eqs.(6) (7) (8) and (9) respectively:

$$X_{DCAA}(\%) = 100\times (C_{DCAA}^{i} - C_{DCAA}^{f})_t / C_{DCAA}^{i} = \quad (6)$$

$$Y(\%) = 100\times C_{MCAA}^{i} / C_{DCAA}^{i} \quad (7)$$

$$CE = 100\times nFV\, C_{DCAA}^{i}\, Y/(It) = \quad (8)$$

$$P = (60/100)\times Y\, C_{DCAA}^{i}\, V/t \quad (9)$$

where C_{DCAA}^{i} and C_{DCAA}^{f} are the initial and final concentration of dichloroacetic acid (DCAA) respectively, C_{MCAA}^{i} the initial concentration chloroacetic acid (MCAA) inside the electrochemical cell, n is the number of electrons exchanged for the reduction of dichloroacetic acid, F the Faraday constant (96487 C mol^{-1}), I the applied current intensity, t the average residence time of the solution in the cell (s), V the volume of the cell (L).

References

[1] C.A. Martinez-Huitle, S. Ferro, A. De Battisti, J. Appl. Electrochem. 35 (2005)1087–1093.

[2] S. Garcia-Segura, F. Centellas, C. Arias, J.A. Garrido, R.M. Rodriguez, P.L. Cabot,E. Brillas, Electrochim. Acta 58 (2011) 303–311.

[3] O. Scialdone, C. Guarisco, A. Galia, G. Filardo, G. Silvestri, C. Amatore, C. Sella, L.Thouin, J. Electroanal. Chem. 638 (2010) 293.

[4] O. Scialdone, A. Galia, C. Guarisco, Electrochim. Acta 58 (2011) 463–473.

[5] O. Scialdone, A. Galia, S. Sabatino, Electrochem. Commun. 26 (2013)45–47.

CHAPTER 4

4. ABATEMENT OF ACID ORANGE 7 IN MACRO AND MICRO REACTORS: EFFECT OF THE ELECTRO-CATALYTIC ROUTE

4.1. Introduction

As described in detail in the previous chapters, the removal of organic pollutants resistant to conventional biological processes from water often requires the adoption of advanced oxidation processes (AOPs). These processes involve chemical, photochemical or electrochemical techniques to allow chemical degradation of organic pollutants. Electrochemical methods are considered to be among the more efficient AOPs and can offer new sustainable routes for the abatement of toxic and bio-refractory organic pollutants. Worth mentioned these methods use a clean reagent, the electron, and mild operative conditions with limited operative costs. However, electrochemical processes present some important disadvantages when performed in conventional reactors. In particular, to achieve reasonable cell potentials when the medium has not an adequate conductivity, one needs adding to the system a supporting electrolyte. This is certainly a main obstacle for a wide application of electrochemical tools. Indeed, adding chemicals is often a problematic issue, since this may lead to the formation of secondary products, makes more difficult the separation procedures and increases the operative costs. As explained in the chapter …, it has been demonstrated that microfluidic reactors can improve the electrochemical processes for the treatment of wastewaters contaminated by recalcitrant pollutants [1-4].

In this chapter, the treatment of water contaminated by a model organic pollutant, the Acid Orange 7 (AO7) was studied, by different electrochemical procedures:

- Direct electrochemical oxidation (EO) with different anodes;
- Indirect electro-oxidation with active chlorine (IOAC);
- Electro-Fenton (EF).

These processes, used alone or in a combined way, were widely and systematically studied to evaluate as the electro catalytic route affects the degradation process.

The azo dye Acid Orange 7 (AO7), also called Orange II (Figure 4.1), was often chosen as model compound to evaluate promising approaches because, being a simple molecule, it is very useful as test and since it is widely used in paperboard industries, for coloration, and in wool textile dyeing.

The electrochemical oxidation of aqueous solutions of AO7 was previously investigated by various authors [4-10]. Fernandes et al. studied the electrochemical oxidation at BDD anodes both in the absence and in the presence of chlorides. An almost complete colour removal and very high COD removal were obtained. In the presence of KCl a faster colour removal was achieved as a consequence of active chlorine formation [4]. A detailed study on the effect of the supporting electrolyte on the oxidation of AO7 at BDD anode was carried out by Zhang and co-authors [6]. Hernandez et al. compared the performances of hydrogen peroxide based processes (direct photolysis, electro-Fenton process and photoelectro-Fenton process) [7]. Electro-Fenton process (EF) was, in particular, studied in detail by various authors [7-10]. Segura et al. [10] studied the abatement of monoazo, diazo and triazo dyes by EF in the presence of a gas diffusion cathode and a BDD anode. According to the literature, the performances of the electrochemical treatment of dyes are likely to strongly depend on the adopted electro-catalytic route [2].

Here, the effect of various operating parameters, such as the initial concentration of the AO7, the flow rate and the current density, was also investigated in detail. Both conventional cells and microfluidic apparatus (described in chapter 3) were used in order to select more effective electrochemical conditions for the treatment of such compound.

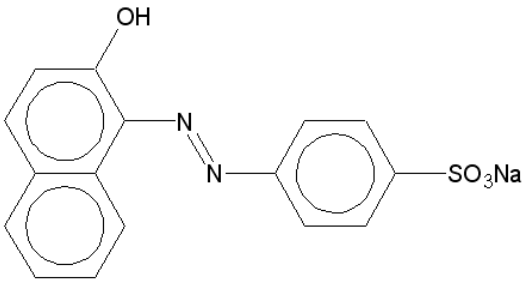

Figure 4.1 *Chemical structure of Acid orange 7*

4.2 Direct electrochemical oxidation

The direct anodic oxidation of organic pollutants (EO) has been extensively investigated in the last years. It was shown that EO can present higher abatements with limited costs with respect to ozonation and Fenton oxidation processes [17]. The performances of the process in terms of complete mineralization of organic pollutant and current efficiency depends dramatically on the nature of the anode [18,19]. The direct electrochemical oxidation of AO7 was performed in conventional cells equipped with magnetic stirring (as described in paragraph 3.3.1) and in micro reactors with a distance between the electrodes of about 50 µm (as described in paragraph 3.3.2.1). BDD and Ti/IrO_2-Ta_2O_5 were used as anodes. In both cases, the process was performed at high anodic potentials necessary to allow the oxidation of water, thus maintaining the anode activity. As shown in figure 4.2, a drastically higher color removal was obtained at BDD anodes with respect to that achieved at iridium based anode.

This is due to the fact that at BDD, very reactive free or loosely adsorbed hydroxyl radicals are formed (Eq. (1)) which have a strong oxidation power.

In the presence of low organic concentrations as usually occurs with the treatment of pollutants, the oxidation at BDD occurs under the kinetic control of the mass transfer of the pollutant to the anode surface [21].

4.2a

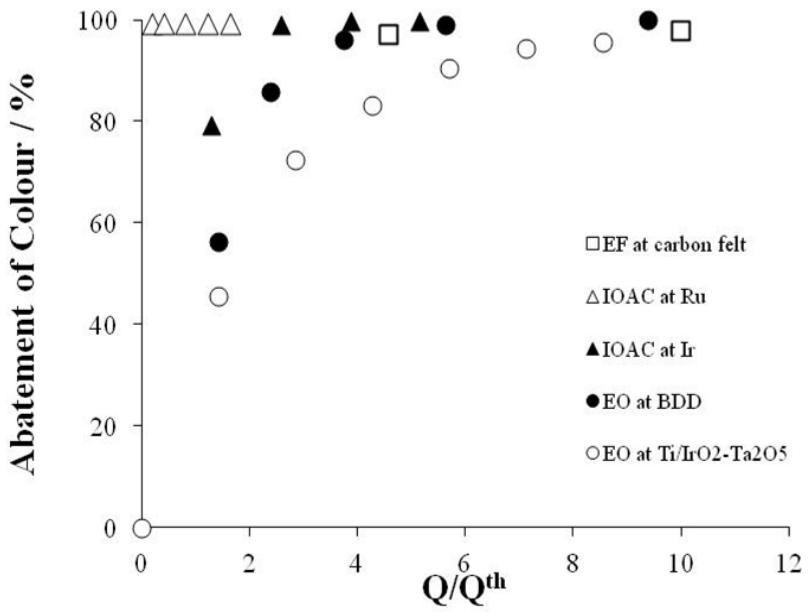
Abatement of Colour / %
Q/Q^th
EF at carbon felt
IOAC at Ru
IOAC at Ir
EO at BDD
EO at Ti/IrO2-Ta2O5

4.2b

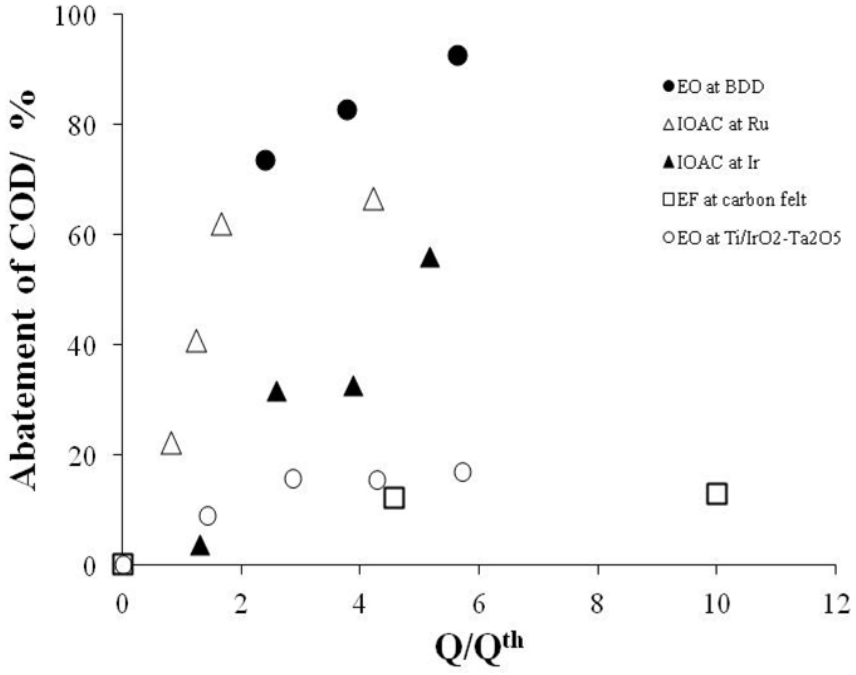
Abatement of COD/ %
Q/Q^th
EO at BDD
IOAC at Ru
IOAC at Ir
EF at carbon felt
EO at Ti/IrO2-Ta2O5

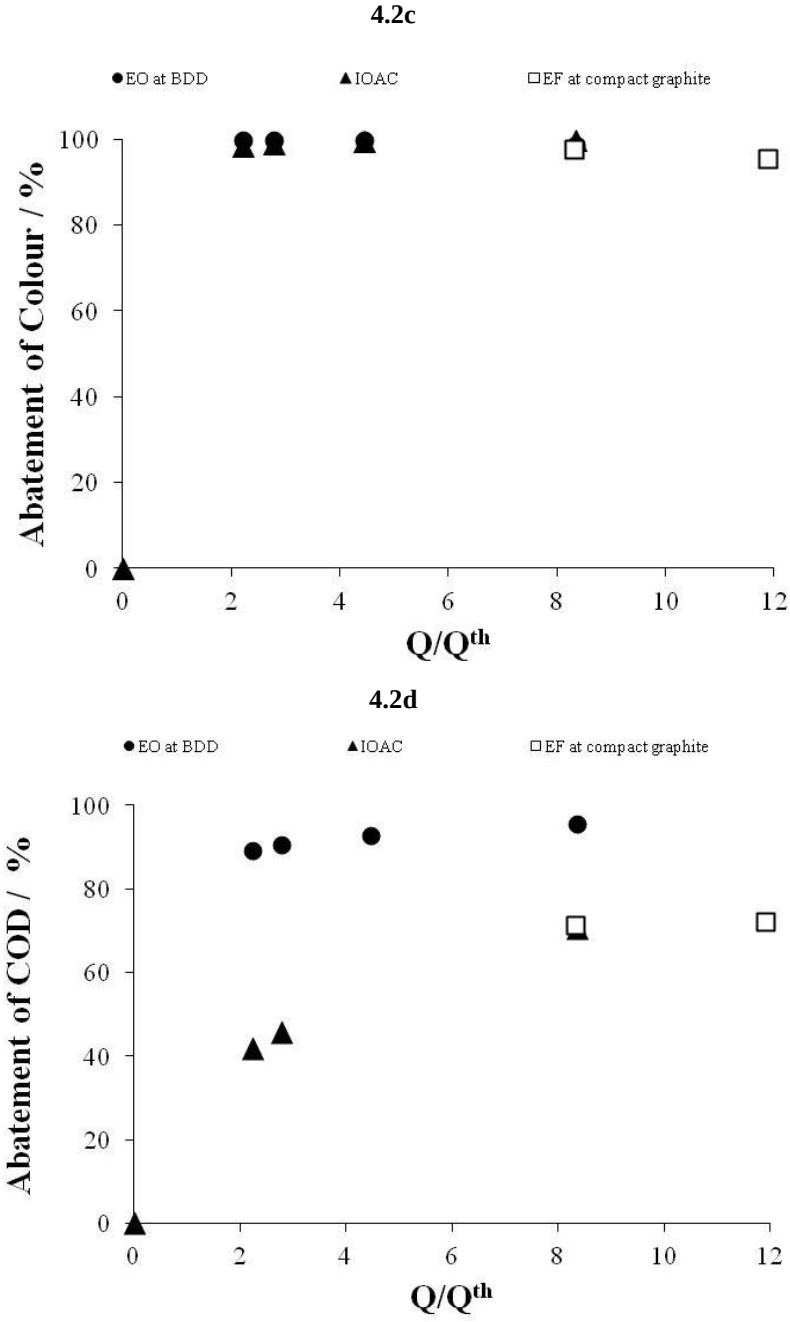

Figure 4.2 *Plot of colour (Figures 4.2a and 4.2c) and COD abatement (Figures4.2b and 4.2d) vs. dimensionless passed charge (the ratio charge passed/theoretical charge) Q/Q^{th} for*

the electrochemical treatment of a water solution of AO7 in a conventional (Figures 2a and 2b) and micro cell (Figures 4.2c and 4.2d). The electrochemical oxidation was performed by direct anodic oxidation at Ti/IrO_2-Ta_2O_5 (o) and BDD anode (●), indirect oxidation by means of electrogenerated active chlorine at Ti/IrO_2-Ta_2O_5 (▲) and Ti/RuO_2-IrO_2 (Δ) anode with 17 mM of NaCl and Electro-Fenton (□). Current density: 20 A/m^2 for electro-Fenton in micro device, 100A/m^2 for other experiments. Room temperature. Initial AO7 concentration 0.43 mM. Na_2SO_4 (0.035 M) was used as supporting electrolyte for experiments carried out in the macro device. $FeSO_4$ (0.5 mM) was used as catalyst for EF processes. Cathode for EO and indirect oxidation by active chlorine: nickel. Cathode for electro-Fenton: carbon felt for conventional cell and compact graphite for micro device. Anode for electro-Fenton: Ti/IrO_2-Ta_2O_5. Nominal distance between the electrodes in the micro reactor 50 μm. Flow rate in the micro reactor: 0.1- 0.4 ml/min. Theoretical charge Q^{th} is the charge necessary to mineralize all the initial COD with a process with a current efficiency of 100 %.

Under adopted operative conditions, the applied current density i was higher than the limiting current density expected for a process under a mass transfer control $i_{lim} = nk_mC_{AO7}$ (where n is the number of electrons necessary for the oxidation of the pollutant to carbon dioxide and k_m and C_{AO7} are the mass transfer coefficient and the bulk concentration of AO7) for almost all the process (initial i_{lim} = 55 A/m^2 < i = 100 A/m^2) and, as shown in figure 4.3.a, the abatement of COD at the BDD anode was very similar to that theoretically expected for a process under mass transfer kinetic control [12,21-22]. The lower abatement achieved at iridium based anodes is due to the fact that the oxidation of water results in the formation of chemisorbed oxygen (Equations (2)-(3)) that have a less oxidation power and that gives rise more easily to the competitive oxygen evolution (Eq. (4)) [12,22-23].

$$BDD + H_2O \rightarrow BDD(^{\bullet}OH) + H^+ + e^- \quad (1)$$

$$MO_x + H_2O \rightarrow MO_x(^{\bullet}OH) + H^+ + e^- \quad (2)$$

$$MO_x(^{\bullet}OH) \rightarrow MO_{x+1} + H^+ + e^- \quad (3)$$

$$MO_{x+1} \rightarrow MO_x + 0.5\ O_2 \quad (4)$$

According to above considerations, the performances of the process at BDD anode are expected to depend mainly on the flowdynamic conditions. Hence,

experiments were repeated in a micro reactor that offers the advantage of fast mass transport kinetics, lower cell potentials and the possibility of working in the absence of supporting electrolytes also in water solutions with low conductivity as it can happen for discharged waters from textile dyeing industry [15].

4.3a

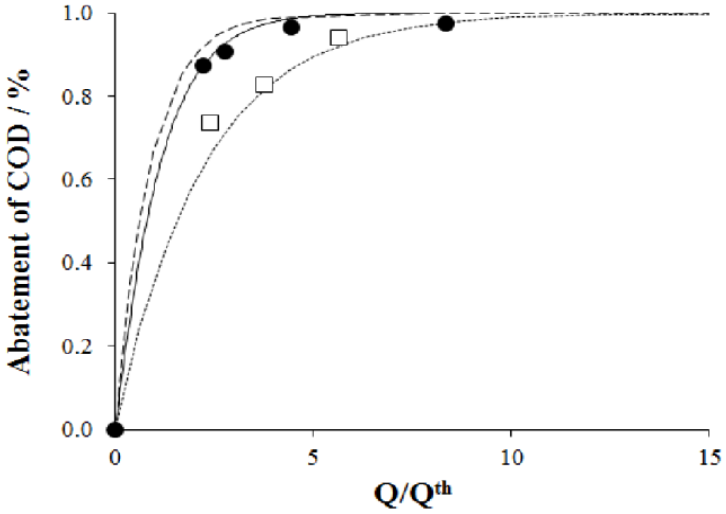

4.3b

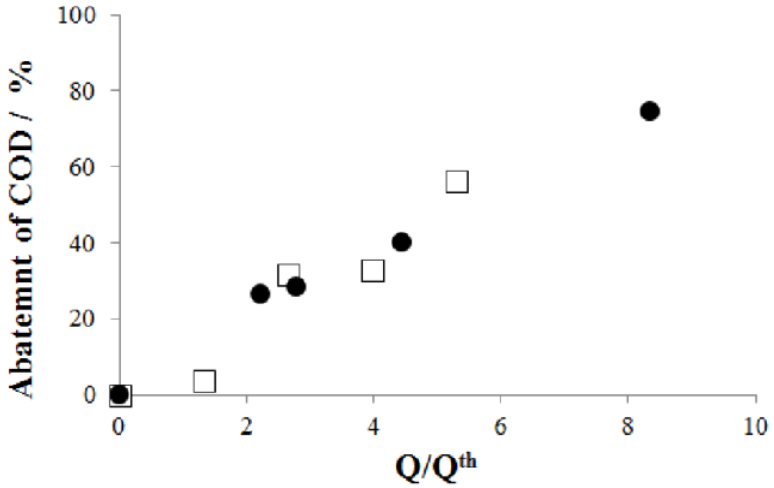

Figure 4.3 *Trend of Abatement of COD vs. Q/Q^{th} for the electrochemical oxidation of AO7 by direct oxidation at BDD (a), electrogenerated active chlorine at Ti/IrO_2-Ta_2O_5 with 17mM of*

NaCl (b) in conventional cell (□) and in the micro reactor (●) at 100 A/m^2 and room temperature. Initial AO7 concentration 0.43 mM. Na_2SO_4 (0.035 M) was used as supporting electrolyte for experiments carried out in the macro device. Cathode: Nickel. Nominal distance between the electrodes in the micro reactor 50 µm. Flow rate in the micro reactor : 0.1- 0.4 ml/min. a) reports also the theoretical predictions for a process under mass transfer control in a conventional cell (...) and in a microfluidic reactor (--) and for a process under a mixed kinetic regime in a micro fluidic reactor (—) computed according to literature [12].

Higher abatements were achieved in the micro cell for the same amount of charge passed, as a result of the fast mass transport, with respect to that recorded in the conventional cell (Figure 4.3.a). Increasing the flow rate (i.e., lowering the treatment time), one has lower abatements (Figure 4.4) but higher current efficiencies and productivity of the cell. In this perspective, the flow rate and as a consequence the productivity of the cell can be properly selected for each target abatement for a given geometry of the microcell.

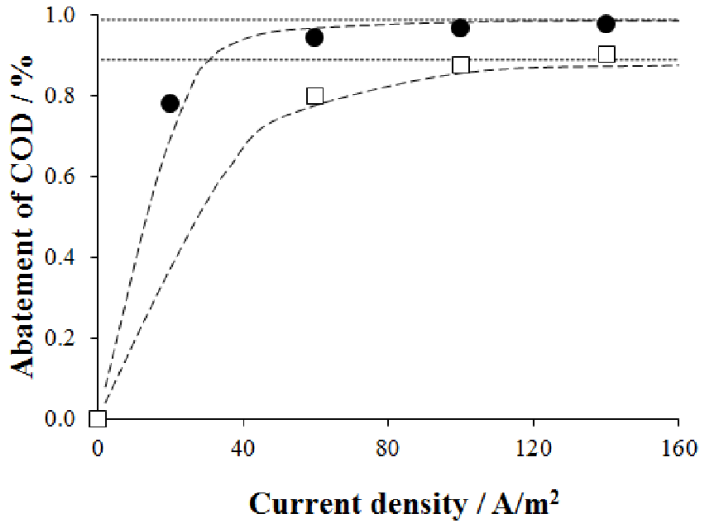

Figure 4.4 *Direct electrochemical oxidation of AO7 at BDD anode in the micro reactor. Effect of current density on the abatement of COD at 0.2 (●) and 0.4 (□) ml/min. Nominal distance between the electrodes 50 µm. Initial AO7 concentration 0.43 mM. Cathode: nickel. Theoretical curves are the predictions for a process under mass transfer control (...) and under mixed kinetic regime (--) computed according to literature [12].*

Higher current efficiencies but lower abatements can be obtained also reducing the current density (Figure 4.4).

In this case the process is no longer under a pure kinetic control of the mass transport of the organics to the anode surface and a more complete theoretical model has to be adopted to describe the experimental results [12].

As shown in figures 4.3 and 4.4, data were well fitted by theoretical predictions. The model involves a fitting parameter named [*RH*]* that is defined as the concentration of the organic which gives a current efficiency of 50% in the absence of mass transfer limitations, e.g., the concentration of the organic *RH* at the anode surface $[RH]_x^{y=0}$ which gives a current density for the *RH* mineralization equal to the current density involved for the oxygen evolution reaction [12]. Of course, the higher is the value of [*RH*]* more favored is the oxygen evolution while the lower is [*RH*]* more favored is the mineralization of the organic.

Hence, the fitted value of [*RH*]* can be used to evaluate the mineralization power of an anode for a selected organic pollutant. In our case a fitting value of [*RH*]* of about 3 x 10^{-2} mM was obtained which confirms that BDD anodes are very suitable for the mineralization of AO7.

HPLC analyses showed that the abatement of AO7 gave rise to the formation of very few by-products (namely, oxalic and formic acids) that were however mineralized at longer times. Indeed, it has been shown in literature that carboxylic acids such as oxalic, formic and maleic acids are usually the main intermediates formed during the oxidation at BDD anodes of more complex substrates such as aromatic ones [40].

4.3 Oxidation by electro-generated active chlorine

Aqueous solutions of organic pollutants can be decontaminated by indirect oxidation with electro-generated active chlorine (IOAC), where anodic oxidation of chloride ions leads to the formation of free chlorine, hypochlorous acid and/or hypochlorite, depending on the pH (Eqs. (5-7)), that can oxidize the organics near to the anode or/and in the bulk of the solution (Eq. (8) in alkaline medium) [24-26].

$$2\,Cl^- = Cl_2 + 2e^- \quad (5)$$

$$Cl_2 + H_2O = HOCl + H^+ + Cl^- \quad (6)$$

$$HOCl = H^+ + OCl^- \quad (7)$$

$$Organics + OCl^- \rightarrow intermediates \rightarrow CO_2 + Cl^- + H_2O \quad (8)$$

These reactions take place in competition with oxygen evolution, chlorate chemical and electrochemical formation and cathode reduction of oxidants in the presence of undivided cells [25-28]. To account for some experimental results and in particular for the different distribution of byproducts observed in the electrochemical treatment in the presence of Cl^- and in the chemical oxidation with NaClO [25,29], some authors have suggested that an important role can be played also by surface electrochemical reactions. In particular, it has been proposed [29-30] that adsorbed chloro- and oxychloro-radicals could be involved in the oxidation mechanism (see as an example Eqs. (9-10) for the oxychlroradicals).

$$MO_x(OH) + Cl^- \rightarrow MO_x(HOCl) + e^- \quad (9)$$

$$Org.+MO_x(HOCl) \rightarrow interm.\rightarrow MO_x+CO_2+Cl^-+H_2O+H^+ \quad (10)$$

This method allows to avoid the transport and storage of dangerous chlorine, gives faster destruction of organic matter and lower costs than in chemical oxidation. On the other hand, the formation of undesirable toxic chloro-organic derivatives such as

chloroform and of chlorine–oxygen by-products such as ClO_2, ClO_3 and ClO_4 can occur. The electrochemical oxidation of numerous dyes with active chlorine in aqueous solutions was studied by various authors [2]. DSA-type anodes (metal oxides supported on Ti) were mainly used due to the high generation of active chlorine expected at these anodes [24,31]. BDD anodes are often not used in the presence of high concentrations of chlorides due to their low efficacy for the conversion of chlorides to active chlorine [24] and for the possible generation of chlorates and perchlorates [32-34]. In the presence of DSA, high color removal was always observed while the removal of COD strongly depended on the investigated system [2]. However, data are available in literature on the utilization of IOAC for the treatment of aqueous solutions of AO7 were mainly based on the utilization of a BDD anode [4]. To evaluate the electrochemical oxidation of AO7 with active chlorine, first experiments were here carried out at Ti/IrO_2-Ta_2O_5 and Ti/RuO_2-IrO_2 anodes that are characterized by a quite low overpotential for oxygen and chlorine, respectively, in the presence of 17 mM of NaCl. Thus, Ir and Ru based anodes gives very low removal of the color by direct EO but high current efficiency for the oxidation of chloride ion to active chlorine (data not shown and reference [24]). A very high abatement of color (Figure 4.2a) and AO7 was achieved at both electrodes, thus showing that active chlorine can be effectively used to oxidize this azoic dye and to remove the color or the solution. A slower abatement of COD occurred (Figure 4.2b). In particular an higher abatement of COD was obtained at Ruthenium based electrodes as a result of the fact that this electrode is expected to generate an higher amount of active chlorine [24]. On the other hand, a less removal of COD was observed in the experiments performed with electro-generated active chlorine with respect to EO at BDD anode (Figure 4.2b). Furthermore, the formation of a colored precipitate was observed during the electrolysis carried out at Iridium based anodes. Hence, it is possible to conclude that electrogenerated active chlorine is very active for the oxidation of AO7 and for de-colorization purposes but less for its mineralization due to the formation of organic intermediates that present a higher resistance to the oxidation by means of active chlorine. In particular, as mentioned in detail in the following, numerous byproducts were detected, the main relevant

being hydroquinone and oxalic, lactic and malonic acids. No chlorinated hydrocarbons were however detected. The latter is a very relevant point since the possible formation of chlorinated organic is considered the main disadvantage given by IOAC processes.

A second series of experiments was carried out in microfluidic devices. It was the first study devoted to the utilization of electro generated active chlorine for the abatement of organic pollutants in water in microfluidic devices. Very similar abatements of both color and COD (Figure 4.3b) were obtained in conventional cells and in microfluidic reactors, thus showing that the oxidation process takes place mainly in the bulk of the solution and that eventual surface processes (as that reported in Eqn.s (9) – (10)) are not limited by mass transfer kinetics.

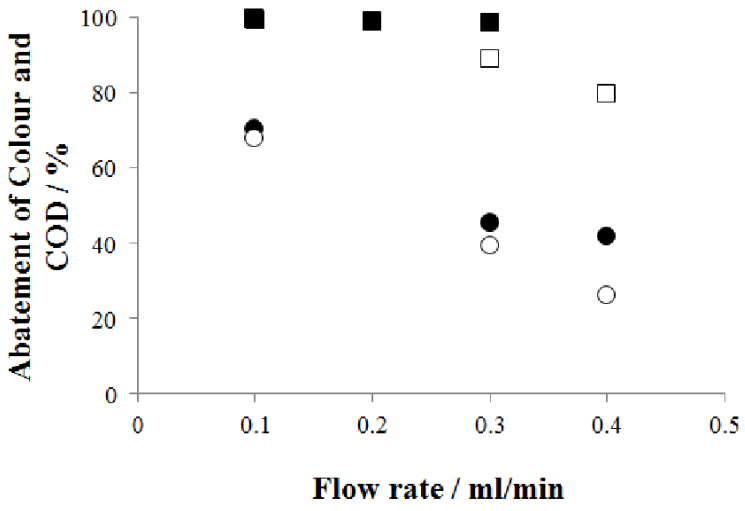

Figure 4.5 *Oxidation of AO7 by electrogenerated active chlorine in the micro reactor. Effect of flow rate on the abatement of colour (□ 60, ■ 100 A/m^2) and COD (○ 60, ● 100 A/m^2). Nominal distance between the electrodes 50 µm. Initial AO7 concentration 0.43 mM. Anode: Ti/IrO$_2$-Ta$_2$O$_5$. Cathode: nickel. Initial concentration of NaCl 17mM.*

To evaluate the effect of residence time and current density on the performances of the process, a series of experiments was performed in the micro-fluidic cell by changing both the current density and the flow rate. As shown in Figure 4.5, the abatement of both color and COD decreased with the flow rate (e.g., lowering the residence time) and increased with the current density. According with the literature, the increase in the current density results in higher bulk concentrations of active chlorine that allow an higher abatement of COD for the same time of contact (e.g., for the same flow rate). Quite interestingly, a drastic effect of current density was observed for the higher values of the flow rate while similar abatements were observed by changing the current density for experiments performed at 0.1 ml/min. This should indicate that for high enough residence times, the concentration of active chlorine is no longer the limiting factor for the abatement of COD.

4.4 Oxidation by Electro-Fenton process

As above mentioned in the paragraph 2.2.4.2 in Chapter 2, the Electro-Fenton process (EF) is based on the electro-generation of hydrogen peroxide in aqueous solution by two-electron reduction of dissolved oxygen (eq. (11)) on a cathode such as mercury pool, compact graphite, carbon felt, activated carbon fiber and carbon-polytetrafluoroethylene-O_2 diffusion cathode (ADE) [2,35]:

$$O_2 + 2H^+ + 2e^- \rightarrow H_2O_2 \qquad (11)$$

$$H_2O_2 + Fe^{2+} \rightarrow Fe^{3+} + OH^{\bullet} + OH^- \qquad (12)$$

The oxidizing power of H_2O_2 is enhanced in the presence of Fe^{2+} via classical Fenton's reaction (Eq. (12)) which leads to the production of hydroxyl radicals. Reaction (12) is propagated through the continuous electro-generation of Fe^{2+} by cathode reduction of Fe^{3+} formed by reaction (12).

$$Fe^{3+} + e^- \rightarrow Fe^{2+} \quad (13)$$

The abatement of AO7 in water by EF processes was studied by vary authors [7-10]. According to literature [10], the addition of 5 mmol dm^{-3} H_2O_2 to AO7 solution did not cause a relevant removal of color. The color removal at ADE was very poor in the absence of iron but quite quick in the presence of 0.5 mM Fe^{2+} [10]. Ozcan and co-authors studied the EF process at carbon felt cathodes [8]. Identification of main intermediates was achieved, thus allowing to propose a plausible mineralization pathway [8]. Malonic, formic, acetic and glioxylic acids and various aromatic products such as hydroquinone, 1,2-naphtaquinone, 4-amminiphenol and 4-amminobenzenesulphonic acid were found as by-products [8].

Since the EF treatment is based on the H_2O_2 electro-generation for the •OH production from Fenton's reaction, a first trial of experiments was carried out to evaluate the production of H_2O_2 in adopted systems. Figure 4.6 shows the time course of this species during the electrolysis of water solutions in the absence of Fe^{2+} and organics at compact graphite and ADE cathodes in conventional cells (as described in paragraph 3.3.1). In all cases H_2O_2 was gradually accumulated during the first 240 min, reaching a steady value that depended dramatically on adopted electrode. Hydrogen peroxide is consumed by electrochemical reduction at the cathode surface, disproportion in the bulk and, for undivided cells that are often used to avoid the voltage penalty of the separator, oxidation to oxygen at the anode (Eq. 14) [36]. Consequently the accumulation of H_2O_2 is lower than its electro-generation.

$$H_2O_2 \rightarrow O_2 + 2H^+ + 2e^- \quad (14)$$

At both graphite (Figure 4.6) and carbon felt, according to literature [9,38], a steady value lower than 1 mM was reached as a result of the low solubility of oxygen in water (about 40 or 8 mg L^{-1} at 1 atm and 25 °C for pure oxygen or air, respectively, [36]) that imposes a slow mass transfer of oxygen to the cathode

surface (see theoretical predictions in Figure 4.6). In the case of the ADE, according to literature very high steady values slightly lower than 100 mM were observed as a result of the dramatic enhancement of kinetics of the cathode process which no longer suffers from mass transfer limitations in the liquid phase [37]. When experiments were repeated at ADE cathode in the presence of iron (II) a lower concentration of hydrogen peroxide was detected as a result of the reaction between Fe(II) and H_2O_2 (Eq. (12)).

The generation of hydrogen peroxide in a micro cell equipped with a graphite electrode in the absence of added air was also studied in our laboratory (Figure 4.6b). At the best adopted operative conditions (i close to 20 - 60 A/m^2, inter-electrodic distance h = 120 μm), the reduction of electro-generated oxygen in the microdevice gave rise to a concentration of H_2O_2 of about 6 mM, one order of magnitude higher than that achieved in conventional cells equipped with the same graphite cathode.

4.6a

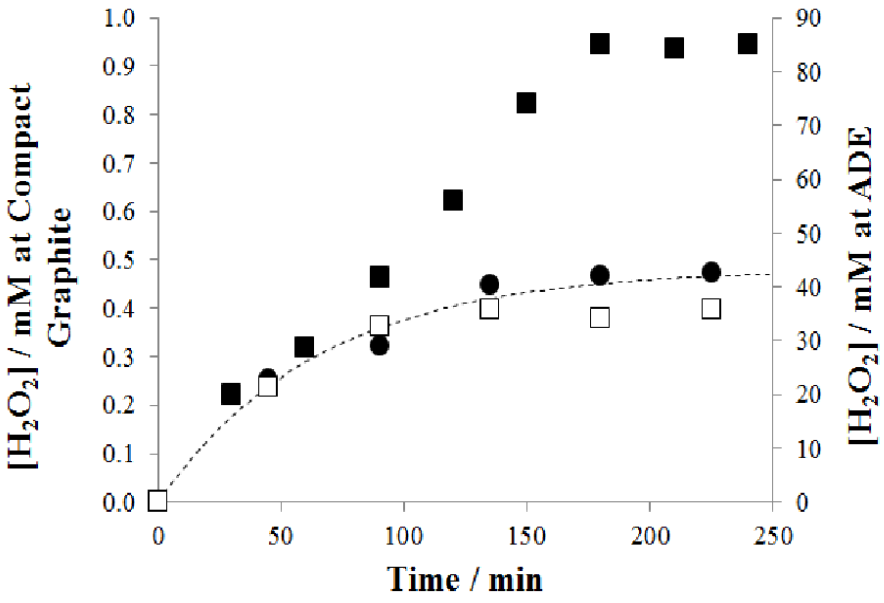

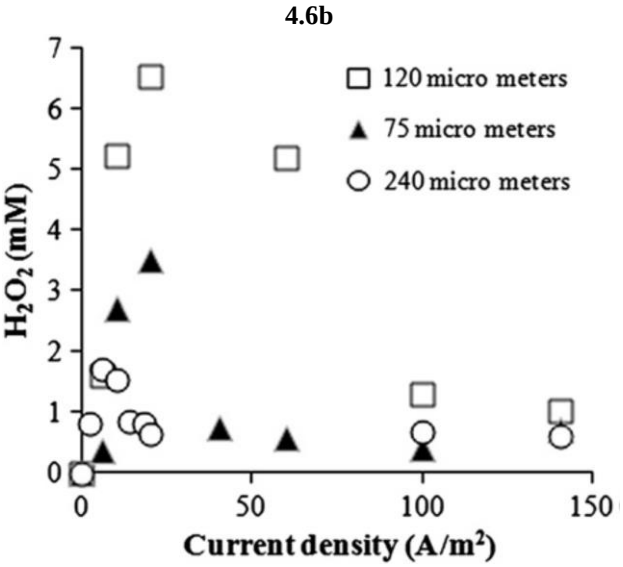

Figure 4.6 *a) Evolution of the concentration of H_2O_2 accumulated during the electrolysis of 50mL of 35mM Na_2SO_4 solutions of pH 3.0 at 25 °C using a conventional undivided tank glass cell equipped with graphite (●) or ADE (■) cathode and a Ti/IrO_2-Ta_2O_5 anode at 500 A/m^2. Some experiments were repeated with Fe(SO_4) (0.5 mM) at ADE cathode (□).Theoretical curve are the predictions for a process of reduction of oxygen to hydrogen peroxide under kinetic mass transfer control (…). b)Concentration of H_2O_2 achieved by the electrolysis of a water solution of pH 3.0 at 25 °C using a microreactor equipped with graphite cathode at various current densities and h of 75 (▲), 120 (□) and 240 (○) µm.*

When electrolyses were performed with both Fe(II) and AO7, the abatement of color was quite fast and similar at all adopted electrodes (carbon felt, compact graphite, ADE) both in conventional and microfluidic cell (Figure 4.7a) even if not complete. On the other hand, the abatement of TOC (Figure 4.7b) depended strongly on both adopted cathode and electrochemical cell.

Higher abatements of TOC were achieved at ADE and lower ones at compact graphite in conventional cell, as a result of the low generation of hydrogen peroxide recorded on this electrode.

The utilization of microfluidic cell equipped with compact graphite allowed to increase dramatically the abatement of TOC (Figure 4.7b) and AO7 (Figure 4.8e) with respect to that achieved in the conventional cell equipped with the same

graphite cathode. The higher abatement of TOC and AO7 achieved in the micro reactor is likely to be due to the ability of micro device to generate high amounts of H_2O_2, thus accelerating the formation of HO● and consequently the oxidation of organics. Furthermore, in macro cell a supporting electrolyte was necessarily added to the system, thus resulting in the formation of catalytic complexes with ferrous ions with lower catalytic activity [9], while in the microfluidic devices experiments were carried out in the absence of supporting electrolyte.

To evaluate the effect of iron concentration and current density on the performances of the process, a series of experiments was performed in the micro-fluidic cell with a nominal inter electrode gap of 120 μm by changing both the current density (in the range 10 – 800 A/m^2) and the concentration of Fe(II). Very similar color and COD removal were achieved at all adopted Fe(II) concentrations (0.25, 0.5, 0.75, 1 mM). Higher abatements were achieved between 20 and 40 A/m^2.

4.7a

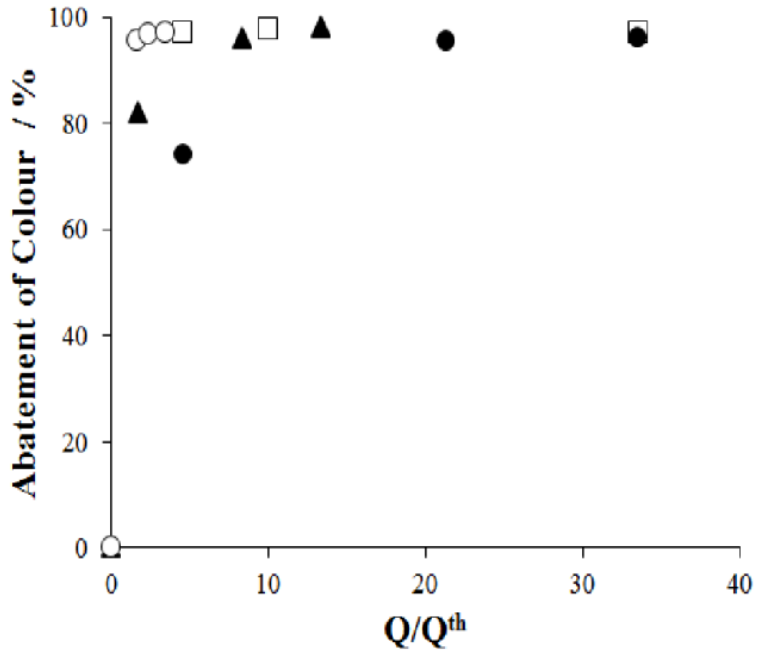

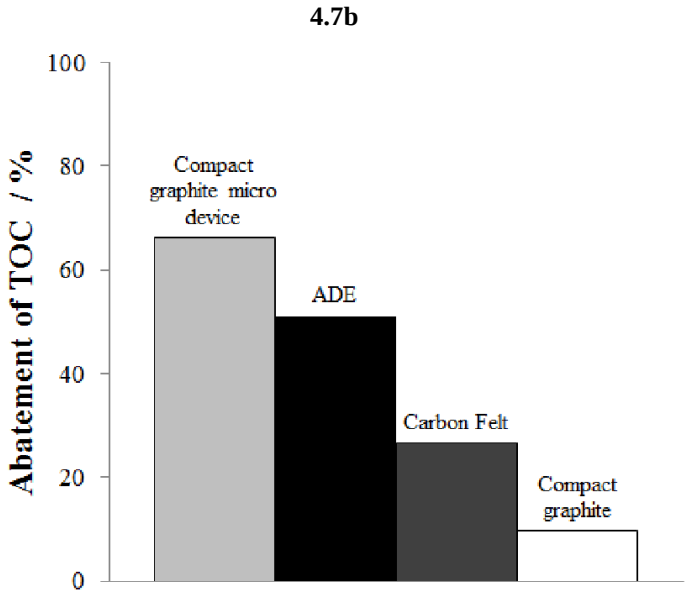

Figure 4.7 *Abatement of colour vs. Q/Q^{th} (a) for a solution of 50 mL of AO7 (0.43 mM) and $Fe(SO_4)$ (0.5 mM) at graphite (●), carbon felt (□), ADE (▲) cathode with a geometric surface of 5 cm^2 at a pH=3. Anode: Ti/IrO_2-Ta_2O_5. Experiments performed in conventional cell (in the presence of Na_2SO_4 35 mM) at 500 A/m^2 and in a micro cell without supporting electrolyte at compact graphite cathode (○) with a nominal distance between the electrodes of 120 µm (Δ) at 20 A/m^2 at flow rate between 0.05 - 0.1 mL/min. (b) reports the abatement of TOC of 50 ml of solution after 23.5 h in the conventional cell and 8.3 h in the microfluidic cell.*

According to the literature, numerous byproducts were detected by HPLC also in this work for the experiments carried out in the conventional cell.

The main relevant byproducts were hydroquinone, oxalic and maleic acids (Figure 4.8e) which remained in the solution after very long times. When the experiments were repeated in the micro device less byproducts were detected by HPLC (8 and 3 peaks were detected by using the Prevail column under conditions suitable for the evaluation of carboxylic acids, in macro and micro devices, respectively).

Regarding the main by-products, maleic acid was present in significantly lower concentrations in the micro device while hydroquinone and oxalic acid were still formed in similar amounts (Figure 4.8e).

4.5 Comparison of oxidation routes

The Figure 4.2 reports the abatement of AO7 and of COD achieved in a conventional cell by the investigated oxidation routes. As shown in Figure 4.2a, higher abatement of AO7 was achieved by electro-generated active chlorine with respect to that obtained by EO at both BDD and Iridium based anode. Thus, indirect oxidation routes are not affected by the slow mass transfer of organic pollutant to the anode surface that decreases the performances of the EO process.

On the other hand, a less removal of the COD was observed in the experiments performed with electrogenerated active chlorine with respect to EO at BDD anode (Figure 4.2b). Thus, electrogenerated active chlorine is very active for the oxidation of AO7 but not for its mineralization due to the formation of organic intermediates that present a higher resistance to the oxidation by means of active chlorine. Electro-Fenton process gave a very fast but not complete abatement of color. The lower abatement of COD was achieved by EF. This is probably due to the formation of iron complexes of carboxylic acids that are very resistant to the oxidation by means of bulk hydroxyl radicals.

The formation of byproducts was evaluated for all investigated electrocataytic routes by focused HPLC analyses. Oxalic acid was formed in all investigated processes even if in different amounts, maleic acid and hydroquinone in EF and IOAC, formic acid only during EO experiments and lactic and malonic acids only during IOAC ones. Furthermore, a very large number of small peaks was observed by HPLC for the two indirect oxidation processes and in most of cases peaks with different retention times were observed for EF and IOAC. On the other hand, for EO at BDD, the chromatograms presented only the peaks attributable to AO7 and oxalic and formic acids. Figure 4.8 reports a plot of the concentrations of AO7 and main common byproducts (namely, hydroquinone, oxalic and maleic acid) vs. time for the three investigated electrocatalytic routes. The degradation of AO7 was faster by EO at BDD and slower for EF (Figure 4.8a). For EF, a small but not negligible residual concentration of AO7 was observed also after 3 h thus giving rise to a residual coloration of the solution. The lower concentrations of hydroquinone, oxalic and

maleic acids were found for EO process. For these compounds, a plot with a maximum was observed for IOAC process. Thus, in the first part of the experiments the generation rate of these compounds is faster than their oxidation rate while the opposite behavior takes place in the second part of the electrolyses an effect of the lower concentration of AO7. On the other hand, for electro-Fenton process, a plot with a maximum was observed for maleic acid while the concentrations of both hydroquinone and oxalic acids still did not decrease also after 3 (Figure 4.8) and 24 h of experiments as a result of their higher resistance to oxidation by means of EF. Figures 4.2c and 4.2d report the abatement of AO7 and COD achieved in a micro device. As shown in figure 4.2c, very high abatements of color were achieved by AO at BDD, very close to that obtained by electro-generated active chlorine, as a result of strong intensification of mass transport of the pollutant to the anode surface. Slightly lower abatements were achieved by Electro-Fenton process. The higher abatements of COD were obtained at BDD anode also in the micro device (Figure 4.2d). On the other hand, very similar abatements of COD were recorded by EF and by means of IOAC, as a result of the dramatic improvement of the performances of EF achieved in the micro device. As above mentioned, this is due to the less formation of byproducts achieved in the microreactor as an effect of high hydrogen peroxide generation and absence of supporting electrolyte.

4.8a

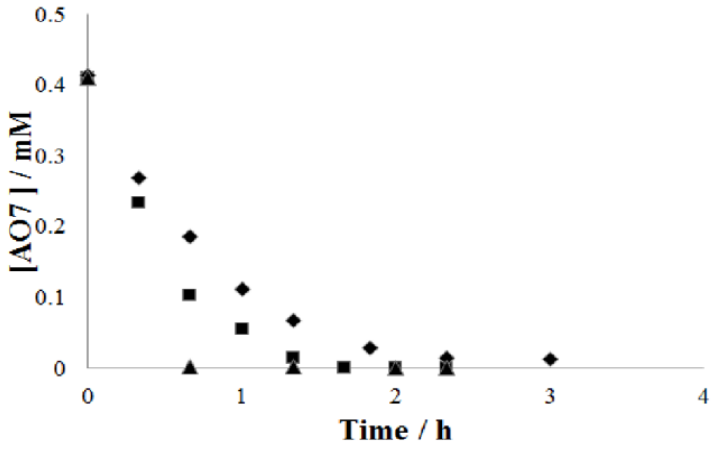

4.8b

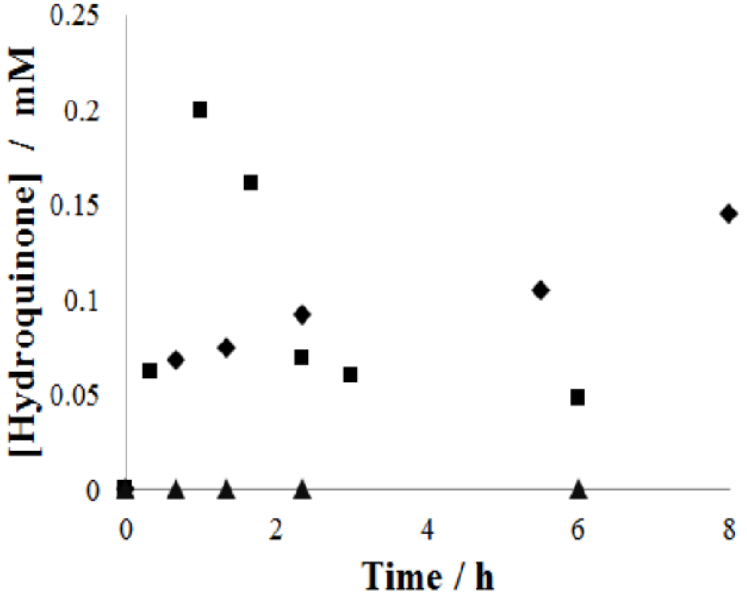
[Hydroquinone] / mM
0.25
0.2
0.15
0.1
0.05
0
0
2
4
6
8
Time / h

4.8c

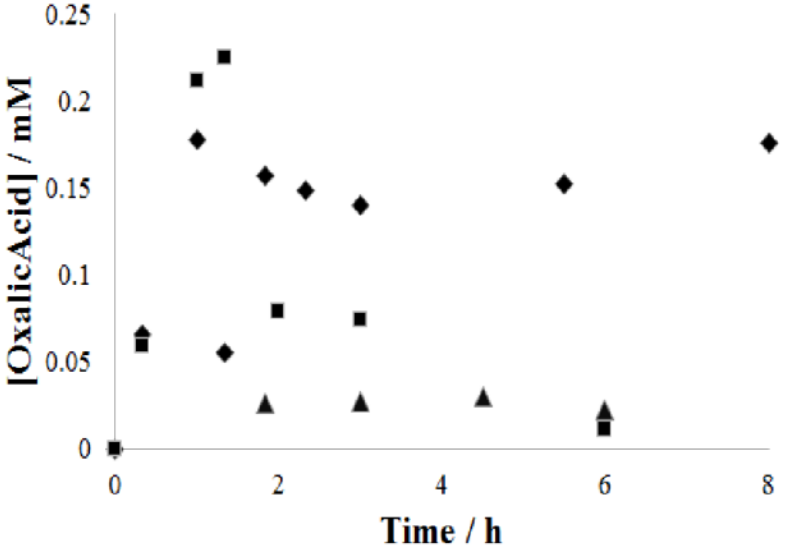
[OxalicAcid] / mM
0.25
0.2
0.15
0.1
0.05
0
0
2
4
6
8
Time / h

4.8d

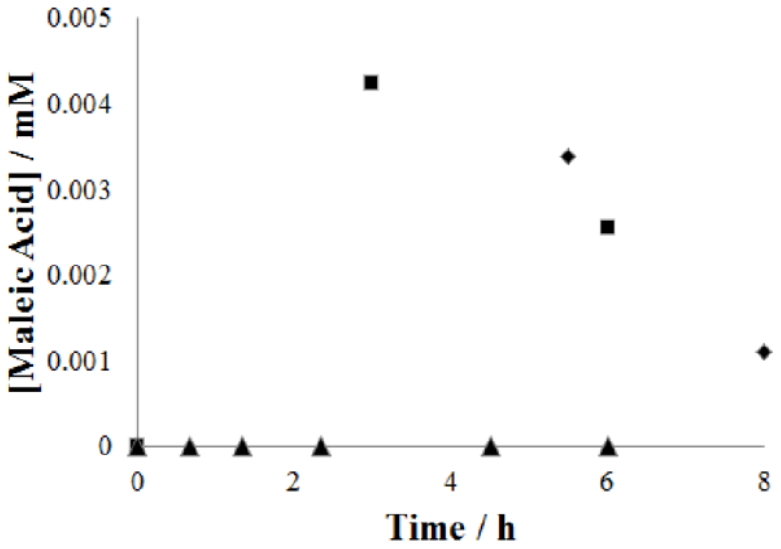

4.8e

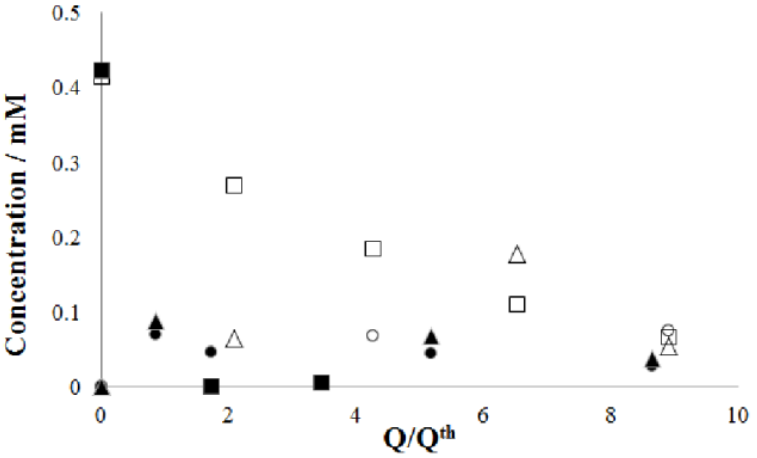

Figure 4.8 *Time-course of AO7 (a), hydroquinone (b) and oxalic (c) and maleic acids (d) during EO at BDD anode and Ni cathode (▲), EF at compact graphite cathde and Ir based anode with Fe_2SO_4 (0.5 mM) (♦) and IOAC at Ru based anode and Ni cathode with 17 mM of NaCl (■) (d) in Na_2SO_4 (35 mM) and AO7 (0.4 mM) medium in conventional macro cell. (e) reports the plot of the concentrations of AO7 (macro (□) and micro (■)), hydroquinone (macro (o) and micro (•)) and oxalic acid (macro (Δ) and micro (▲)) vs. Q/Q^{th} for the EF process performed at compact graphite cathode and Ir based anode in macro (with Na_2SO_4 35mM) and micro devices with Fe_2SO_4 (0.5 mM) and AO7 (0.4 mM) without supporting*

electrolyte with a nominal distance between the electrodes 120 µm at flow rate of 0.1 mL/min and at density current between 20-180 A/m^2.

4.6 Coupled approaches

It has been recently stressed that coupled abatement processes, using both cathode and anode reactions, can allow to enhance significantly the performances of electrochemical approaches in terms of overall abatement of the organic pollutants and current efficiency. Figure 4.9a reports the abatement of AO7 achieved by electro-Fenton at graphite cathode (with DSA anode and $FeSO_4$ as catalyst), EO at BDD anode (with Ni cathode) and coupled process at BDD anode and graphite cathode with $FeSO_4$ as catalyst. An higher abatement of color was achieved in the coupled process with respect to that observed in both uncoupled processes, for the same amount of charge passed, as a result of the combined action of hydroxyl radicals generated at the BDD anode (BDD-HO•) by the water oxidation and in the bulk of the solution (bulk HO•) by the Fenton process.

As shown in Figure 4.9b, the adoption of a coupled process involving both EO at BDD and electro-Fenton at graphite gave higher abatements of COD with respect to the sole electro-Fenton but lower than that achieved by EO at BDD with a Nickel cathode. It is known that iron ions form complexes with carboxylic acid that are quite resistant to oxidation. BDD-HO• are capable to mineralize also these compounds but longer times are necessary [2]. Very similar results in terms of abatement of color were achieved when the graphite cathode was substituted with an ADE one for both single and coupled process (Figure 4.9a). However, as shown in Figure 4.9f the abatement of TOC by the coupled process increased drastically in the presence of an ADE cathode.

Figures 4.9c and 4.9d report the abatement of color and COD, respectively, achieved by EF at carbon felt cathode (with an iridium based anode and $FeSO_4$ as catalyst), by IOAC at Ru based anode (with Ni cathode and 17 mM of NaCl) and coupled process at Ru based anode and carbon felt cathode (with $FeSO_4$ and 17 mM of NaCl). In this case, the abatement of color was very high with all the processes

performed in the presence of electro-generated active chlorine (Figure 4.9c) while the abatement of COD was higher for the coupled process (Figure 4.9d).

Thus, the utilization of a coupled process allows one to use the charge passed at both electrodes to generate oxidants that can react with both AO7 and intermediates formed by the two processes. Furthermore the utilization of NaCl instead of Na_2SO_4 is expected to favor the Fenton process.

Indeed, both Cl^- and SO_4^{2-} are regarded as radical scavenger that may retard the oxidation action by means of hydroxyl radicals generated by electro-Fenton process. On the other hand, it is reported that about 80 % or 20 % of iron (III) is complexed in the presence of 0.05 M sulfate or chlorides, respectively [38].

Thus, removal rate of AO7 was reported to be slower in the presence of sulphate ions. On the other hand iron ions form complexes with carboxylic acid that are quite resistant to oxidation and that can adversely affect the oxidation by means of electrogenerated active chlorine.

Figures 4.9e and 4.9f report the abatement of color and TOC recorded in tested coupled processes. Very high abatements of color were achieved by EF- IOAC processes for quite low charge passed (Figure 4.9e). On the other hand, EF-EO (at carbon cathodes and BDD anode) gave higher abatement of TOC (Figure 4.9f) with respect to coupled processes with electro-generated active chlorine. For both coupled processes higher abatement of TOC were achieved at ADE electrodes.

Coupled EF-EO process was investigated also in microfluidic devices and gave higher abatements of COD with respect to uncoupled processes at all adopted distances between the electrodes, i.e. 50, 120 and 240μm, (see an example data reported in Figure 4.10b for an inter-electrodic distance of 50 μm). As shown in Figure 4.10a, the performance of EF-EO processes in the micro device strongly depended on the inter-electrodic distance: the higher abatements were achieved at 50 and 120 μm while lower ones were recorded at both 75 and 240 μm. These interesting results are due to the fact that EO benefits from lower inter electrodic distances while EF process gave best results by using an intermediate distance of about 120 μm [13]. As a consequence, when experiments were carried out with an

inter electrodic distance of 50 μm, best results were achieved at higher current densities that favor the EO process and, when a spacer of 120 μm was used, higher abatements of COD were obtained by working with the current densities that optimize the EF process (e.g., close to 40 A/m^2).

4.9a

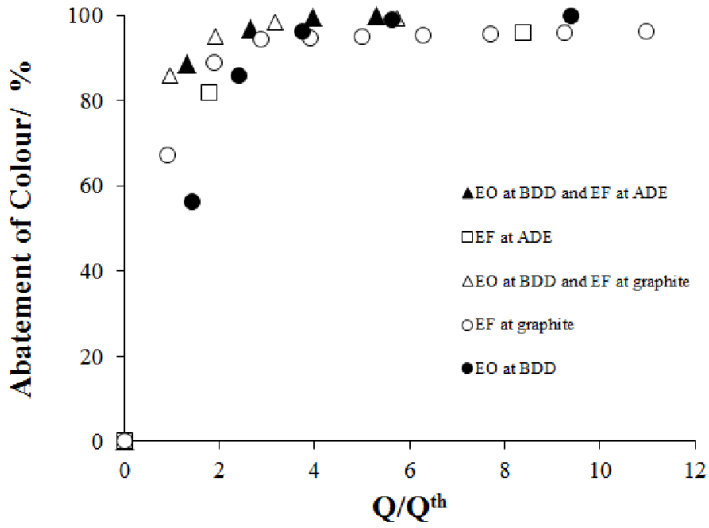

4.9b

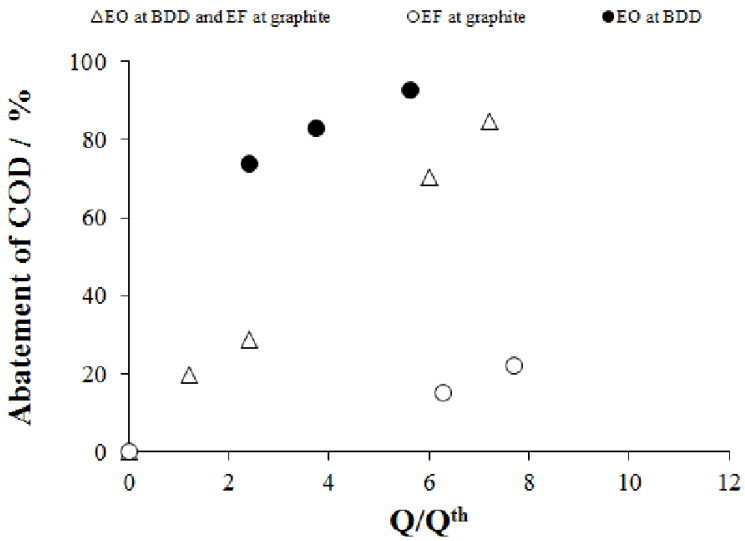

4.9c

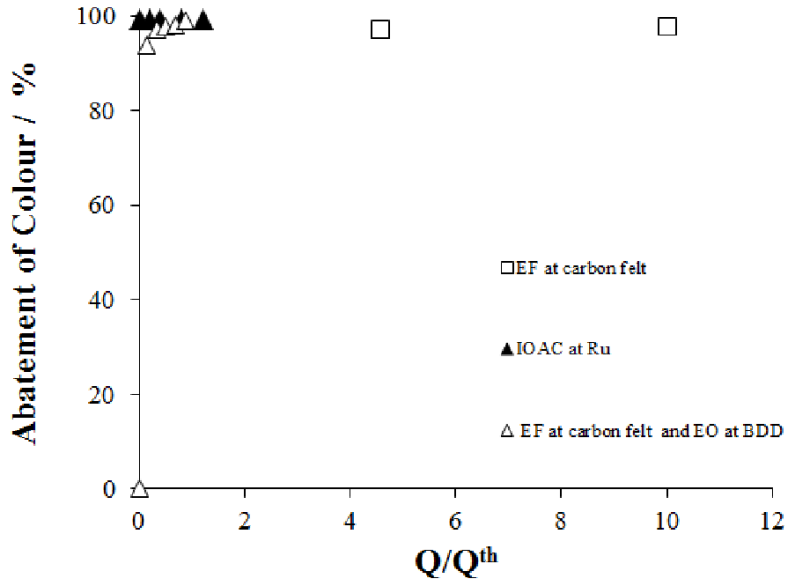
Abatement of Colour / %
100
80
60
40
20
0
0
2
4
6
8
10
12
Q/Q^th
EF at carbon felt
IOAC at Ru
EF at carbon felt and EO at BDD

4.9d

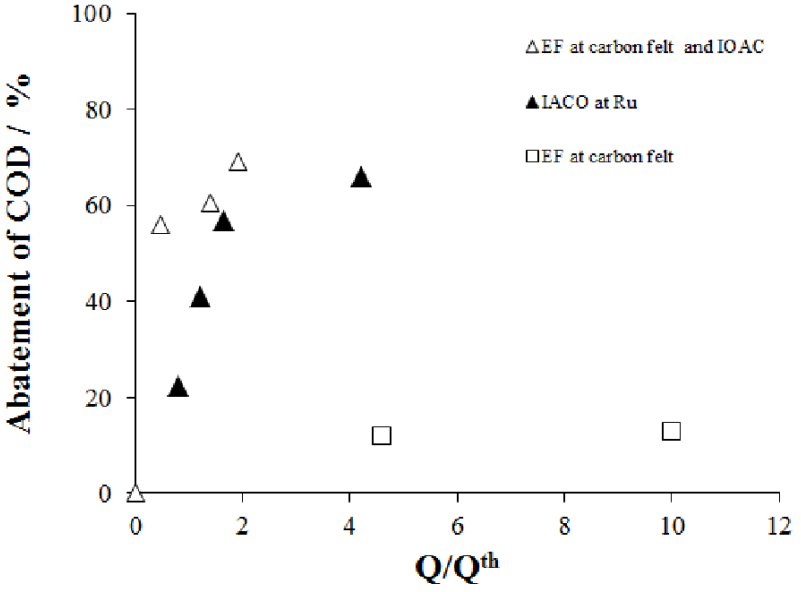
Abatement of COD / %
100
80
60
40
20
0
0
2
4
6
8
10
12
Q/Q^th
EF at carbon felt and IOAC
IACO at Ru
EF at carbon felt

4.9e

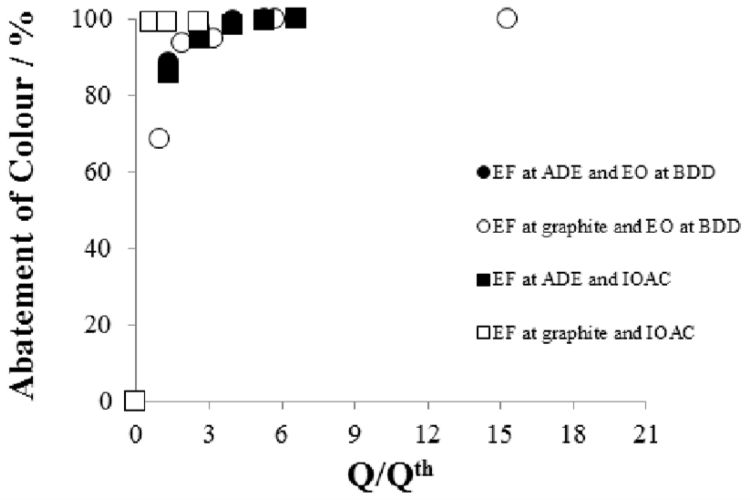

4.9f

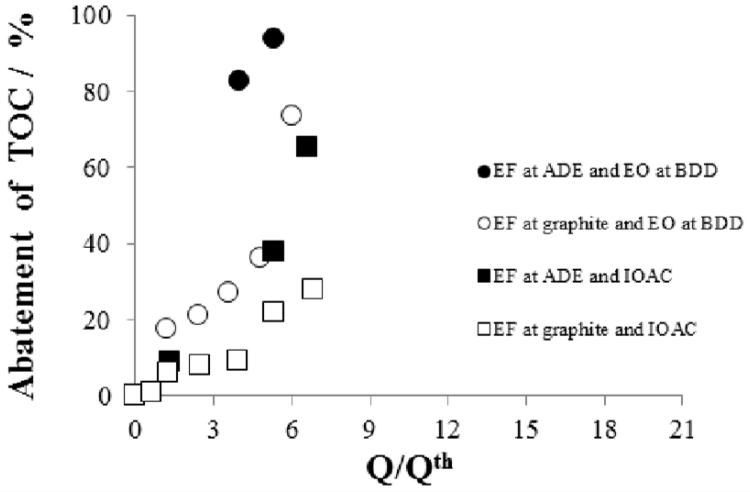

Figure 4.9 *Comparison between single and coupled processes. Figures a) and b) report the abatement of colour and COD, respectively, vs. Q/Q^{th} by EO at BDD (with Ni cathode), electro-Fenton at graphite (○) or ADE (□) cathode with Ti/IrO_2-Ta_2O_5 anode and coupled process at BDD anode and graphite (Δ) or ADE (▲) cathode. Figures c) and d) report the abatement of AO7 and COD, respectively, achieved by electro-Fenton at carbon felt cathode with Ti/IrO_2-Ta_2O_5 anode (□), by active chlorine electro-generated at Ru based anode with Ni cathode (▲) and coupled process at Ru based anode and carbon felt cathode (Δ). A*

comparison between coupled processes in terms of abatement of AO7 and TOC is reported in Figures 9e and 9f. Coupled processes: Electro-Fenton at ADE (●) or graphite (○) cathode and EO at BDD anode, Electro-Fenton at ADE (■) or graphite (□) cathode and electro-generation of active chlorine at Ru based anode. Data achieved during the treatment a solution of 50 mL of AO7 (0.43 mM) in conventional cell (in the presence of Na_2SO_4 0.035 M) at a pH = 3. For electro-Fenton and coupled processes, $Fe(SO_4)$ (0.5 mM) was added to the solution. Experiments at Ru based anode were performed with 17mM of NaCl. Electrodes with a geometric surface of 3-5 cm^2. Current density: 100 A/m^2.

4.10a

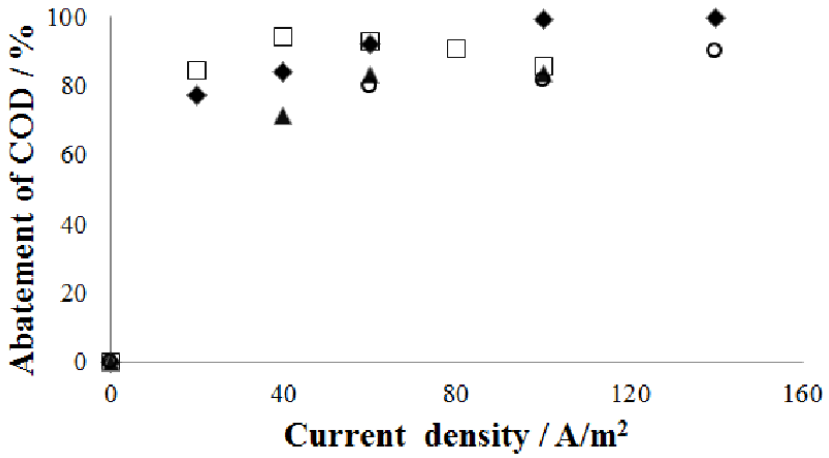

4.10b

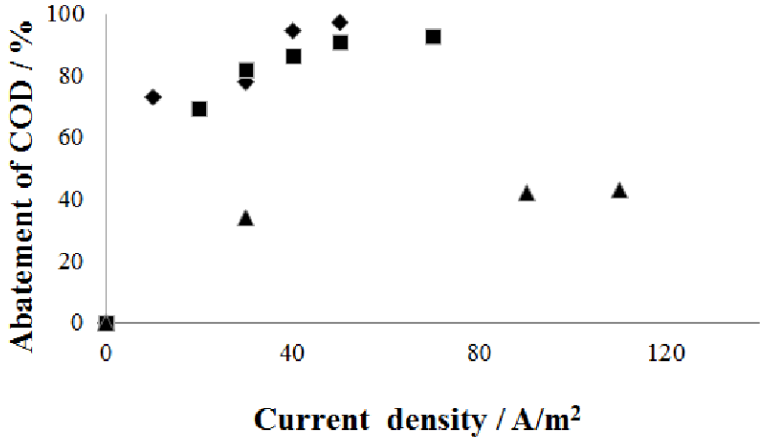

Figure 4.10 *Comparison between coupled processes. Figure a) report the abatement of COD vs. density current in a micro cell without supporting electrolyte at compact graphite cathode and BDD with a nominal distance between the electrodes of 240 µm (▲) 120 µm (□) 75 µm (○) 50 µm (♦) at density current between 20 - 140 A/m^2. Figure b) reports the abatement COD vs. density current by EO at BDD anode (with Ni cathode) (■), electro-Fenton at graphite (▲) at Ru based anode and coupled process at BDD anode and graphite (♦) cathode in a micro cell without supporting electrolyte with a nominal distance between the electrodes 50 µm at flow rate of 0.3 mL/min and at density current between 20 - 140 A/m^2. Data achieved during the treatment a solution of AO7 (0.43 mM). For electro-Fenton and coupled processes, Fe(SO$_4$) (0.5 mM) was added to the solution.*

4.7 Experiments with reactors in series

In the previous paragraphs it was shown that EO with BDD and the EF with graphite strongly benefited by the utilization of a microfluidic reactor. Very different operating conditions were set for EF and EO to optimize their performances with electrochemical microfluidic reactors. To improve the performances to the use of microreactors with low energetic consumptions and high productivity a set of experiments was performed under a continuous mode using various micro electrochemical cells in series. The possibility of operating EF and EO in two different reactors in series was also investigated in order to select the best operating conditions for each process.

In the following paragraphs the possibility to use more reactors in series for the abatement of AO7 was evaluated, with the aim of optimizing the process in terms of abatements, electrode costs, productivity and energetic consumptions.

4.7.1 Direct electrochemical oxidation at BDD in the micro reactor

As above mentioned, the direct electrochemical oxidation at BDD of AO7 strongly benefit from the utilization of a microfluidic electrochemical cell. It was found that higher abatements was achieved working with a very low inter-electrodic distances

(50 µm) and high current intensity. A set of experiments were carried to evaluate the productivity and energetic consumptions of the EO of AO7 in the microreactor at the best operative conditions (50 µm) [14], for different current densities (2, 10 and 20 mA cm^{-2}), initial concentrations of AO7 (150-500 mg/l) and flow rates (0.1-0.3 ml/min). Under all adopted operating conditions, the EO process allowed the total decolourization of the solution in one single passage through the cell. On the other hand, the abatement of TOC, CE and EC strongly depended on current, flow rate and initial concentration of AO7 (Figure. 4.11).

Increasing the current density gave rise to an enhancement of the abatement of the TOC (Figure. 4.11a), because of the higher charge passed, but to higher anodic and cell potentials (data not shown) and lower *CE* (because of higher impact of parasitic oxygen evolution) (Figure. 4.11b), thus involving higher *EC* (Figure. 4.11c).

4.11a

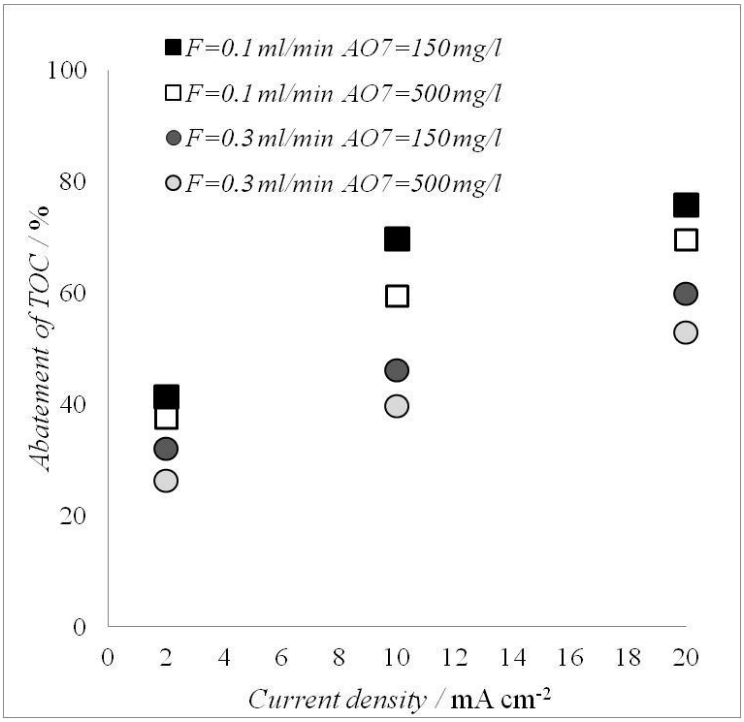

4.11b

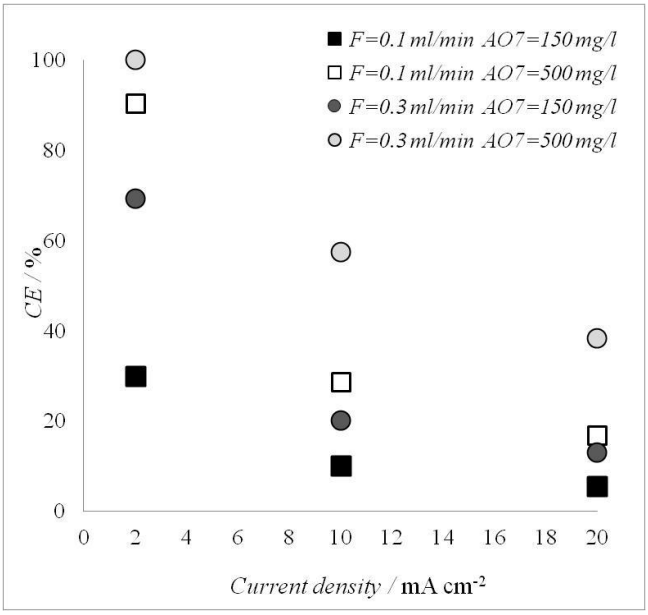

4.11c

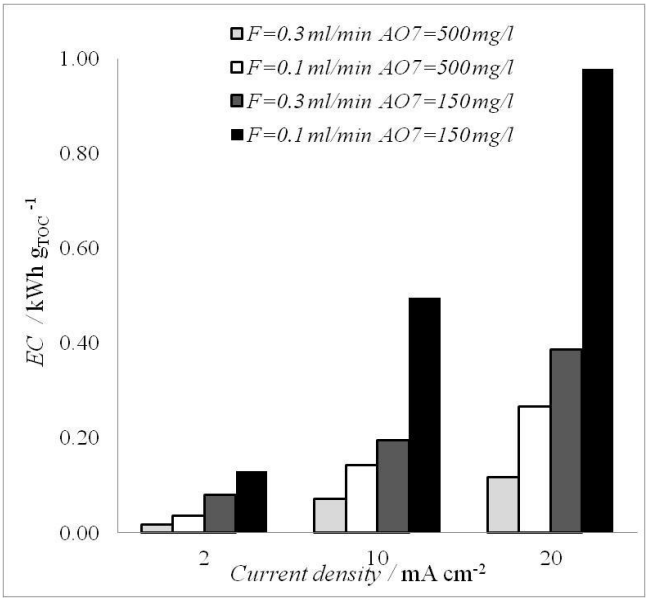

Figure 4.11 *Direct electrochemical oxidation of AO7 at BDD anode in a single micro reactor. Effect of current density on the abatement of TOC (Figure. 4.11a), Current Efficiency*

(CE) (Figure. 4.11b) and Energy Consumption (EC) (Figure. 4.11c). Flow rate 0.1 ml/min (■ C_{iAO7} = 150 mg/l, □ C_{iAO7} = 500 mg/l) and 0.3 ml/min (● C_{iAO7} = 150mg/l, ○ C_{iAO7} = 500 mg/l). Nominal distance between the electrodes 50 µm. Cathode: nickel.

According to literature [7], higher abatements (Figure. 4.11a) but lower *CE* (Figure. 4.11b) and higher *EC* (Figure. 4.11c) were achieved decreasing the flow rate (i.e., increasing the treatment time). The utilization of more concentrated solutions of AO7 (C_{iAO7} = 500 instead of 150 mg/l) gave rise to lower percentage abatement of TOC (Figure. 4.11a), but a drastic decrease of *EC* (Figure. 4.11c), as a result of the lower impact of parasitic anodic processes. In general, quite high energetic consumptions were achieved to obtain high abatements. As an example, an energy consumption of 0.27 kWh g_{TOC}^{-1} and an abatement of TOC of about 70% were obtained for high initial concentrations of the dye (500 mg/l) and low flow rate (0.1 ml/min) at 20 mA cm^{-2}.

4.7.2 Electro-Fenton at graphite in the micro reactor

As above mentioned, the abatement of organic pollutants by EF strongly benefits from the utilization of a microfluidic electrochemical cell. It was found that the higher concentration of H_2O_2 was achieved working with relatively high inter-electrodic distances (120 µm) and low current densities (about 2-5 mA cm^{-2}). Indeed, the EF experiments were here performed in a single microreactor equipped with an inter-electrodic distances of 120 µm, in the presence of the catalyst $FeSO_4$, with a concentration of 0.5 mM at a pH of 3 obtained by addition of sulfuric acid.
As shown in Figure 4.12, higher abatements of TOC (about 70%) were obtained for low current density (2 mA cm^{-2}). Worth mentioning, at this low current density, very low cell potentials and *EC* (0.055 kWh g_{TOC}^{-1}) were obtained, thus confirming the optimum performance of micro reactors for EF. Please consider that in order to achieve a similar abatement of the TOC under the same operating conditions (in terms of initial concentration of AO7 and flow rate), the EO at BDD required a current density of 10 mA cm^{-2}, thus resulting in a tenfold higher *EC* (0.5 kWh g_{TOC}^{-1}).

4.12a

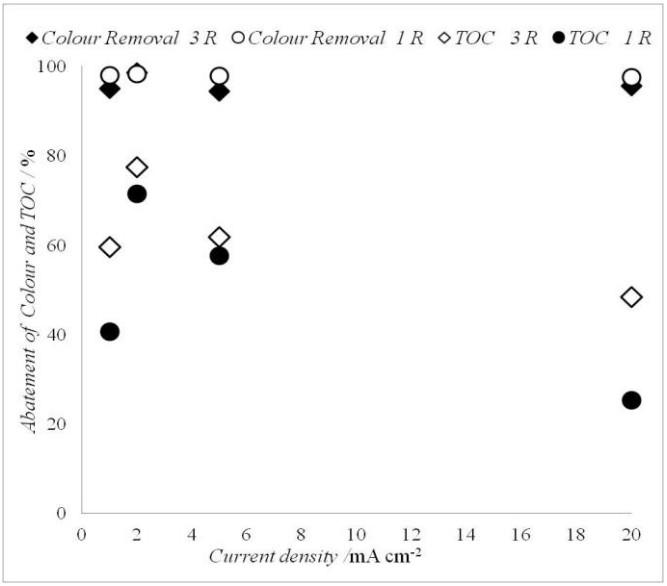

4.12b

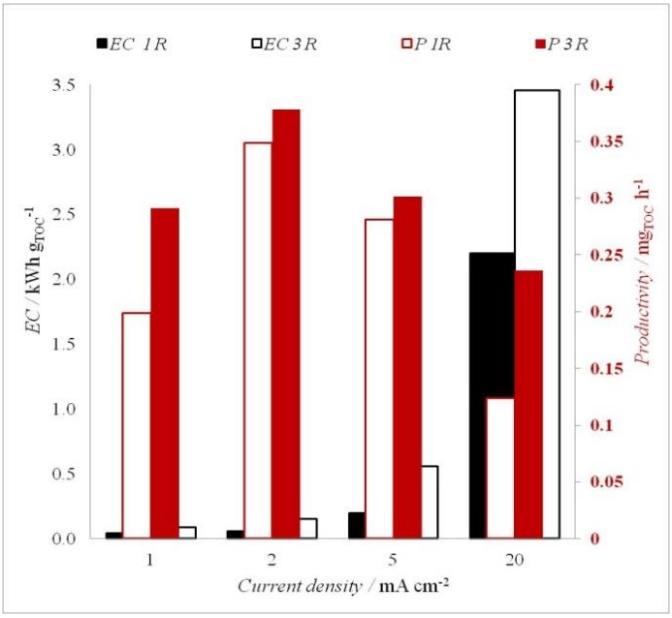

Figure 4.12 *Comparison of EF at graphite cathode in a single and in three microreactors in series. Effect of current density on the abatement of colour and TOC (a) and on energy*

consumption (b) at 0.1 ml/min with C_{iAO7} = 150 mg/l and $FeSO_4$= 0.5 mM at a pH=3. Nominal distance between the electrodes 120 µm. Anode: DSA.

4.7.3 Utilization of three reactors in series

To achieve high abatements also in the presence of high initial concentrations of the dye and high flow rates (in order to increase the productivity of the cell), the utilization of a cascade of more reactors in series was considered (as described in paragraph 3.3.2.3).

First, the experiments were performed using three reactors in series (with an overall surface area of 12 cm^2), all of them performing EO or EF processes. For EO at BDD anode, the utilization of three reactors in series allowed to operate with relatively high initial concentration of AO7 (500 mg/l) and flow rate (0.3 ml/min), affording high abatements of TOC and an increase of the productivity of the system (in terms of mass of TOC removed in one hour) with respect to the results achieved using only one micro reactor (Figure 4.13). As an example, at 10 mA cm^{-2}, using three reactors instead than one, the removal of TOC increased from 40 to 90% and the productivity from 2.3 to 5.3 mg_{TOC}/h. Conversely, *EC* increased just from 0.06 to 0.09 kWh g_{TOC}^{-1} as a result of the higher removal of TOC. At 20 mA cm^{-2}, a further enhancement of the abatement of TOC up to 98% was obtained but the *EC* value increased significantly (Figure. 4.13a and 4.13b).

Three reactors in series were also used for the EF process (with an overall surface area of 12 cm^2). Quite similar TOC profiles were obtained when the experiments were performed in one or three reactors in series. Indeed, using three reactors, we obtained very slight increases of the abatements of TOC with obvious enhancement of EC, thus showing that the process gives rise to the formation of by-products that are very resistant to EF. Hence, for EF the utilization of a cascade of more reactors is not an interesting option.

4.13a

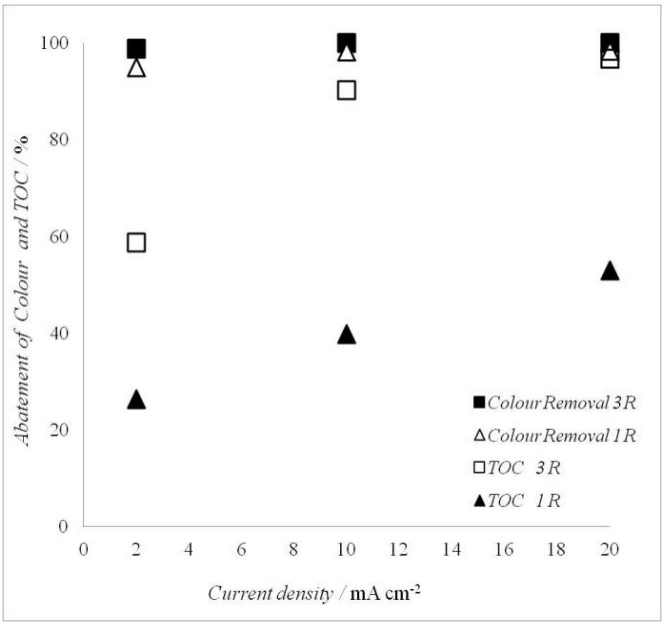

4.13b

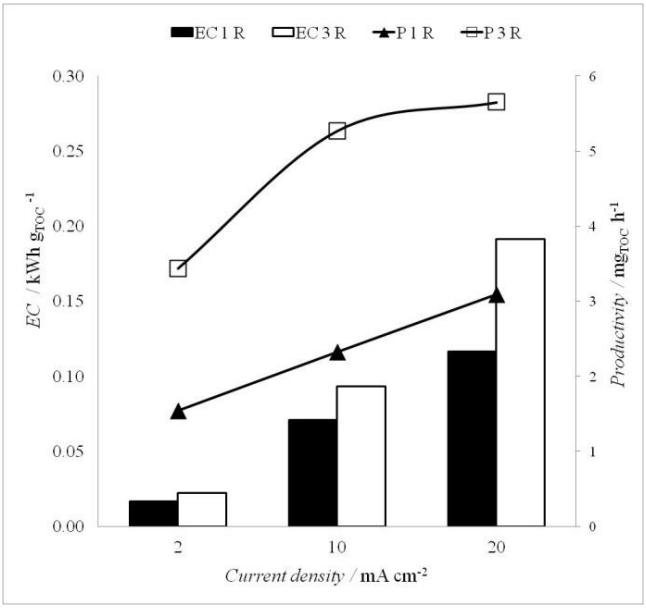

Figure 4.13 *Comparison of direct electrochemical oxidation of AO7 at BDD anode in a single reactor and in three microreactors in series. Effect of current density on the abatement*

of colour and TOC (a) and on energy consumption and productivity (b) at 0.3 ml/min with C_{iAO7} = 500 mg/l. Nominal distance between the electrodes 50 µm. Cathode: nickel.

4.7.4 Utilization of different processes in series

As shown in the previous paragraphs, EO and EF present very different characteristics. In particular, EF works with low *EC* and cheap electrodes, but it does not allow a complete mineralization of AO7. Conversely, EO at BDD requires drastically higher *EC* and a very expensive anode, but gives very high abatements of the TOC. Hence, in order to synergize the different characteristics of these processes, we have studied the utilization of two reactors with the following approach:

- In the first reactor, the wastewater was treated by EF with the aim to reduce the TOC content with low *EC* and cheap electrodes;
- In the second reactor, the wastewater was treated by EO with the aim to achieve the degradation of organics formed in EF.

Worth mentioning, these two processes are optimized under very different operating conditions (see above). Hence, in order to benefit in an efficient way of both processes, we have tried to operate differentiating the operating conditions for the two reactors. In particular, a nominal distance between the electrodes of 120 and 50 µm was used for the reactors devoted to EF and EO, respectively.

First experiments were carried out with a flow rate of 0.1 ml/min, a concentration of AO7 of 150 mg/l and using a current density of 20 mA cm^{-2} in both reactors. As shown in Figure. 5a, high abatements of TOC (about 76 %) were coupled with high *EC* because of the relatively high cell potentials. Worth mentioning, the utilization of only one reactor with a BDD anode, with the same operating parameters, gave a very similar abatement, thus showing that the reactor with EF at these high current densities gives a very small contribution to the performances of the system.

When the experiments were repeated with a quite low current density (2 mA cm^{-2}) for both reactors, a slightly lower abatement of the TOC was obtained (about 70 %) but very small values of *EC* were achieved. It is interesting to observe, that a single

reactor devoted to EF at these operative conditions gave an abatement close to 70 %, thus showing that at these very low values of current densities the contribution of the reactor equipped with BDD is negligible. Hence, in both cases only one of the processes was fully exploited (e.g., at high and low current density the contribution of EF and EO were, respectively, very small, according to the results presented in previous paragraph). Hence, the following experiments were performed using a different current density for each reactor.

In particular, as shown in Figure. 4.14a, when the experiments were repeated with 2 and 20 mA cm^{-2} in the first and in the second reactor, respectively, a significant increase of the abatement of TOC was achieved (about 86 %) with respect to the experiments performed using the same current density for both reactors. Furthermore, a drastically lower *EC* was obtained with respect to the experiment carried out imposing 20 mA cm^{-2}. Indeed, in these conditions, both processes are fully exploited: in the first micro reactor, the EF process at graphite allowed to degrade a large part of AO7 with the formation of some by-products, such as, according to the literature, hydroquinone, oxalic and maleic acids. Afterwards, the solution passed in the second micro reactor where the EO process at BDD allowed to continue the degradation of these resistant by-products.

Worth mentioning, a further decrease of *EC* was obtained imposing 2 and 10 mA cm^{-2} in the first and in the second reactor, respectively, coupled with a still high abatement of TOC (about 84%). Similar trends were obtained when the previous mentioned experiments were repeated at higher flow rate (0.3 ml/min) (Figure. 4.14c). Also in this case, the higher abatement of TOC (about 82 %) was achieved imposing 2 and 20 mA cm^{-2} in the first and in the second reactor, respectively (Figure. 4.14b and Figure. 4.14d). Furthermore, as a result of the lower residence time (and consequently of the lower passed charge), a drastic decrease of *EC* (to 0.32 kWh g_{TOC}^{-1}) was achieved.

Interesting results in term of both *EC* and abatement of TOC were obtained also working with higher initial concentrations of AO7 (500 mg/l) adopting 2 and 20 mA cm^{-2} in the first and in the second reactor, respectively. At 0.3 ml/min the abatement of TOC was 73 % and *EC* about 0.09 kWh g_{TOC}^{-1} (Figure. 4.14d).

4.14a

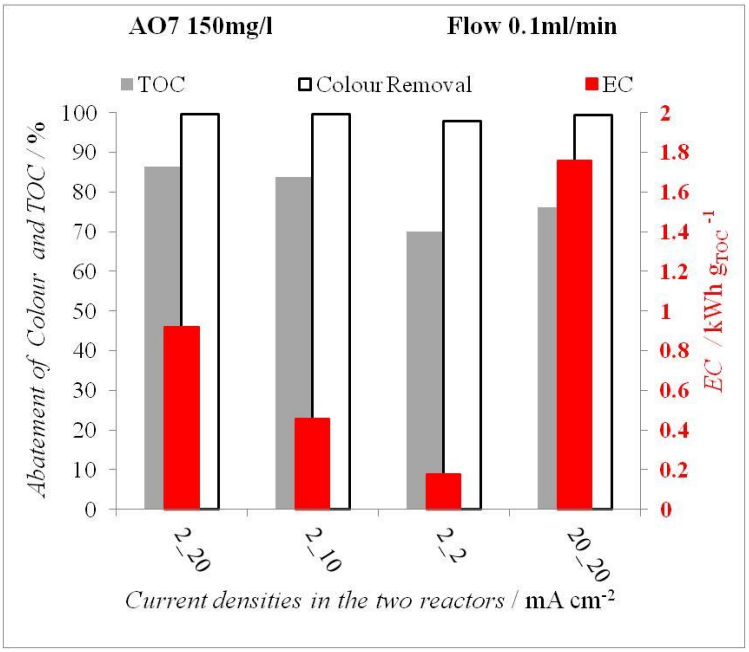
AO7 150mg/l
Flow 0.1ml/min
TOC
Colour Removal
EC
Abatement of Colour and TOC / %
EC / kWh g_TOC^-1
2_20
2_10
2_2
20_20
Current densities in the two reactors / mA cm-2

4.14b

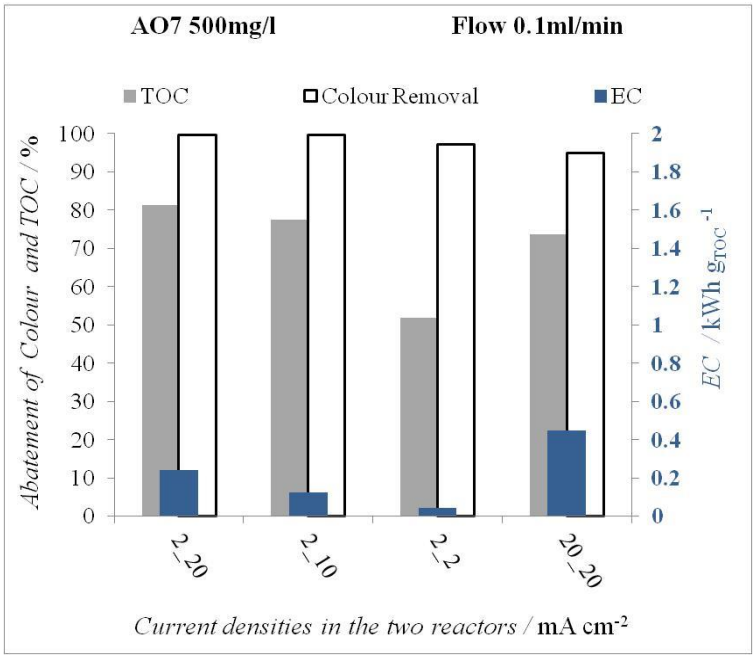
AO7 500mg/l
Flow 0.1ml/min
TOC
Colour Removal
EC
Abatement of Colour and TOC / %
EC / kWh g_TOC^-1
2_20
2_10
2_2
20_20
Current densities in the two reactors / mA cm-2

4.14c

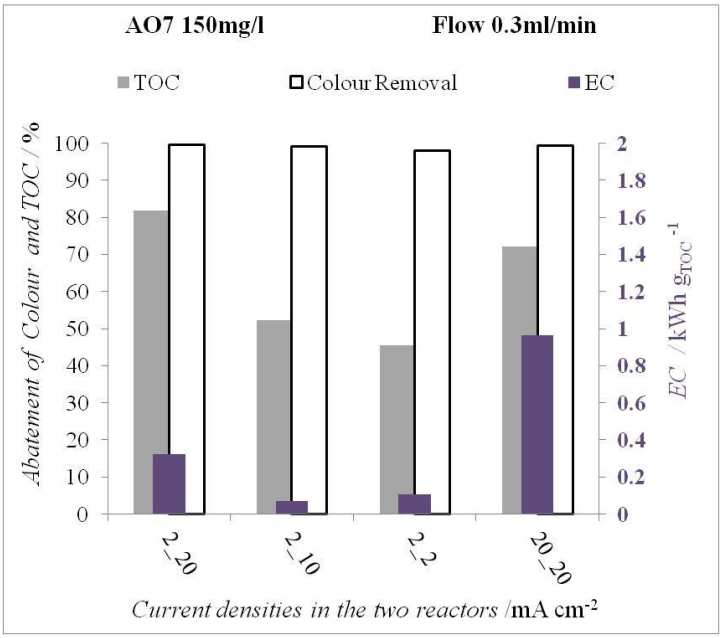
AO7 150mg/l
Flow 0.3ml/min
TOC
Colour Removal
EC
Abatement of Colour and TOC / %
EC / kWh g$_{TOC}$$^{-1}$
2_20
2_10
2_2
20_20
Current densities in the two reactors /mA cm^{-2}

4.14d

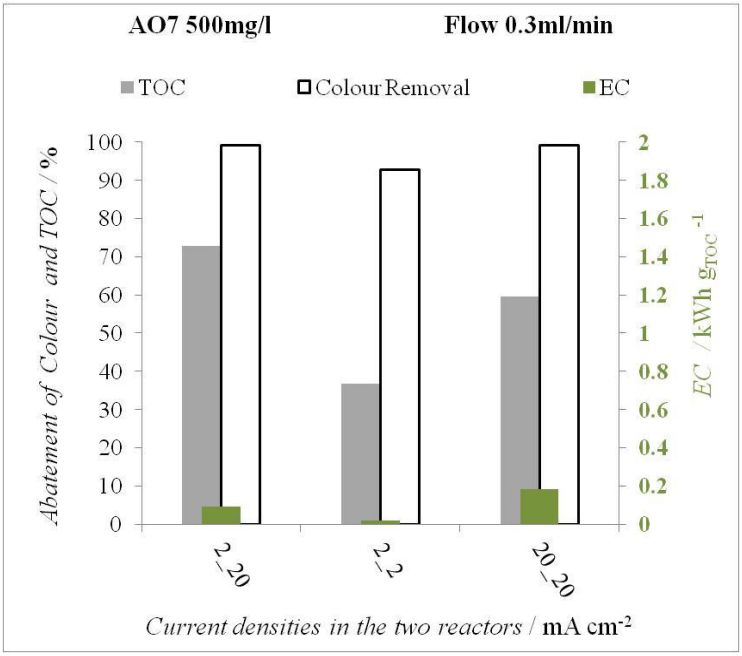
AO7 500mg/l
Flow 0.3ml/min
TOC
Colour Removal
EC
Abatement of Colour and TOC / %
EC / kWh g$_{TOC}$$^{-1}$
2_20
2_2
20_20
Current densities in the two reactors / mA cm^{-2}

Figure 4.14 *Effect of current density on the abatement of colour, TOC and on EC for two micro reactors in series. First reactor was devoted to EF at graphite cathode, with a nominal distance between the electrodes of 120 µm. Second reactor was devoted to the direct electrochemical oxidation of AO7 at BDD anode, with a nominal distance between the electrodes of 50 µm. a): 0.1 ml/min; C_{iAO7} = 150 mg/l. b): 0.1 ml/min; C_{iAO7} = 500 mg/l. c): 0.3 ml/min; C_{iAO7} = 150 mg/l. d): 0.3 ml/min; C_{iAO7} = 500 mg/l. The iron catalyst was added to the solution as $FeSO_4$= 0.5 mM at a pH=3.*

Some experiments were repeated with three reactors in series. The first two reactors were devoted to EF with graphite cathodes and the third one to EO with BDD. As shown in Figure. 4.15, also in this case the best results in terms of high abatement of TOC coupled with limited EC were achieved differentiating the current density for EF and EO.

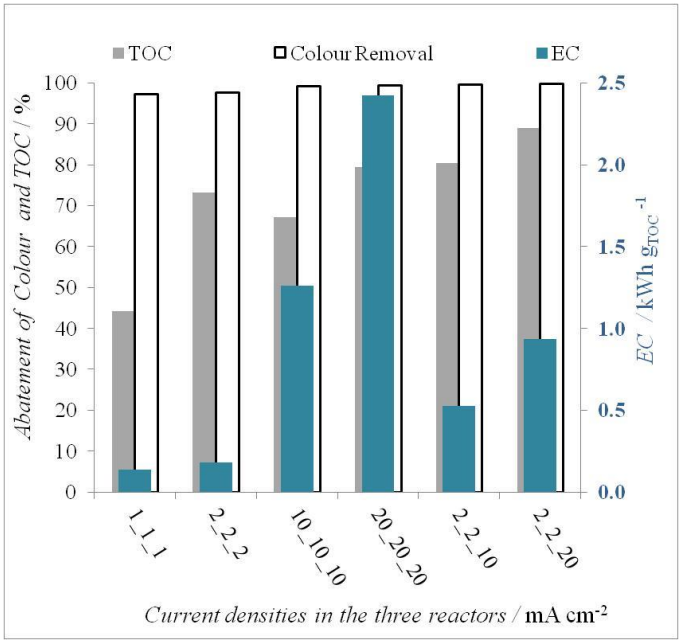

Figure 4.15 *Effect of current density on the abatement of colour, TOC and on EC achieved using three reactor in series at 0.1 ml/min C_{iAO7} = 150 mg/l First two reactor were devoted to EF at graphite cathode, with a nominal distance between the electrodes of 120 µm. The third reactor was devoted to the direct electrochemical oxidation of AO7 at BDD anode, with a nominal distance between the electrodes of 50 µm. The iron catalyst was added to the solution as $FeSO_4$= 0.5 mM at a pH=3.*

However, the enhancement of the TOC abatement was quite small with respect to that achieved in two reactors, thus probably indicating that the second reactor does not provide a high contribution to the overall abatement because of the resistance to EF of products formed in the first reactor.

Worth mentioning, as shown in Figure. 4.16, the utilization of two reactors in series equipped with EF and EO, respectively, seems a very interesting option to achieve high abatements of the TOC (not obtainable with an EF process) limiting the energy consumptions (and the cost of the electrodes) with respect to processes that use only EO with BDD.

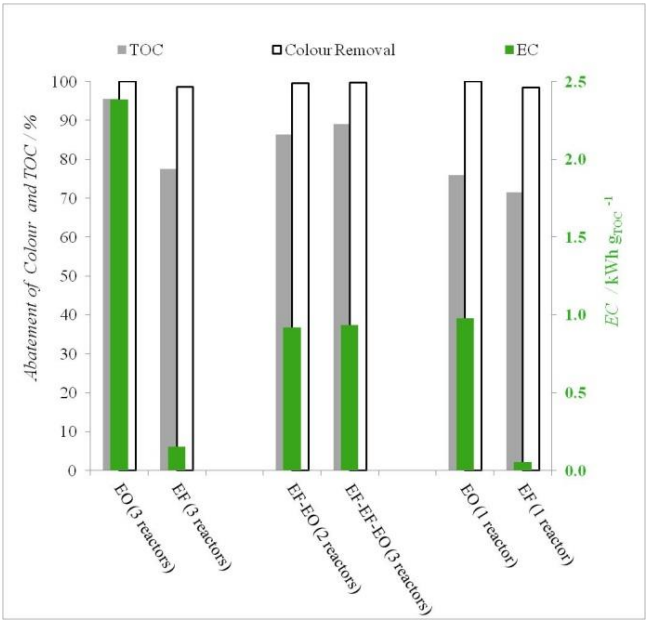

Figure 4.16 *Electrochemical abatement of AO7 in water using one, two or three micro reactors in series with different processes. EF was performed at graphite cathode with a nominal distance between the electrodes 120 µm and a current density of 2 mA cm^{-2} and direct electrochemical oxidation of AO7 at BDD anode, with a nominal distance between the electrodes of 50 µm and a current density of 20 mA cm^{-2}. Flow rate: 0.1 ml/min C_{iAO7} = 150 mg/l. For the EF process the iron catalyst was added to the solution as $FeSO_4$= 0.5 mM at a pH=3.*

4.8 Effect of air pressure on the electro-generation of H_2O_2 and the abatement of Acid Orange 7 by electro-Fenton process

Asabove mentioned, the Electro-Fenton process is a very promising tool for the treatment of wastewater contaminated by a wide series of organic pollutants resistant to conventional biological processes. The utilization of air is usually preferred for its low cost with respect to oxygen. Due to the poor solubility of O_2 in aqueous solutions at 1 atm and 25 °C (about 40 or 8 mg L^{-1} in contact with pure oxygen or air, respectively) [41] two dimensional cheap graphite electrodes give quite slow generation of H_2O_2, thus resulting in low H_2O_2 bulk concentrations especially in undivided cells [4,7]. The generation of H_2O_2 is usually accompanied by the parasitic cathodic evolution of hydrogen (eq. (15)) while at the anode the oxygen evolution reaction is expected (eq. (16)).

$$2H^+ + 2\,e^- \rightarrow H_2 \qquad (15)$$

$$2\,H_2O \rightarrow O_2 + 2\,H^+ + 2\,e^- \qquad (16)$$

Various approaches have been described in the literature to increase the local concentration of H_2O_2. Concentrations of H_2O_2 higher than 50 mM in divided cells separated by cationic membranes [36-38] were reached by injecting the gas through GDEs which have higher costs and require a more complicated electrochemical cell layout. An increase of the concentration of H_2O_2 of about one order of magnitude was obtained using microfluidic electrochemical devices as described in paragraph ….

A high concentration of hydrogen peroxide could be theoretically also obtained by increasing the solubility of oxygen in water by using pressurized air or oxygen, thus potentially improving the performances of the EF process. In this context, we report here, for the first time to the best of our knowledge, a study on the effect of the air pressure on both the electro-generation of hydrogen peroxide and the abatement of organic pollutants in water by an electro-Fenton process. Moderate air pressures (1-

11 bar) easily achievable in applicative scale electrochemical reactors were used. An increase of the concentration of H_2O_2 of more than one order of magnitude was obtained by working at proper operating conditions with moderate air pressure (up to 11 bar) with an high pressure reactors as described in paragraph 3.3.3. Similarly, a drastically higher abatement of the Acid Orange 7 (AO7) was obtained by performing the electro-Fenton process upon increasing the air pressures.

4.8.1 Electro-generation of H_2O_2

First experiments were performed with air at atmospheric pressure under galvanostatic mode at various current intensities (50, 80 and 110 mA) with a water solution of Na_2SO_4 (35 mM) and H_2SO_4 (pH 3) for 2 h. At 80 mA and atmospheric pressure, the concentration of H_2O_2 increased with time up to a plateau value of 1.2 mM (Fig.4.17) as a concomitant result of slow H_2O_2 cathodic formation (due to the low mass transfer kinetics of oxygen to the cathode surface, caused by its low solubility) and its anodic consumption (Fig. 4.17). When the experiments were repeated at 50 and 110 mA, quite similar H_2O_2 concentrations profiles were obtained, resulting in final concentrations of hydrogen peroxide close to 1.2-1.3 mM after 2 h (table 4.1), as a result of the fact that the process was likely to be kinetically controlled by the mass transfer of oxygen to the cathode surface. These final concentrations of H_2O_2 were achieved with low current efficiency (*CE*) ranging from 1.5 to 3.5 % for experiments performed at 110 and 50 mA, respectively (Table 4.1).

Worth mentioning, the profiles of H_2O_2 concentration and of *CE* were fitted by a very simple theoretical model based on the assumption that both the cathodic reduction of oxygen to hydrogen peroxide and the anodic oxidation of H_2O_2 take place under mass transfer control (see Fig. 4.17 and Appendix A1).

In order to enhance the electro-generation of H_2O_2, a set of amperostatic electrolyses was repeated at 80 mA for 2 h, increasing the air pressures from 1 to 6 and 11 bar, corresponding to oxygen partial pressure of about 0.2, 1.2 and 2.2 bar, respectively. As shown in Figure 4.17a and Table 1, the increase of the pressure gave rise to a

drastic enhancement of the concentration of H_2O_2. In particular, upon increasing the air pressure from 1 to 6 bar, the concentration of H_2O_2 reached a value of about 7 mM. A further increase of the air pressure to 11 bar gave rise to a final concentration of H_2O_2 of about 12 mM. Therefore, upon enhancing the air pressure from 1 to 11 bar, the *CE* increased from about 2 to 21 % (Table 4.1 and Fig. 4.17b).

Table 4.1 *Effect of pressure and current density on cathodic electro-generation of* H_2O_2 [a]

Pressure (bar)	Current (mA)	$[H_2O_2]$ (mM)	Current efficiency (%)
1	50	1.3	3.4
1	80	1.2	1.9
1	110	1.2	1.5
6	50	6.5	17
6	80	6.9	12
6	110	6.2	8
6	200	5.0	3
11	50	7.0	19
11	80	12.3	21
11	110	12.2	15
11	200	12.2	8
11	300	4.7	2

[a] *Electrolysis of 50 mL of 35 mM* Na_2SO_4 *solutions (pH 3.0) at 22 °C at compact graphite cathode. Time: 2 h. Value indicate as 1 bar stays for atmospheric pressure (1.013 bar).*

These drastic enhancements were due to the higher concentration of oxygen molecularly dissolved in water associated, according to the Henry's law, with the higher oxygen partial pressure. Indeed, as shown in Fig. 4.17, the experimental data achieved at both 6 and 11 bar were well predicted by the above mentioned theoretical model using the same fitting parameters obtained at 1 bar, just changing the oxygen concentration according to the Henry's law (Appendix A1). Worth mentioning, at 11 bar the chromatographic area of the peak of hydrogen (generated by the parasitic cathodic reduction of water) was strongly reduced with respect to that obtained in the experiment performed at 1 bar (data not shown).

To evaluate the effect of the current intensity (*I*) on the electro-generation of H_2O_2 under different air pressure values, the experiments at 6 and 11 bar were repeated at different *I*. Quite interestingly, at both 6 and 11 bar a maximum value of $[H_2O_2]$ was achieved increasing the current value; however, after a certain current values, the $[H_2O_2]$ started decreasing (Table 4.1).

In the experiments performed at 11 bar, for the lower adopted value of *I* (50 mA), a final concentration of H_2O_2 slightly lower than 7 mM was achieved with a corresponding *CE* close to 20 %.

4.17a°

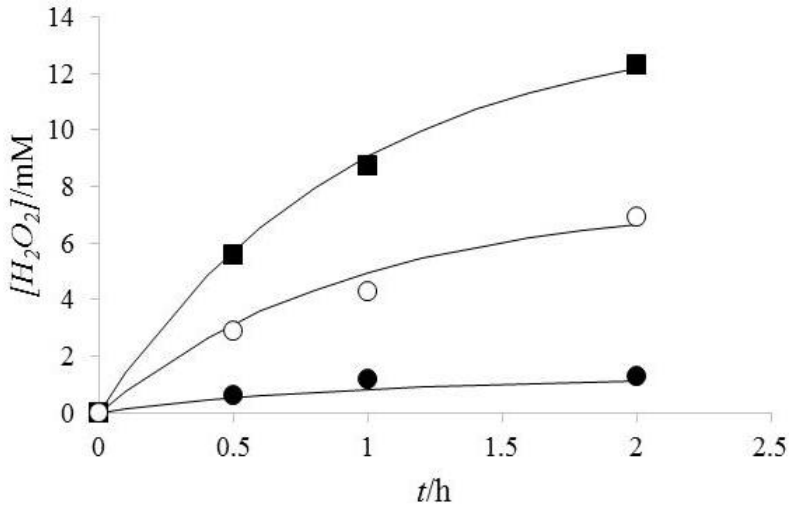

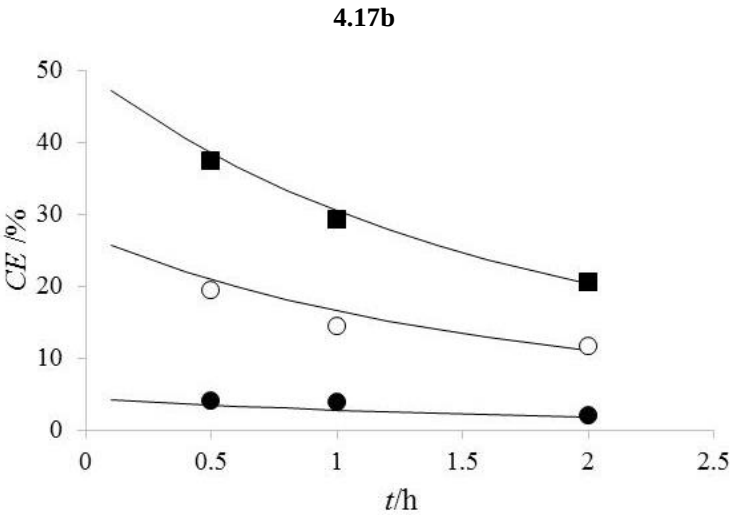

Figure 4.17 *Evolution of the concentration of H_2O_2 (4.17a) and of CE (4.17b) during the electrolysis of 50 mL of 35 mM Na_2SO_4 solutions (pH 3.0 by addition of H_2SO_4) at 25 °C and 80 mA and various pressures: 1 (●), 6 (o) and 11 (■) bar. Theoretical curves (-) are the predictions under the hypothesis that both the cathodic reduction of oxygen to hydrogen peroxide and the inverse reaction at the anode are mass transfer-controlled reactions with fitting parameters obtained for the experiments performed at 1 bar (see the Appendix A1).*

An increase of the current to 80 mA gave higher amounts of H_2O_2 but similar *CE* values, due to the larger passed charge. When *I* was increased up to 200 mA, very similar profiles of H_2O_2 concentration vs. time were achieved (Fig. 4.18a) as a probable result of the fact that the electro-generation of H_2O_2 at these current densities is limited by the oxygen transfer to the cathode surface (mass transfer-controlled process). Hence, in this range of current intensity (80 – 200 mA), the increase of the current gave rise to a decrease of the *CE* (Fig.4.18b). Worth mentioning, a further increase of the current up to 300 mA gave rise to a strong decrease of the concentrations of H_2O_2 (Table 4.1 and Fig. 4.18b).

This result is probably due to the fact that at high current densities, quite high cathodic potentials are reached and part of the excess of the charge passed is likely to be used for the cathodic reduction of H_2O_2. Consequently, the profiles of *CE* vs.

time were in good agreement with the theoretical trends expected for the processes occurring under mass transfer kinetics only in the range 80 - 200 mA (Fig. 4.17b).

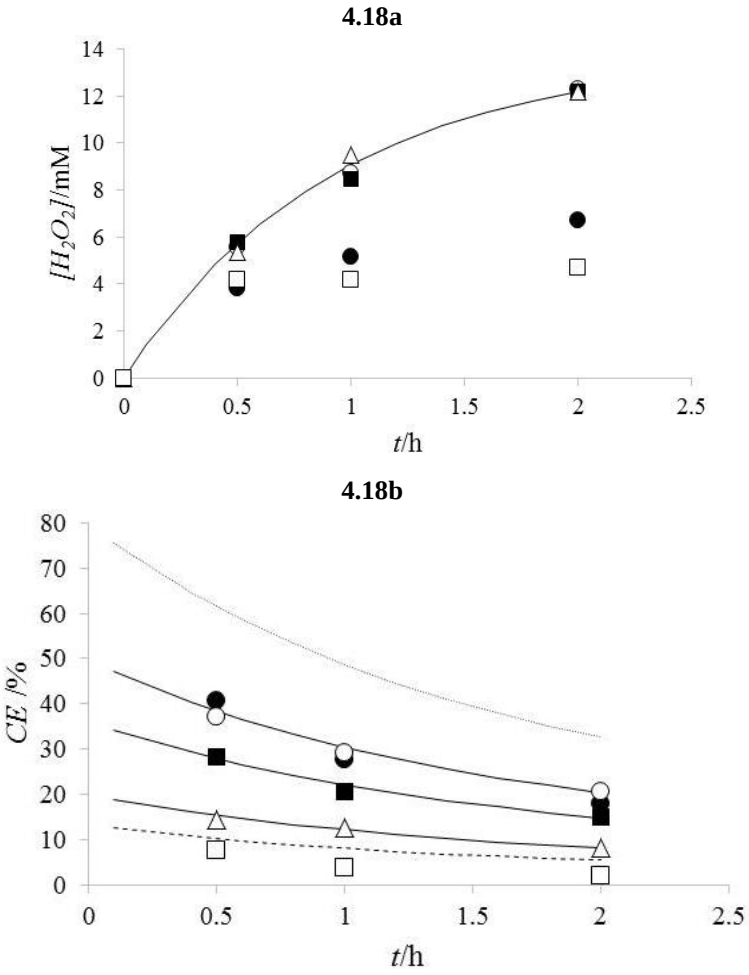

Figure 4.18 *Evolution of the concentration of H_2O_2 (a) and of CE (b) during the electrolysis of 50 mL of 35 mM Na_2SO_4 solutions (pH 3.0 by addition of H_2SO_4) at 25 °C and 11 bar at various currents: 50 (●), 80 (o), 110 (■), 200 (Δ) and 300 (□) mA. Theoretical curves are the predictions under the hypothesis that both the cathodic reduction of oxygen to hydrogen peroxide and the anodic oxidation of hydrogen peroxide take place under mass transfer control with fitting parameters obtained for the experiments performed at 1 bar (see the Appendix A1). For the concentration of H_2O_2 (a), the theoretical predictions (–) do not*

depend on the adopted current density. For the CE (3B), the theoretical predictions change with the current density: 50 (...), 80, 110 and 200 (–) and 300 (--) mA.

4.8.2 Electro-Fenton

Here, the abatement of AO7 was studied by galvanostatic electrolyses mainly at graphite cathode and iridium based anode with 0.5 mM of $FeSO_4$ as catalyst, Na_2SO_4/H_2SO_4 as supporting electrolyte at pH 3 with an initial concentration of the dye of 0.43 mM. Iridium based anode was chosen since it gives very poor abatement of AO7 by electro-oxidation. According to the literature, using air at 1 bar as oxygen source and 110 mA current intensity, a very fast abatement of the color was coupled with a slow abatement of TOC (Table 4.2) as a result of the low concentration of hydrogen peroxide and of the generation of resistant intermediates [7-8,14]. In order to enhance the abatement of the TOC, the experiments were repeated at 110 mA and higher air pressures (4, 6 and 11 bar). As shown in Table 4.2 and Fig.4.19, the utilization of higher pressures allowed to achieve drastically higher abatements of TOC after the same passed time, reasonably as a consequence of the enhanced H_2O_2 generation.

In particular, an increase of the pressure from 1 to 6 bar allowed to enhance the final abatement of the TOC from 48 to 63%. A further increase of the pressure to11 bar gave an abatement of the TOC of about 74 %. Hence, it is possible to conclude that the utilization of quite moderate air pressures, that are easily achievable in industrial electrolyzers, can allow to increase substantially the efficacy of EF process.

According to the literature, an acceleration of the abatement rate can be achieved in electro-Fenton process by using carbon felt cathodes which present high electrode surfaces. Quite interestingly, when the abatement of AO7 was performed at a carbon felt cathode using air at 1 bar, a lower abatement (about 55 %) was achieved with the same treatment time with respect to that obtained at compact graphite at pressures of 6 or 11 bar.

Table 4.2 *Effect of pressure and current density on abatement of AO7 by electro-Fenton*[a]

Pressure (bar)	Current (mA)	Abatement of color (%)	Abatement of TOC (%)	Current efficiency (%)
1	50	> 99	50	7.3
1	110	> 99	48	2.9
4	110	> 99	54	3.2
6	110	> 99	63	3.7
11	110	> 99	74	4.7
11	50	> 99	65	9.2
11	200	> 99	75	2.4

[a]*Electrolysis of 50 mL of 35 mM Na_2SO_4, 0.5 mM $Fe(SO_4)$ and 0.43 mM AO7 aqueous solutions (pH 3.0 by H_2SO_4 addition) at 18 °C on compact graphite cathode. Reaction time: 7 h. Anode: Ti/IrO_2-Ta_2O_5.*

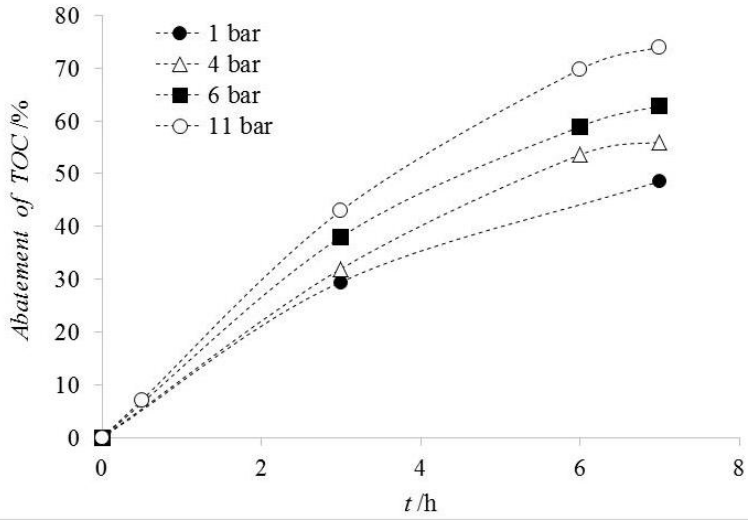

Figure 4.19 *Electrolysis of 50 mL of 35 mM Na_2SO_4, 0.5 mM $Fe(SO_4)$ and 0.43 mM AO7 aqueous solutions (pH 3.0) at 18 °C nd 100 mA at compact graphite cathode at various pressures (1, 4, 6 and 11 bar). Anode: Ti/IrO_2-Ta_2O_5.*

This result clearly highlights that a moderate enhancement of the operating pressure allows the operator to work with compact planar electrodes that are much easier to be modeled in terms of current distribution, mass transfer kinetics and electrochemical performances and that are characterizeb by low costs.

In order to evaluate the effect of the current density on the abatement of TOC, some experiments were performed with air at 11 bar and 50, 110 and 200 mA. As shown in Table 4.2, an higher abatement was achieved at 110 and 200 mA with respect to that obtained at 50 mA, according to the results obtained from the experiments of electrogeneration of H_2O_2 (see paragraph 4.8.1).

Worth mentioning, the applicative utilization of electrochemical processes for the treatment of wastewater is up to now often limited by the energetic costs. In this context, EF process presents the advantage to utilize quite low working potentials since the cathodic reduction of oxygen to H_2O_2 requires potential close to 0.5 V vs. SCE. However, EF process usually suffers of lower abatements with respect to other electrochemical processes such as the direct electrochemical oxidation at Boron-doped diamond (BDD) that, on the other hand, requires very high anodic potential and cell potentials.

In this context, it is important to observe that, according to our experimental results, the utilization of mild air pressures can allow to increasee drastically the abatement of the TOC, while maintaining low energetic costs. Indeed, according to the data shown in Table 4.3, the utilization of pressurized air allowed to decrease dramatically the energetic consumptions necessary for the abatement of the pollutant, due to the lower cell potentials and the higher current efficiencies.

The energetic costs necessary to provide air at 6 or 11 bar were estimated considering an hypothetic adiabatic compression (polytropic transformation in which the warms up), followed by cooling of the system back to room temperature just via heat exchange with the surrounding environment (without any energy supply).

Even assuming an overall compression efficiency of 50%, the energetic costs for compression result drastically lower with respect to the energetic gain obtained from the improvement of the energetic efficiency of the electrochemical process.

Table 4.3 *Effect of air pressure on energy consumption related to the abatement of AO7 by electro-Fenton*[a].

Pressure (bar)	Cell potential (V)	Abatement of TOC (%)	Energy Consumption (kWh/gTOC)
1	9.4	48	3.8
4	7.6	54	2.7
7	8.0	73	2.1
11	7.4	74	1.9

[a] *Electrolyses of Table 4.2.*

4.9 Conclusion

It was shown that the performances of the electrochemical degradation of AO7, in terms of abatement of colour, AO7 and COD and formation of by-products, depend dramatically on the adopted electro-catalytic route:

– Electrochemical treatment with electro-generated active chlorine (IOAC) gave the faster abatement of colour.
– The higher abatement rate of COD was achieved by the direct electrochemical oxidation (EO) process at BDD that gave rise to a very small generation of by-products, while the lower one was observed for electro-Fenton (EF) process as a result of the formation of quite resistant by-products that remains in the electrolytic medium also after long electrolysis times.
– Intermediate abatement of COD were given by IOAC as a result of the formation of a number of intermediates that are oxidized with higher rate with respect to EF.

Optimization of investigated catalytic routes occurs under very different operative conditions:

– Performances of IOAC, in terms of abatement of both colour and COD, were improved by working with a Ru based electrode (that gives high generation of active chlorine) and higher current densities and residence times but were not affected by the adopted reactor.
– The performances EO depended obviously on the nature of anode. At BDD anode, higher abatements of both colour and COD were achieved in the microfluidic cell that enhances the mass transport phenomena. Higher abatements of COD but lower current efficiencies were achieved by increasing the current density and lowering the flow rate.
– The abatement of AO7 by electro-Fenton (EF) strongly benefited by the utilisation of air diffusion electrode or of a microfluidic reactor or working at high pressures. For experiments carried out in the microfluidic reactor, higher abatements of both colour and COD were achieved by working at intermediate values of the current density (between 20 and 40 A/m^2). A dramatic increase of

the generation of H_2O_2 (up to one order of magnitude) was readily achievable simply through a moderate increase of the air pressure contacted with the electrolytic solution in a pressure range (1 – 11 bar) that can be easily reached in industrial applicative scale electrochemical reactors.

Performances of coupled processes (EF-IOAC, EF-EO) were improved using microfluidic devices which furthermore allowed to work in the absence of supporting electrolytes.

References

[1] T. Robinson, G. McMullan, R. Marchant, P. Nigam, Bioresour. Technol. 77 (2001) 247–255.

[2] C. A. Martınez-Huitle, E. Brillas, Appl. Catal. B: Environ 87 (2009) 105–145.

[3] E. Forgacs, T. Cserhati, G. Oros, Environ. Int. 30 (2004) 953–971; G.M. Atenas, E. Mielczarski, J.A. Mielczarski, J. Colloid Interf. Sci. 289 (2005) 171–183.

[4] A. Fernandes, A. Morao, M. Magrinho, A. Lopes, I. Goncalves, Dyes and Pigments 61 (2004) 287–296.

[5] W. L. Chou, C. T. Wang, C. P. Chang, Desalination 266 (2011) 201-207.

[6] C. Zhang, J. Wang, T. Murakami, J. Electroanal. Chem. 638 (2010) 91–99.

[7] J.M. Peralta-Hernandez, Y. Meas-Vong, F. J. Rodrı´guez, T. W. Chapman, M. I. Maldonado, L. A. Godınez, Dyes and Pigments 76 (2008) 656 – 662.

[8] A. Ozcan, M. A. Oturan, N. Oturan, Y. Sahin, J. Hazard. Materials 163 (2009) 1213-1220.

[9] N. Daneshvar, S. Aber, V. Vatanpour, M. H. Rasoulifard, J. Electroanal. Chem. 615 (2008) 165–174.

[10] S. Garcia-Segura, F. Centellas, C. Arias, J. A. Garrido, R. M. Rodriguez, P. L.

[11] O. Scialdone, C. Guarisco, A. Galia, G. Filardo, G. Silvestri, C. Amatore, C. Sella, L. Thouin, J. Electroanal. Chem. 638 (2010) 293.

[12] O. Scialdone, A. Galia, C. Guarisco, Electrochimica Acta 58 (2011) 463– 473.

[13] O. Scialdone, A. Galia, S. Sabatino, Electrochem. Commun. 26 (2013) 45-47.

[14] O. Scialdone, A. Galia, S. Sabatino, Appl. Catal. B: Environ. 2014, 148-149, 473-483.

[15] P. He, P. Watts, F. Marken, S.J. Haswell, Electrochem. Commun. 7 (2005) 918–924.

[16] J. M. Aquino, G. F. Pereira, R. C. Rocha-Filho, N. Bocchi, S. R. Biaggio, Journal of Hazardous Materials 192 (2011) 1275– 1282.

[17] C. A. Martinez-Huitle, S. Ferro, A. De Battisti, J. Appl. Electrochem. 35 (2005) 1087-1093.

[18] P. Canizares, R. Paz, C. Saez, M. A. Rodrigo, J. Envir. Manag. 90 (2009) 410.

[19] C. A. Martinez-Huitle, S. Ferro, Chem. Soc. Rev. 35 (2006) 1324-1340;

[20] O. Scialdone, A. Galia, G. Filardo, Eletrochim. Acta 53 (2008) 7220-7225.

[21] M. Panizza, G. Cerisola, Electrochim. Acta 51 (2005) 191-199.

[22] O. Scialdone, A. Galia, C. Guarisco, S. La Mantia, Chemical Engineering Journal 189-190 (2012) 229-236.

[23] O. Scialdone, Electrochim. Acta 54 (2009) 6140–6147.

[24] C. Comninellis, Electrochim. Acta 39 (1994) 1857-1862.

[25] O. Scialdone, S. Randazzo, A. Galia, G. Silvestri, Wat. Res. 43 (2009) 2260-2272.

[26] L. Szpyrkowicz, J. Naumaczky, F. Zilio-Grandi, Toxicology and Environmental Chemistry 44 (1994) 189-202.

[27] C. H. Yang, C. C. Lee, T. C. Wen, Journal of Applied Electrochemistry 30 (2000) 1043-1051.

[28] L. C. Chiang, J. E. Chang, T. C. Wen, Water Research 29 (1995) 671-678.

[29] Ch. Comninellis, A. Nerini, Journal of Applied Electrochemistry 25 (1995) 23-28.

[30] F. Bonfatti, S. Ferro, F. Lavezzo, M. Malacarne, G. Lodi, A. De Battisti, Journal of the Electrochemical Society 147 (2000) 592-596.

[31] C. A. Martinez-Huitle, S. Ferro, A. De Battisti, Electrochemical and Solid-State Letters 11 (2005) D35-D39.

[32] L. C. Chiang, J. E. Chang, T. C Wen, Water Research 29 (1995) 671-678.

[33] A. Sánchez-Carretero, C. Sáez, P. Ca˜ nizares, M.A. Rodrigo, Chem. Eng. J. 166 (2011) 710-714.

[34] A.M. Polcaro, A. Vacca, M. Mascia, S. Palmas, J. Rodriguez Ruiz, J. Appl. Electrochem. 39 (2009) 2083-2092.

[35] M.E.H. Bergmann, J. Rollin, T. Iourtchouk, Electrochim. Acta 54 (2009) 2102-2107.

[36] E. Brillas, I. Sires, M. A. Oturan, Chem. Rev. 109 (2009) 6570.

[37] J. S. Do, C. P. Chen, J. Electrochem. Soc. 140 (1993) 1632.

[38] A. Da Pozzo, L. Di Palma, C. Merli, E. Petruccci, J. Appl. Electrochem. 35 (2005) 413-419.

[39] J. De Laat, G. T. Le, B. Legube, Chemosphere 55 (2004) 715-723.

[40] O. Scialdone, A. Galia, S. Randazzo, Chemical Engineering Journal 266 (2011)174.

[41] J. S. Do, C. P. Chen, J. Electrochem. Soc, 140 (1993) 1632.

CHAPTER 5

5 ELECTROCHEMICAL CONVERSION OF DICHLOROACETIC ACID TO CHLOROACETIC ACID IN CONVENTIONAL CELL AND IN MICROFLUIDIC REACTORS

5.1 Introduction

Electrochemical processes are considered very promising tools for the synthesis of fine chemicals. As above mentioned, such processes use a clean reagent, the electron, under mild operative conditions without the use of toxic/hazardous reactants. Furthermore, electrochemical processes can allow the selective synthesis of a large variety of compounds by a proper tuning of the working potential with limited operative costs. However, in spite of these promising features, electrochemical tools have found a quite limited number of applications on an industrial scale for the synthesis of fine chemicals. This is due to various factors such as the utilization of less usual apparatuses and the cost of electric energy. The more relevant disadvantage is given by the fact that electrochemical processes require high conductivity of the solution in order to limit the cell potential, thus imposing the addition of a supporting electrolyte to the solvent. This addition enhances the costs of the process and makes more difficult the work-up procedures due to the necessity to separate the supporting electrolyte from the products.
Furthermore, the supporting electrolyte can be potentially involved in lateral reactions, giving rise to less interesting product mixtures.
Worth mentioned, the utilization of microfluidic reactors can dramatically improve the appealing of electrochemical processes for the synthesis of fine chemicals.

Here the utilization of different microfluidic devices for the electrosynthesis of chloroacetic acid in water was evaluated.

As described in detail in paragraph 2.3.1 chloroacetic acid (MCAA), an important reagent for several chemical reactions, is industrially synthesized by

hydrolysis of trichloroethylene or chlorination of acetic acid.[24] The production of MCAA by chlorination of acetic acid, the prevalent route, is accompanied by the formation of relevant amounts of dichloroacetic acid (DCAA) and to a small extent of trichloroacetic acid (TCAA).

The conversion of DCAA to MCAA acid is of industrial interest in order to recover the so formed dichloroacetic acid and to increase the overall yield in MCAA. The electrochemical reduction of DCAA to MCAA acid was, in particular, investigated in detail both in bench and pilot scale with promising results.

In this work, the electrochemical conversion of DCAA to MCAA was studied both in a conventional cell and in different microfluidic devices above mentioned. The effect of some operative parameters including the nature of cathode material, adopted electrochemical cell, current density, flow rate and inter-electrodic gap (for experiments performed in the micro reactors) was investigated in detail.

5.2 Preliminary electrolyses in macro cells

First electrolyses were carried out in a conventional undivided cell (as described in paragraph 3.31) in the presence of a water solution of DCAA (0.1 M) and Na_2SO_4 (0.1 M) as supporting electrolyte with a current density of 230 A/m^2 with the aim of evaluating the effect of the nature of the cathode on the process. Silver, copper, graphite and lead were used as cathodes while Ti/IrO_2-Ta_2O_5 as anode. Silver and copper were chosen for their electrocatalytic activity towards the reduction of chlorinated organic compounds and, in particular, of chloracetic acids. Graphite and lead were also selected as cathodes since, according to literature, they allow good conversions of DCAA acid to MCAA. A pH close to 1 was obtained as a result of the presence of DCAA.

The target cathodic process was the reduction of DCAA to MCAA (eq. (1)). The successive reduction of MCAA to acetic acid (AA) (eq. (2)) and the reduction of water (eq. (3)) could potentially take place as lateral unwanted processes. Thus, the reduction to AA would lead to a decrease of yield, selectivity and current efficiency in MCAA while the reduction of water would cause a decrease of conversion and

current efficiency of the process. The counter-process was the anodic oxygen evolution (eq. (4)).

$$Cl_2CHCOOH + 2e^- + H^+ = Cl^- + ClCH_2COOH \quad (1)$$

$$ClCH_2COOH + 2e^- + H^+ = Cl^- + CH_3COOH \quad (2)$$

$$H_2O + e^- = 0.5\ H_2 + OH^- \quad (3)$$

$$H_2O = 0.5\ O_2 + 2H^+ + 2e^- \quad (4)$$

As shown in fig. 5.1a, at all adopted electrodes the conversion achieved after the theoretical charge Q^{th} necessary to convert the moles of DCAA with a bi-electronic process was significantly lower than 100 %. An almost complete conversion was achieved after about 2.5 – 3.0 Q^{th} because of parasitic reactions such as that reported in eq. (2) and (3). Silver gave the lower yields in MCAA (fig. 5.1b) because of its extraordinary catalytic activity towards the reduction of chlorinated compounds, thus resulting in high yields in AA (fig. 5.1c). AA was also formed at copper and lead cathodes, even if in minor amounts (fig. 5.1b). No formation of AA was observed at graphite as a result of its less catalytic activity towards the reduction of chlorinated compounds. In all cases, the sum of the yields in MCAA and AA assumed the same values of the conversion of DCAA. On the other hand, the sum of current efficiencies in MCAA and AA ($CE_{MCAA+AA}$) was significantly lower than 100 % for all adopted cathodes (data not shown) because of the probable occurrence of parasitic water reduction (eq. (4)).

The higher $CE_{MCAA+AA}$ was achieved for silver due to its very high selectivity towards the reduction of chlorinated organic compounds. After the electrolyses, lead and graphite did not show any apparent macroscopic modification of the surface while the silver electrode presented some black points. SEM analyses showed silver dissolution phenomena while EDAX ones suggested the formation of silver oxides and chlorides. In the case of copper, very small degradation phenomena were observed by SEM analyses. According to above-mentioned results, silver was

discarded due to its low performances in terms of yield and selectivity. In addition, lead was discarded due to its toxicity and since it is expected to show low resistance in the employed conditions for long times.[25] Hence, further studies were focused on graphite and copper cathodes.

According to literature, the reduction of chloroacetic acids is expected to depend on pH. Hence, some electrolyses were repeated at Cu cathode at different values of pH (namely 1, 4 and 7).

Higher pH resulted in lower conversions (fig. 5.2a) but higher selectivity for the same amount of charge passed. Thus, at pH 4 and 7 no acetic acid was formed (fig. 5.2b).

A pH of 4 seemed particularly interestingly since it provided quite good conversions coupled with very high selectivity.

5.1a

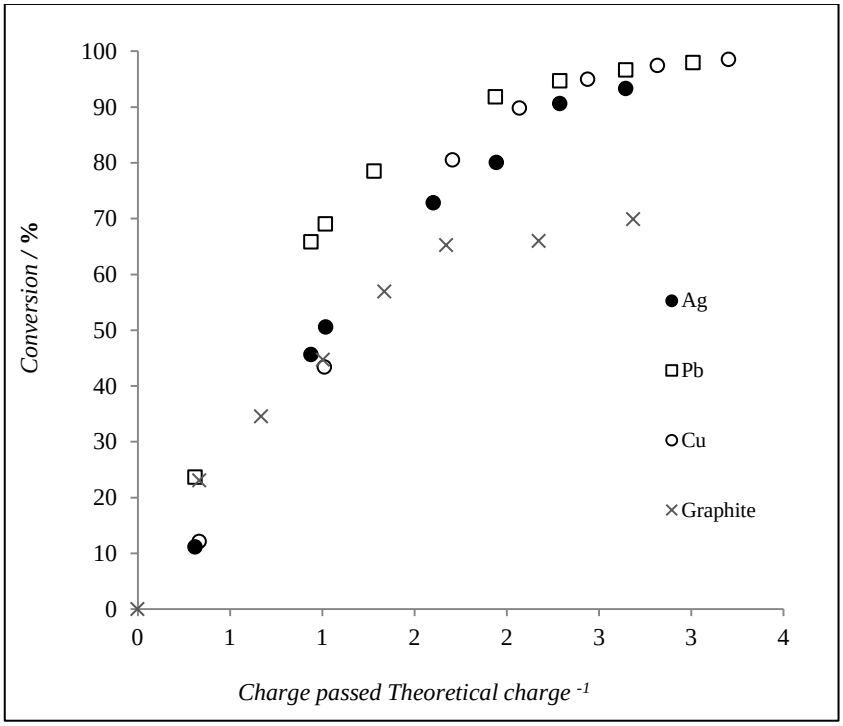

5.1b

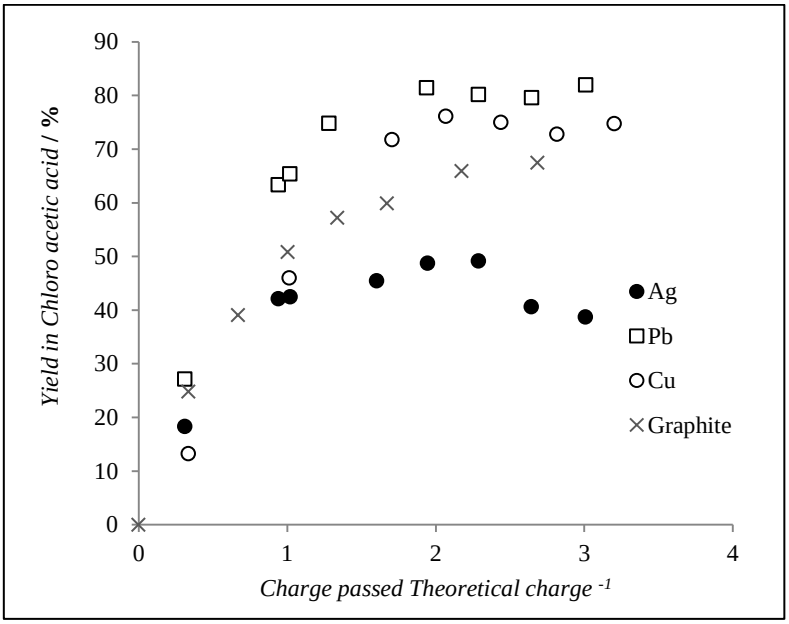

5.1c

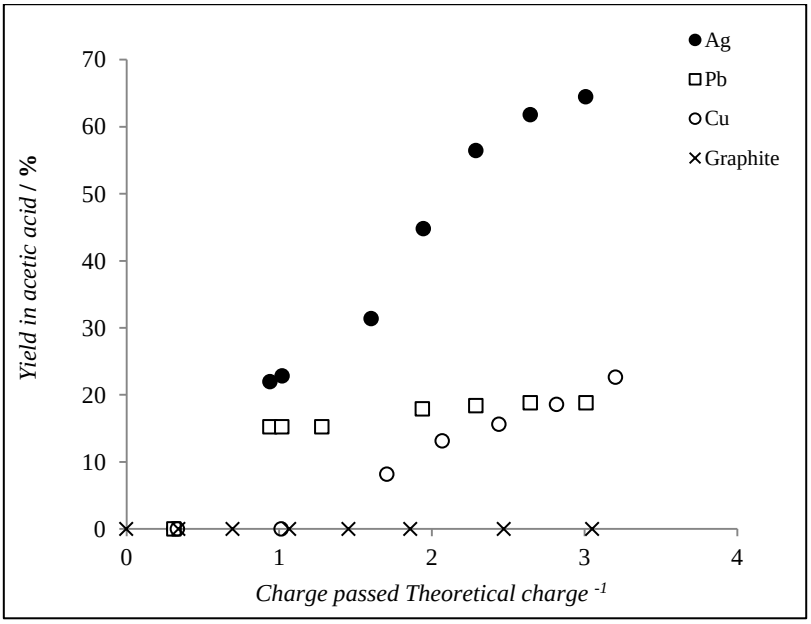

Figure 5.1. *Effect of the nature of the anode on the reduction of DCAA. Plot of DCAA conversion (a), yield in MCAA (b) and AA (C) vs. Q/Q^{th}. Electrolysis of a water solution of*

DCAA (0.1 M) and Na_2SO_4 (0.1 M) at Ag (•), Pb (□), Cu (o) and graphite (x) cathode and Ti/IrO_2-Ta_2O_5 anode in the conventional macro cell. Current density: 230 A/m^2. Q is the charge passed and Q^{th} is the theoretical charge necessary to convert DCAA with a bi-electronic process.

Furthermore, Cu cathode is expected to be more resistant if pH is increased from 1 to 4 as shown also by SEM analyses. To understand the effect of pH on the conversions, please consider that, at higher pH, equilibriums reported in equations (5) and (6) are shifted to the right giving the dissociated form of the acids that are likely to be more resistant to the cathodic reduction due to their anionic charge.
As a result higher pH results in lower current efficiencies but in higher selectivity.

$$Cl_2CHCOOH = Cl_2CHCOO^- + H^+ \quad (5)$$

$$ClCH_2COOH = ClCH_2COO^- + H^+ \quad (6)$$

5.2a

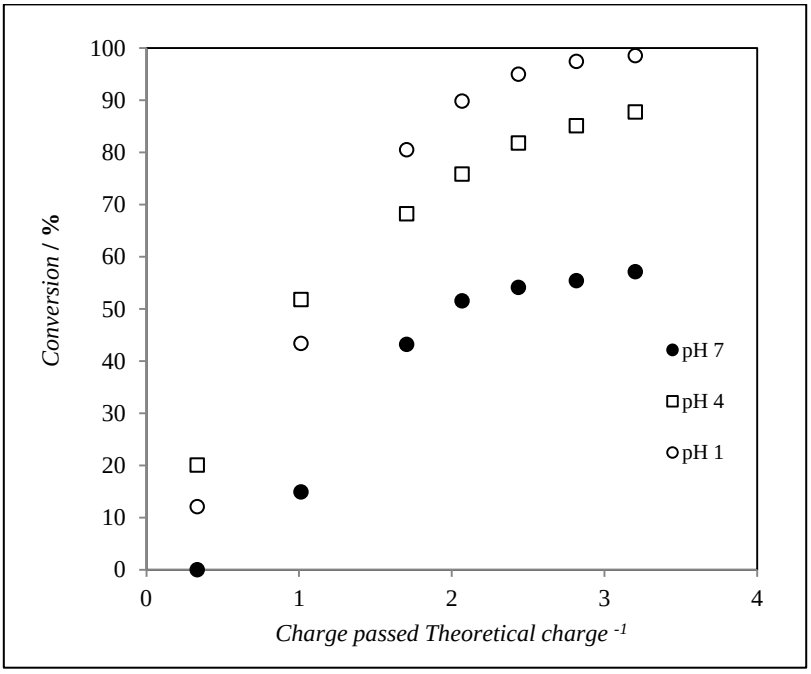

5.2b

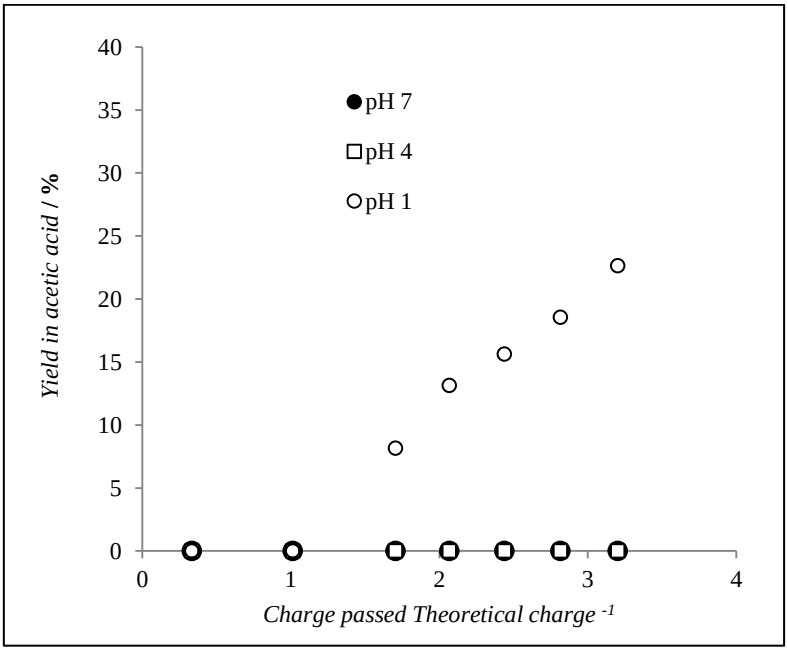

***Figure 5.2**. Effect of pH on the reduction of DCAA at Cu cathode and Ti/IrO_2-Ta_2O_5 anode in the conventional macro cell. Plot of DCAA conversion (a) and yield in AA (b) vs. Q/Q^{th} at pH 1 (•), 4 (□) and 7 (o). Electrolysis of a water solution of DCAA (0.1 M) and Na_2SO_4 (0.1 M). Current density: 230 A/m^2. Q is the charge passed and Q^{th} is the theoretical charge necessary to convert DCAA with a bi-electronic process.*

5.3 Electrolyses in micro-reactors

5.3.1 Effect of cathode and adopted micro-reactor

A second series of electrolyses was carried out in the two microfluidic reactors (as described in paragraph 3.3.2.1 and 3.3.2.2) under a continuous mode with copper and graphite cathodes and Ti/IrO_2-Ta_2O_5 as anode with the aim to evaluate both the effect of the cathode nature and of adopted micro reactor. First experiments were performed in micro-reactor II in the presence of a water solution of DCAA (0.1 M) without the addition of a supporting electrolyte at various flow rates (0.02-0.1 ml/min) and at a current density of 230 A/m^2. A nominal inter-electrodic distance of 100 µm was used. A pH close to 1 was obtained as a result of the presence of DCAA. Quite low cell potentials were recorded in the micro reactor (2.3 - 2.8 V) in spite of the fact that electrolyses in the micro cell were performed in the absence of an added supporting electrolyte because of the very low inter-electrodic distances. The conversions and the yields in MCAA slightly depended on the adopted cathode. Higher conversions, yields and selectivity were recorded at compact graphite cathode (table 5.1, entries 1 and 3 and figure 5.3a). However, very high selectivity in MCAA were achieved in the micro reactor also at copper cathode because of very poor formation of AA. As shown in fig. 5.3b, when experiments were performed in the micro reactor, a drastic increase of the selectivity was achieved at copper cathode with respect to that recorded in the conventional macro cell for the same amount of the ratio Q/Qth. This is an intrinsic advantage of the different flow models characterizing the batch reactor and the microreactors. The batch cell can be approximated by a perfectly mixed reactor with residence time corresponding to the whole time of the electrolysis (about 6 h) while microfluidic apparatuses are substantially tubular reactor with laminar flow characterized by much lower average residence times (lower than 2 min). This is the reason why even if large local concentration of monochloroacetic acid are reached in the outlet stream collected from the microreactor, the follow-up reaction of reduction of MCAA to AA (eq. (2)) has a much lower extent. In order to evaluate the effect of the micro reactor on the

performances of the process, some experiments were performed with compact graphite cathode and Ti/IrO_2-Ta_2O_5 anode in both micro-reactors I and II. Quite interestingly, very similar results were achieved for the two micro reactors in terms of yields, conversions (see table 1, entries 3, 5 and 6 and fig. 5.4a) and cell potentials. Hence, it is possible to conclude that the cathodic conversion of DCAA to MCAA can be carried out without supporting electrolyte with low cell potentials and high selectivity and yields in both adopted micro-reactors. It is quite interestingly to mention that micro-reactor I is particularly adapt for a fast screening of operative parameters for the very easy and fast assembly and disassembly while the micro-reactor II is more suited for scale-up, parallelization and industrialization purposes.

Table 5.1 *Effect of pH, nature of the cathode and kind of micro reactor on the process.*[a]

Entry	Cathode	Micro reactor	pH	Current density (A/m^2)	Conversion and yield (%)
1	Copper	II	1	230	83 - 79
2	Copper	II	4	230	70 - 69
3	Graphite	II	1	230	90 – 89
4	Graphite	I	1	290	83 – 80
5	Graphite	I	1	250	92 – 92
6	Graphite	I	1	200	90 - 90

[a] Electrolysis of a water solution of DCAA (0.1 M) at Cu or compact graphite cathode and Ti/IrO_2-Ta_2O_5 anode in micro-reactor I or II. Nominal inter-electrodic distance in the micro-reactor: 100 µm. Flow rate: 0.05 ml/min.

5.3a

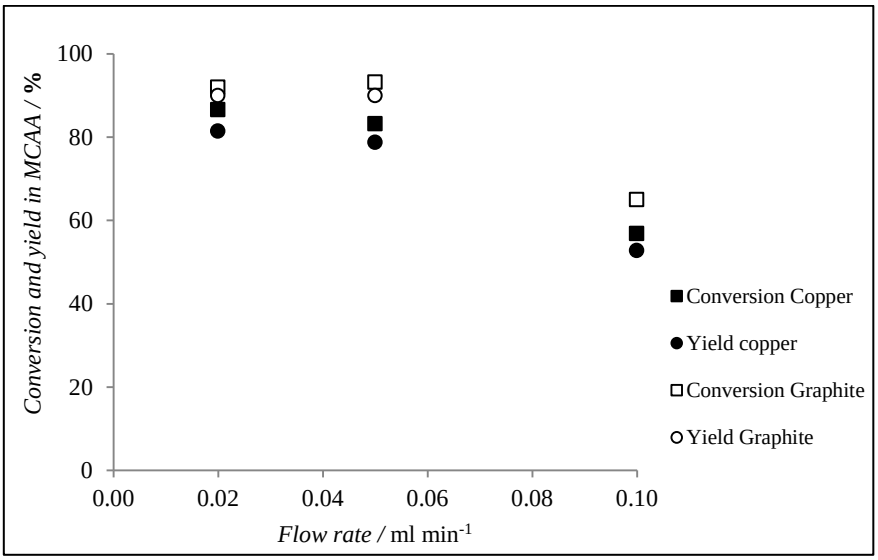

5.3b

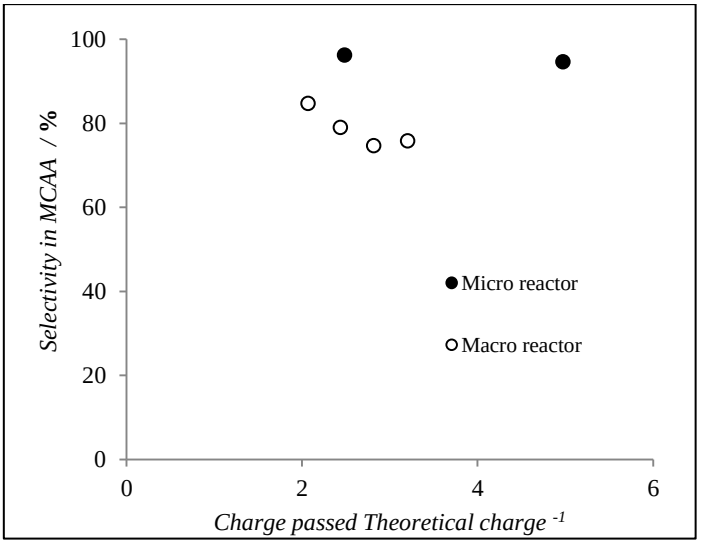

Figure 5.3 *Electrolysis of a water solution of DCAA (0.1 M) at Cu and compact graphite cathode and Ti/IrO_2-Ta_2O_5 anode in the micro-reactor II. a) reports the plot of DCAA conversion (■ copper, □ graphite) and yield in MCAA (• copper, o graphite) vs. flow rate. b) reports the plot selectivity in MCAA vs. Q/Q^{th} achieved in the micro reactor II (•) and in the conventional macro cell (in the presence of 0.1 M Na_2SO_4 as supporting electrolyte) (o)*

equipped with copper cathode. Current density: 230 A/m^2. Q is the charge passed and Qth is the theoretical charge necessary to convert DCAA with a bi-electronic process. Nominal inter-electrodic distance in the micro-reactor: 100 µm.

5.3.2 Longer time experiments

In order to evaluate the long-term reliability of adopted cells and cathodes, the two devices worked for at least two weeks for 10 hours every day without disassembly. Micro reactor I was assembled with a copper cathode while micro reactor II with a compact graphite one. In both cases, no leakages nor significant variations of the cell potentials were observed, thus showing the reliability of adopted cells. Compact graphite cathode gave also very reproducible results in terms of yields and conversions after two weeks of operation while the copper one gave poor reproducibility of results after one week because of the degradation of copper (observed by SEM analyses). Some experiments were repeated by changing the pH (from 1 to 4) with copper cathode to increase the cathode stability. On the other hand, at pH of 4 lower yields were achieved (table 1, entries 1 and 2) and a poor reproducibility of data was still observed after one week of operations.

5.3.3 Effect of flow rate, current density and inter-electrodic gap

To evaluate in detail the effect of flow rate and current density, numerous experiments were performed in the micro reactor I equipped with graphite cathode, Ti/IrO_2-Ta_2O_5 anode and a nominal inter-electrodic distance of 100 µm by working at various flow rates (namely, 0.02, 0.05, 0.1 and 0.2 mL/min) and current densities (50, 150, 200, 250 and 300 A/m^2). As shown in figure 5.4a, at higher adopted flow rates (namely, 0.1 and 0.2 mL/min), yields in MCAA increased with current densities as a result of the higher charge passed. At these flow rates, current densities of 300 A/m^2 were necessary to achieve good yields. Conversely, at 0.05 ml/min, very high yields in MCAA were achieved in a large range of current density because of the high average residence time. Indeed, yields higher than 90% were achieved by working from 200 (current efficiency 18%) to 300 A/m^2 (current

efficiency 12%). Yields in MCAA increased by lowering the flow rate from 0.2 to 0.05 ml/min because of the higher residence times t_{res} (t_{res} is about 48 and 12 sec for 0.05 and 0.2 ml/min, respectively). Similar yields but drastically lower current efficiencies were achieved by a further decrease of the flow rate from 0.05 to 0.02 ml/min (t_{res} is about 48 and 120 sec for 0.05 and 0.02 ml/min, respectively). As an example, at 150 A/m^2 current efficiencies of 21% and 9% were achieved at 0.05 and 0.02 ml/min, respectively. Hence, 48 sec was a sufficient residence time for the quantitative conversion of DCAA at employed conditions. Quite interestingly, at all adopted operative conditions, selectivity was close to 100%. On overall, a flow rate of 0.1 ml/min and a current density of 300 A/m^2 allowed to achieve the best compromise between productivity, yield in MCAA (83%) and current efficiency (22%) among adopted operative conditions. The productivity achieved in these conditions was however not very high (about 0.5 mmol/h).

5.4a

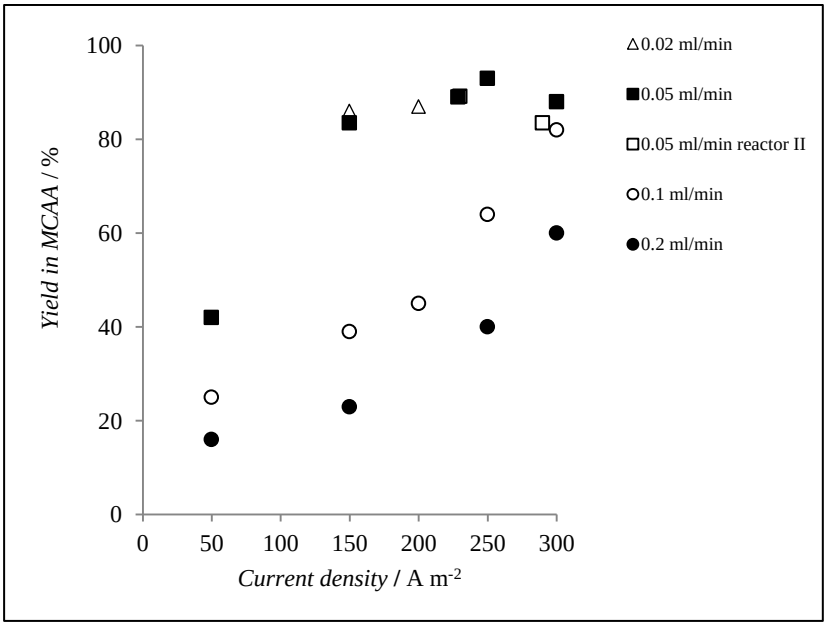

5.4b

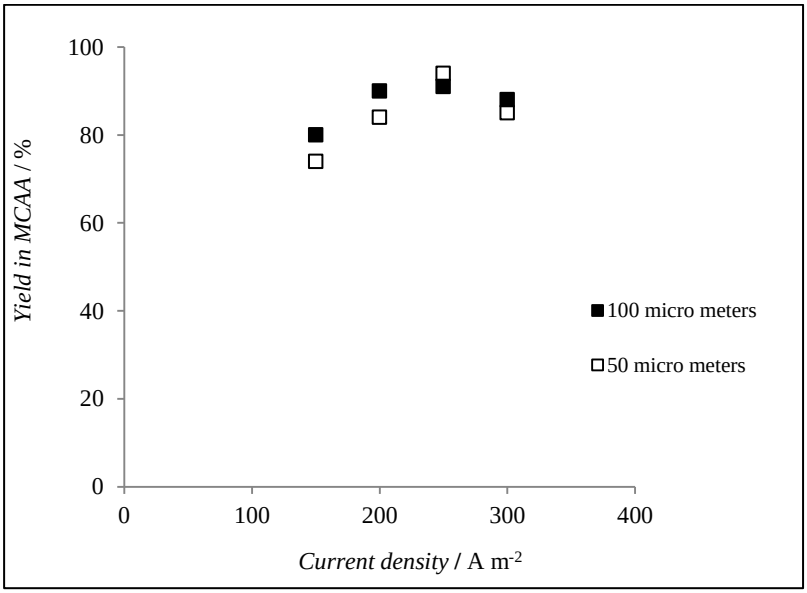

5.4c

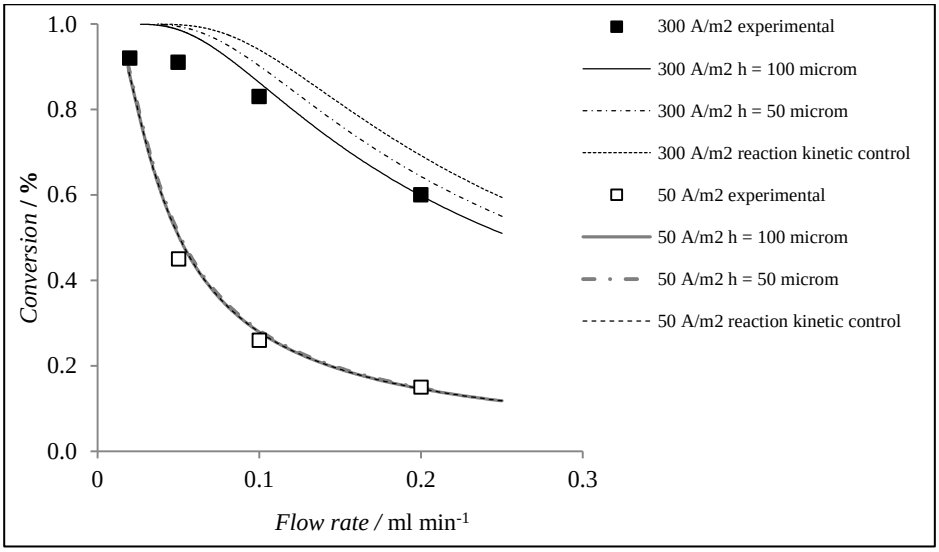

Figure 5.4. *Effect of operative parameters on the electrolysis of a water solution of DCAA (0.1 M) at compact graphite and Ti/IrO_2-Ta_2O_5 anode in the micro-reactor I and II. A reports the effect of current density and flow rates: 0,02 (Δ reactor I), 0,05 (■ reactor I, □ reactor II), 0,1 (o reactor I) and 0,2 mil/min (• reactor I) in micro-reactors with a nominal inter-electrodic distance h of 100 µm. B reports the effect of the inter electrodic distance h (50 (□)*

and 100 µm (■)). C reports the theoretical predictions obtained by using the theoretical model presented in the appendix A2 at 50 (green lines) and 300 A/m^2 (black lines) for h = 50 (dashed lines) or 100 µm ((full lines) by using a value of [RH] = 0.1 M and experimental results obtained by using h = 100 µm at 50 (■) and 300 A/m^2 (□).*

Hence, the devices will be modified in the next future to present higher surfaces and productivities. In particular, this objective should be easily achievable in micro reactor II.

To better rationalize experimental results, a simple theoretical model previously developed by some of authors was used (see Appendix A2). At lower adopted current densities, the process occurred under the kinetic control of charge transfer. Indeed, the applied current density was significantly lower than the limiting current density $i_{lim} = 2FK_m[\overline{RH}]_x$ (where 2 is the number of electrons involved for the reduction of DCAA to MCAA, F is the Faraday constant, $K_m = Sh/2h$ is the mass transfer constant, Sh the Sherwood number, h the inter-electrodic distance, $[\overline{RH}]_x$ the average concentration of the substrate for a given value of the distance x from the inlet of the reactor in the direction of the flow) expected for for a process under mass transfer control. Hence, at the lower adopted current densities, the conversion was just determined by the competition between DCAA and water reduction and by the charge passed that at its turn depends on the flow rate, the electrode surface and the adopted current density. The competition between DCAA reduction and parasitic processes can be described by a fitting parameter $[RH]^*$, the value of $[\overline{RH}]_x$ which gives a current density for the substrate reduction equal to the current density involved for parasitic processes, e.g. the value of $[\overline{RH}]_x$ that gives a current efficiency of 50%, that was assumed, in a first approximation approach, to be constant for a given cathode (see appendix A2).

Also at the higher adopted current densities, the process never occurred under the kinetic control of the mass transfer of the substrate to the cathode surface

because of the relatively high DCAA initial concentration and the reduced inter-electrodic distance. As an example, at 300 A/m^2, the process occurred under the kinetic control of the charge transfer in the first portions of the micro reactor and under a mixed control in the last ones. As shown in figure 5.4c, a quite good fitting between experimental data and theoretical predictions based on the adopted model (appendix A2) was observed in spite of the strong approximations used in the model for both low and high current densities with the exception of the lower flow rates. Indeed, for 0,02 and 0,05 ml/min lower conversions were obtained with respect to that predicted by the model. This is probably due to the fact that for very low flow rates, the axial mixing (not considered by the model) cannot be more neglected, thus giving rise to lower conversions. Since, the process is slightly affected by mass transfer kinetic under all adopted operative conditions, a further reduction of the inter-electrodic distance should not results in significant modification of yields as predicted by theoretical predictions reported in fig. 5.4c. Indeed, when experiments were repeated with a smaller inter-electrodic distance (50 μm), very similar results in terms of yields and conversions were obtained (fig. 5.4b) with respect to that achieved with a nominal distance of 100 μm.

5.4 Utilization of microreactors in series and stack

As shown in previous paragraph, at microfluidic reactors equipped with compact graphite cathode, chloroacetic acid can be obtained at low cell potentials in water with high conversions and selectivity under a single-pass mode without added supporting electrolyte. These proof-of-concept experiments involved quite small electrode surface areas (in most of cases 4 cm^2), thus limiting the productivity of the microreactor and the final concentration of the product. In fact, this is a general issue since most of the studies reported in literature on the electrosynthesis of fine chemicals in microreactors exhibit quite low productivities [1] as a result of low electrode surfaces and small flow rates. Hence, the scaling out of these processes is of paramount relevance in order to assess their feasibility for applicative purposes. Various authors have explained that the parallelization of a large number of cells can

allow to achieve quite high productivity [1-4]. However, the parallelization of devices characterized by too low electrode surfaces is expected to be operated with low initial concentrations of substrate, thus limiting the concentrations of the target product. In order to be able to achieve both high conversions and high initial concentrations of the substrate, using microreactors in series seems an attractive but unexplored solution. In addition, several microreactors operating in series under a continuous mode allow a facile modulation of the current density on each electrode thus adapting it to the input solution which opens new perspectives from the point of view of the optimization of the synthetic processes.

In the next paragraph, we want, in particular, to examine in detail the interest of using more reactors in series for the conversion of dichloroacetic acid to chloroacetic acid. Two different approaches were used: in the first one, three micro reactors operated in series (as described in paragraph 3.3.2.3) in order to modulate the current density in each reactor while in the second case a simple and compact microfluidic stack with different chambers in series was used (as described 3.3.2.4). The effect of some operating parameters including the current density, the flow rate and the initial concentration of dichloroacetic acid was investigated in detail.

5.4.1 Experiments performed using one or three microreactors in series

A first series of experiments was performed using one or three micro reactors in series. Each device was equipped with compact graphite cathode and Ti/IrO_2-Ta_2O_5 anode (electrode surface 4 cm^2) following previous investigations. A nominal inter-electrodes distance of 100 µm was achieved through the use of appropriate spacers. Electrolyses were performed galvanostatically at a current density of 330 A/m^2 on solutions of dichloroacetic acid in water without supporting electrolyte.

As shown in previous paragraph and in Table 5.2, using a single micro device with a cathode surface area of about 4 cm^2 gave quite high yields (close to 90 %) using moderate values of the flow rate (0.05 ml/min) and of the initial concentration of the substrate (0.1 mol/dm^3), thus corresponding to a productivity of about 0.3 mmol/h (Table 5.2, entry 1).

When the current density and/or the flow rate or the initial concentration was significantly enhanced, a drastic decrease of the yield occurred, thus limiting the final productivity of the single microreactor cell. For example, doubling the flow rate from 0.05 to 0.1 ml/min resulted in a decrease of the yield to about 50% while the overall productivity did not change appreciably (Table 5.2, entries 1 and 2).

Table 5.2 *Experiments performed with one or three micro reactors in series or with a stack assembled with two or three cells.*[a]

Entry	Reactor system - overall surface (cm^2)	Current density (A/m^2) / Flow rate (mL/min)	Initial Dichloro acetic acid concent. (M)	Conversion and yield (%)	Productivity (mmol/h)
1	Single reactor 4 cm^2	330 / 0.05	0.1	94 – 93	0.3
2		330 / 0.1	0.1	51 - 50	0.3
3	Three reactors 12 cm^2	330 / 0.1	0.3	89 – 82	1.5
4		480 / 0.1	0.4	82 – 80	1.9
5		350,330, 310[b] / 0.1	0.3	91 – 87	1.6
6	Single reactor 6 cm^2	330 / 0.1	0.1	90 – 86	0.5
7		330 / 0.1	0.3	61 - 57	1.0
8	Stack 12 cm^2	330 / 0.1	0.3	88 - 81	1.5
9	Stack 18 cm^2	330 / 0.1	0.3	97 – 93	1.7
10		430 / 0.2	0.3	89 – 85	3.1
11		370 / 0.1	0.5	92 – 84	2.5

[a] Electrolyses of a water solution of dichloroacetic acid at compact graphite cathode and Ti/IrO_2-Ta_2O_5 anode. Nominal inter-electrodes distance in the micro-reactor: 100 µm.

[b] Electrolyses performed by using different current densities in the three reactors.

Conversely, when the experiments were repeated using three reactors in series (with an overall surface area of 12 cm^2, as described in paragraph 3.3.2.3) a significantly higher productivity was achieved affording good yields while performing at entrance concentrations (0.3 to 0.4 M) of dichloroacetic acid (table 5.2, entries 3 and 4) as a result of developing a high electrode surface area in three segments.

Using three different devices in series operating under a continuous mode allows applying a different current density in each reactor. Hence, a series of experiments was performed by fixing the current density of the second reactor (330 A/m^2) and changing the current density of the first and the third reactors in order to achieve the same overall charge consumption. When the current densities were imposed at increasing values from the first reactor to the last one, low conversions and selectivity were achieved (Fig. 5.5).

Conversely, when the imposed current density decreased from the first to the third reactor, an increase of the selectivity was observed (fig. 5.5). In particular, the selectivity reached a value of 100% when the experiments were performed with 560 and 100 A/m^2 in the first and the third reactor, respectively. In order to understand this result it is useful to recall that the last reactor performs in the presence of the lowest concentration of dichloro acetic acid and the highest one in the more difficultly reduced chloro acetic acid. Thus, a lower current density in the last reactor allows avoiding too high cell potentials which would favor the successive cathodic reduction of chloroacetic acid into acetic acid (eq. (2)). However, a too low current density in the last reactor results in a decrease of the conversion and consequently of the yield (fig. 5.5). For a constant current density of 330 A/m^2 applied to the central microreactor, the highest yield value (87%) due to simultaneous high values of the conversion (91%) and of the selectivity (96%) was achieved using a slight modulation of the current density, i.e., imposing 350 and 310 A/m^2 values in the first and in the last reactor (Figure 5.5 and Table 1, entry 5).

Hence, these results show that the modulation of a constant global current density among the three microreactors offers a suitable mean of increasing the selectivity, the yield and the productivity.

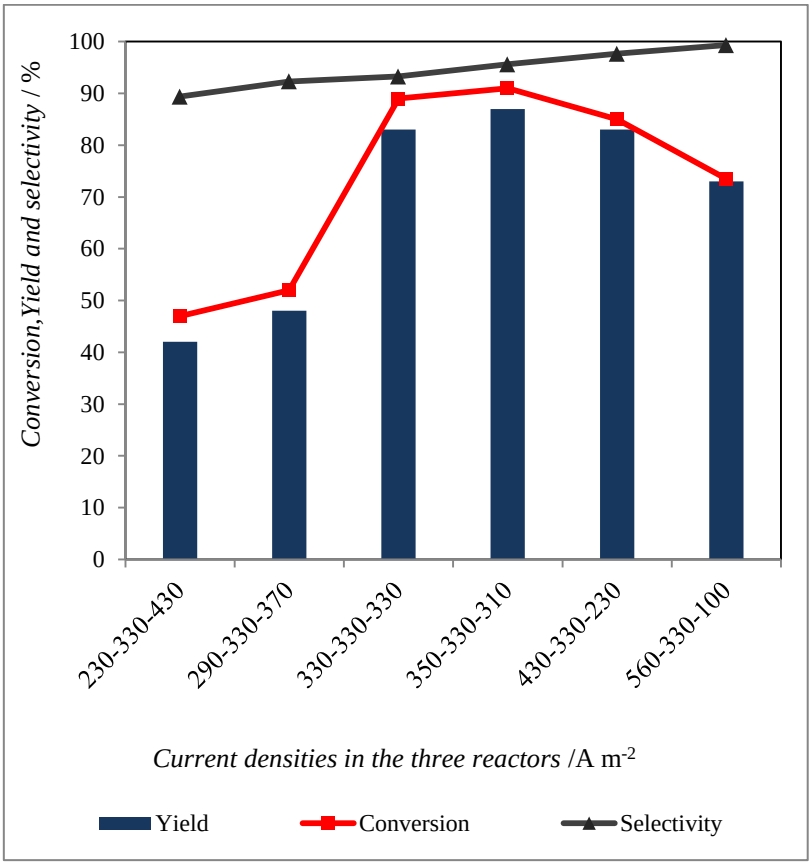

Figure 5.5 *Dichloro acetic acid conversion, yield and selectivity in chloro acetic acid obtained using different current densities in three micro fluidic reactors in series. Electrolyses of aqueous solutions of dichloro acetic acid (0.3 M) at compact graphite cathodes and Ti/IrO_2-Ta_2O_5 anodes. 100 µm nominal inter-electrodes distance and 4 cm^2 electrode surface area in each micro-reactor.*

Quite interestingly, the adopted process is also characterized by quite good performances in terms of yields and selectivity when using a constant current density (Table 5.2, entry 3 and Figure 5.5). Hence, the following experiments were performed by using a stack with high electrode surface with the aim to increase the productivity of the cell with a more compact device.

5.4.2 Experiments performed using a micro fluidic stack equipped with one, two or three electrode chambers

A second series of electrolyses was carried out in a stack equipped with one, two or three electrolytic chambers in series. The electrode surface area of each chamber was 6 cm^2.

First experiments were performed with a single chamber at different values of flow rate (namely, 0.05, 0.1 and 0.2 mL/min), current density (from 100 to 400 A/m^2) and initial concentration of dichloro acetic acid (0.1, 0.2 and 0.3 M). As shown in fig. 5.6a, a very high yield was achieved using 170 A/m^2, 0.05 ml/min and an initial concentration of dichloro acetic acid of 0.1 M as a result of a simultaneous high conversion and selectivity (both close to 97%). However, under these operating conditions, a high value (~ 6.2) of the ratio Q/Q^{th} between the charge passed and the theoretical one required for the conversion of dichloroacetic acid to chloroacetic acid was involved, thus giving rise to quite low current efficiency (15 %) (fig. 5.6c). Furthermore, a quite low productivity was achieved (slightly lower than 0.3 mmol/h) because of required low values of flow rates and initial concentration of the substrate (fig. 5.6b). Indeed, for this low value of the initial concentration, quite high conversions were achieved and an increase of the current density resulted at least in part in an enhancement of the parasitic cathode processes (see equations (2) and (3)). Quite interesting, for this low value of the initial concentration of dichloroacetic acid at 0.05 ml/min the plot yield vs. current density showed a maximum (fig. 5.6a) as a result of the fact that at very high conversions higher current densities resulted mainly in the conversion of chloroacetic acid to acetic acid (eq. (2)).

In order to increase the productivity, some of the above mentioned experiments were repeated in a stack equipped with 2 (12 cm^2) or 3 (18 cm^2) electrolytic microchambers in series and fed with an aqueous solution of 0.3 M dichloroacetic acid.

5.6a

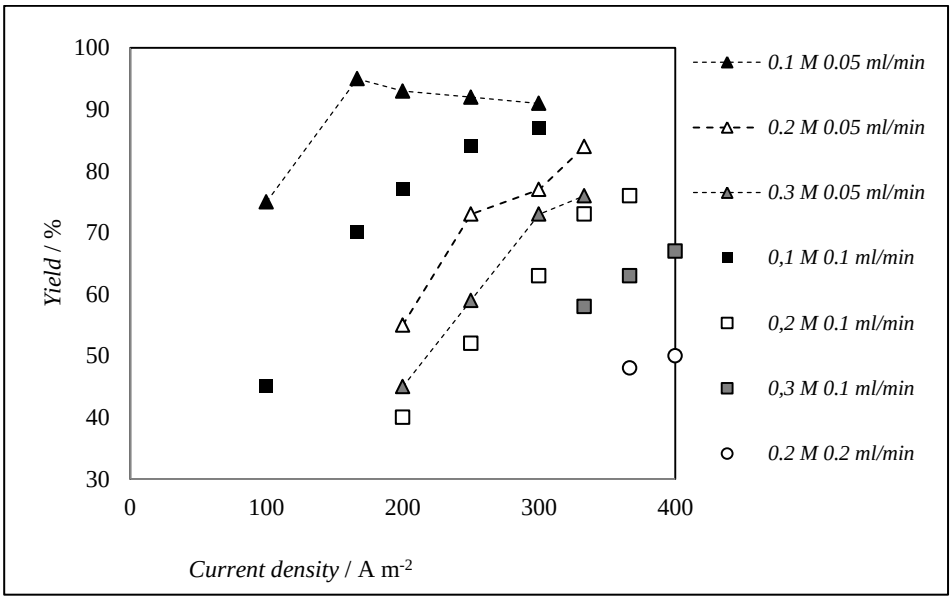
100
90
80
70
60
50
40
30
Yield / %
0
100
200
300
400
Current density / A m-2
0.1 M 0.05 ml/min
0.2 M 0.05 ml/min
0.3 M 0.05 ml/min
0,1 M 0.1 ml/min
0,2 M 0.1 ml/min
0,3 M 0.1 ml/min
0.2 M 0.2 ml/min

5.6b

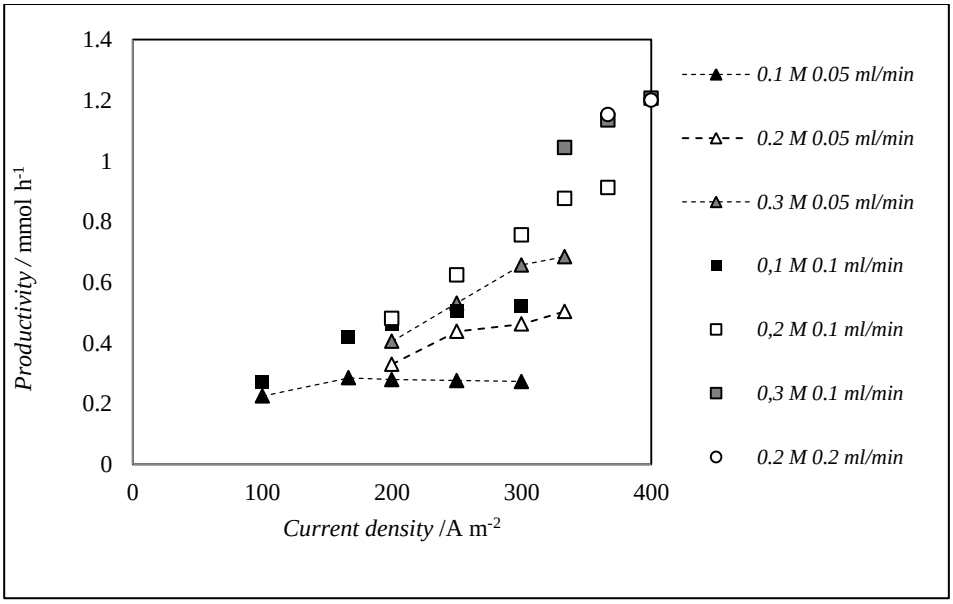
1.4
1.2
1
0.8
0.6
0.4
0.2
0
Productivity / mmol h-1
0
100
200
300
400
Current density /A m-2
0.1 M 0.05 ml/min
0.2 M 0.05 ml/min
0.3 M 0.05 ml/min
0,1 M 0.1 ml/min
0,2 M 0.1 ml/min
0,3 M 0.1 ml/min
0.2 M 0.2 ml/min

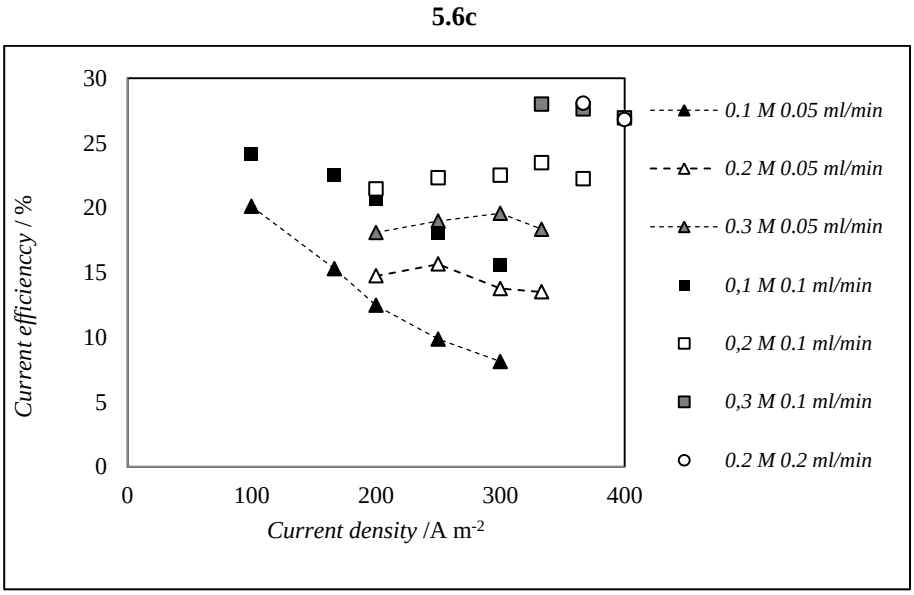

Figure 5.6. *Plot of yield (5.6a), productivity (5.6b) and current efficiency (5.6c) vs. current density. Electrolysis of a water solution of dichloroacetic acid (0.1, 0.2 or 0.3 M) at various flow rates (0.05, 0.1 or 0.2 ml/min) at compact graphite cathode and Ti/IrO_2-Ta_2O_5 anode in a microfluidic cell. Nominal inter-electrodes distance in the micro-reactor: 100 µm. Electrode area for the device: 6 cm^2.*

As shown in fig. 5.7, increasing the number of microcells increased the productivity and the yield in chloro acetic acid as a result of the higher electrode area. For example, when the electrolyses were performed at 0.1 mL/min with one single cell with an initial concentration of the substrate of 0.3 M, the yields were lower than 70 % using a current density up to 400 A/m^2 (fig. 5.7a). When stacks with 2 or 3 electrode microchambers were used, the yield increased from above 80 to close to 95 %, respectively, using a same current density close to 400 A/m^2 (fig. 5.7a). Therefore, the enhanced number of cells gave rise as expected to a significant increase of the productivity (fig. 5.7b). When the flow rate was increased to 0.2 mL/min, using a stack with three compartments allowed to still achieve good yields (fig. 5.7a) and higher productivity (up to 3 mmol/h). A three microcells stack was then expected to yield good productivity for high values of the initial substrate

concentration. To test this issue, a series of experiments was carried out in the three-microcell stack (electrode surface area 18 cm^2) at various flow rates (namely, 0.05 and 0.1 mL/min), current densities (250, 300, 330 and 370 A/m^2) and initial substrate concentrations (0.3, 0.4 and 0.5 M).

5.7a

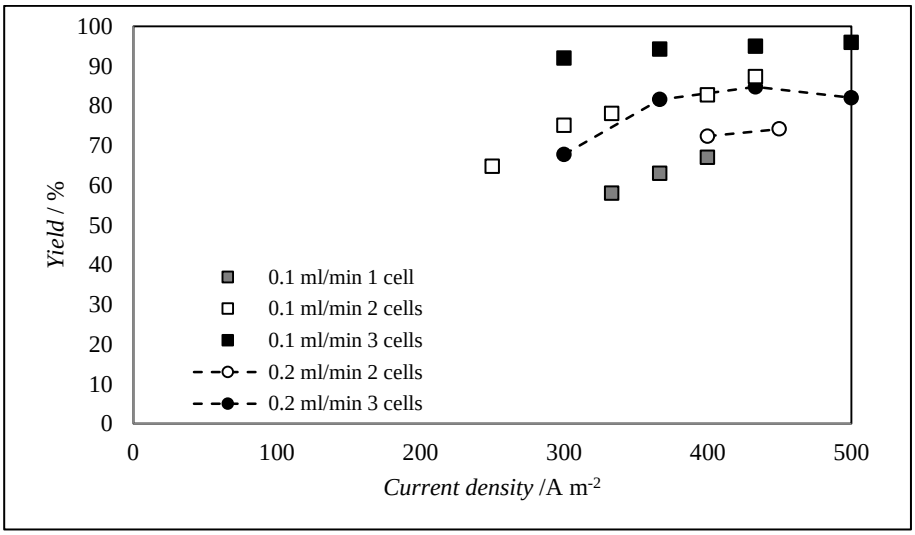

5.7b

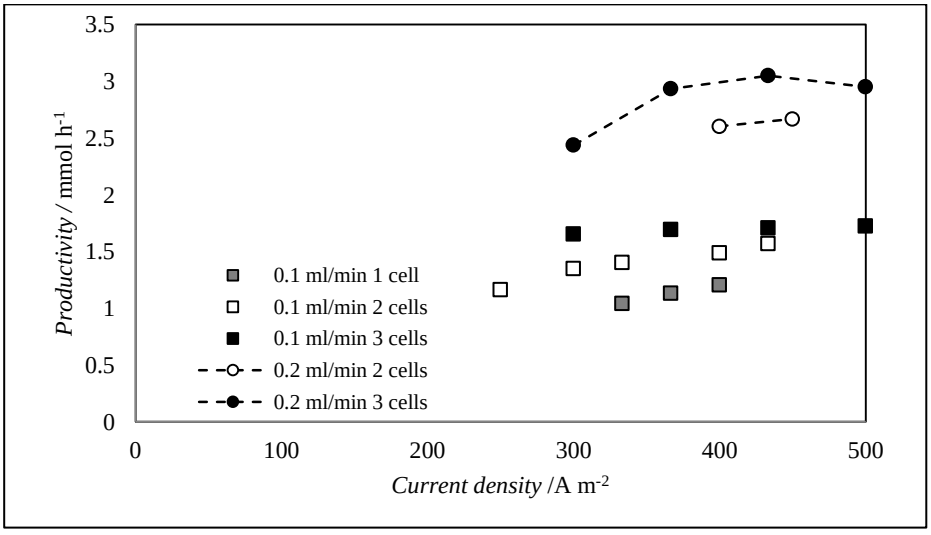

Figure 5.7 *Variations of yield (a) and productivity (b) vs. current density. Electrolyses of aqueous solutions of dichloroacetic acid (0.3 M) at various flow rates (0.1 or 0.2 mL/min) at*

compact graphite cathodes and Ti/IrO_2-Ta_2O_5 anodes. Nominal inter-electrodes distance in the micro-reactor: 100 µm. Electrode area for the stack: 6, 12 (2 cells) or 18 (three cells) cm^2.

Quite interestingly, this afforded pretty good yield (fig. 5.8a) and selectivity (higher than 90 %) for all initial concentrations of dichloro acetic acid tested.

In particular, the highest yields (higher than 90% at 0.1 ml/min using a current density of 300 A/m^2) were obtained using a 0.3 M initial substrate concentration. When the initial concentration of the substrate was increased to 0.4 or 0.5 M, quite good yields could still be achieved upon increasing the current densities or lowering the flow rates (fig. 5.8a). For example, at a 0.5 M initial substrate concentration yields of about 84 and 95 % were obtained using 0.1 mL/min and 370 A/m^2 or 0.05 mL/min and 300 A/m^2, respectively. Notably, such high initial concentrations of the substrate allowed to increase both the productivity (fig. 5.8b) and the current efficiency (fig. 5.8c).

5.8a

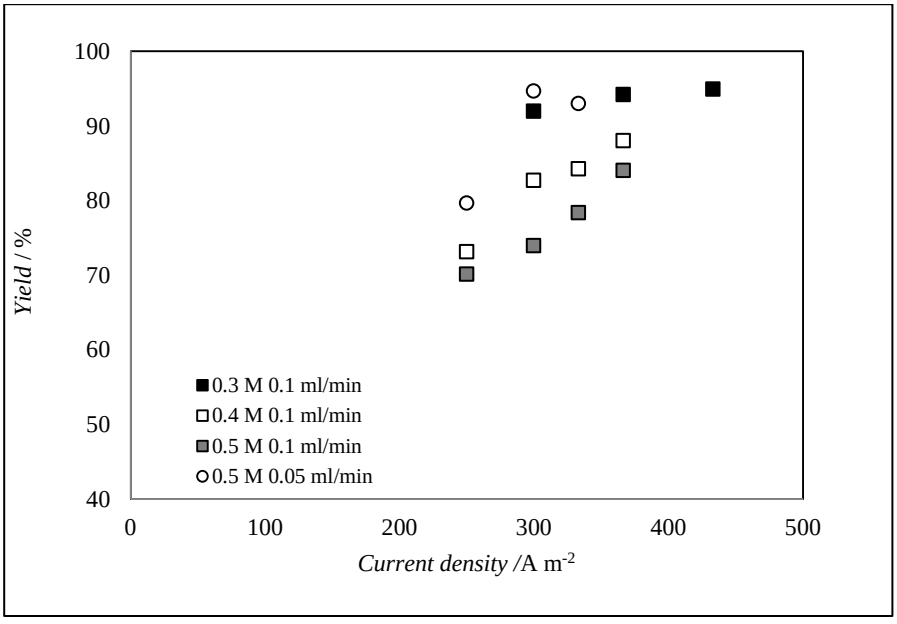

5.8b

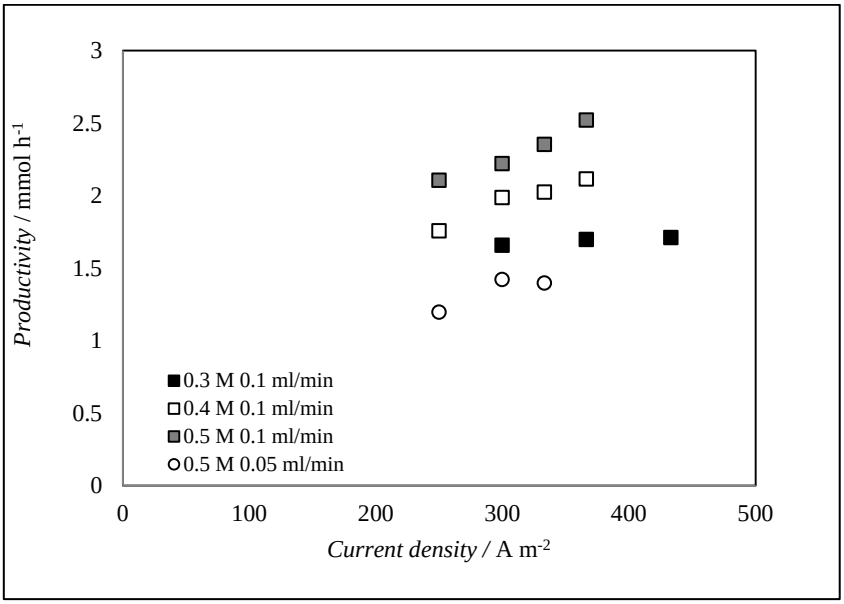

5.8c

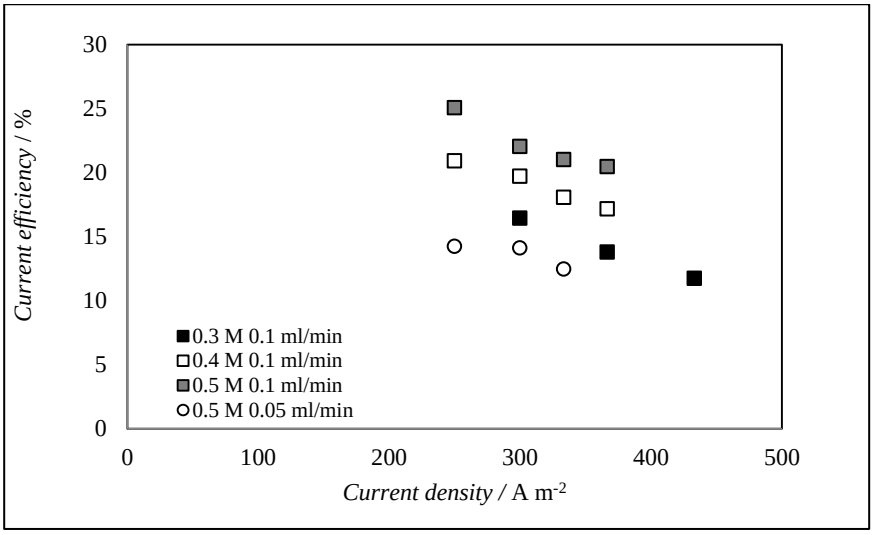

***Figure 5.8**. Plot of yield (a), productivity (b) and current efficiency (c) vs. current density. Electrolysis of a water solution of dichloroacetic acid (0., 0.4 or 0.5 M) at various flow rates (0.05 or 0.1 ml/min) at compact graphite cathode and Ti/IrO_2-Ta_2O_5 anode. Nominal inter-electrodes distance in the micro-reactor: 100 µm. Electrode area for the device: 18 (three cells) cm^2.*

This is worth mentioning since allowance of high initial substrate concentrations is usually desired from applicative points of view in order to obtain more concentrated solutions of the target product and to avoid mass transfer controlled kinetic regimes. In this context, the present method allows to by-pass the classical microfluidic reactors limitation related to low electrode surface areas and which as a consequence are often operated onto low initial substrate concentrations in order to achieve high yields after one single passage. To avoid this limitation, the productivity is usually thought to be increased through a parallelization of the electrodes. This, however, does not allow to increase the final concentration of the product. This report show that cumulating both strategies, viz., parallelizing multi-microcell stacks in series should allow achieving both high productivity and high concentrations of the product.

5.5 Conclusions

The electrochemical conversion of dichloroacetic acid to monochloroacetic acid was performed in a conventional cell and in different microfluidic devices.

The performances of the process in terms of conversion, selectivity and stability of electrodes strongly depended on the nature of the cathode material. Good results were achieved with graphite electrodes while copper and silver cathodes gave worse results in terms of selectivity and stability. The utilization of both employed microreactors allowed to achieve high conversions and selectivity with a single-pass continuous process with low cell potentials and in the absence of supporting electrolyte. Interestingly, the utilization of micro cells allowed to increase the selectivity of the process by reducing the relevance of follow-up reaction as an effect of low residence times. Experiments in microreactors were carried out for long times (up to one month) without leakages.

A stacks of several cells in series allowed a substantial increase of the process productivity and operating at higher initial substrate concentrations. This was coupled to high yields and selectivity in simple and compact devices. Using micro reactors in series allowed also to modulate the current densities in the series reactors,

thus allowing to improve the figures of merit of the process in terms of conversions and selectivity.

The present results offered a proof of concept showing that microreactors in series may result perfectly suitable for operation in the framework of electrochemical synthesis of organics. Work is in progress to improve the design of the cells and to evaluate their feasibility for other chemical reactions.

References

[1] J. Kuleshova, J. T. Hill-Cousins, P. R. Birkin, R. C. D. Brown, D. Pletcher, T. J. Underwood, Electrochimica Acta 56 (2011) 4322-4326.

[2] a) P. He, P. Watts, F. Marken, S. J. Haswell, Lab. Chip. 7 (2007) 141-143; b) P. He, P. Watts, F. Marken, S. J. Haswell, Green Chem.9 (2007)20–22.

[3] C. Paddon, M. Atobe, T. Fuchigami, P. He, P. watts, S. J. Haswell, G. J. Pritchard, S. D. Bull, F. Marken, J. Appl. Electrochem. 36 (2006) 617-634.

[4] A. Ziogas, G. Kolb, M. O'Connell, A. Attour, F. Lapique, M. Matlosz, S. Rode, J. Appl. Electrochem.39 (2009) 2297-2313.

A1. APPENDIX

To rationalize the effect of the air pressure on the electrogeneration of H_2O_2 a simple model was used based on the assumption that both the cathodic reduction of oxygen to hydrogen peroxide and the anodic oxidation of H_2O_2 take place under mass transfer control. Other routes involving H_2O_2 were, in a first approximation approach, neglected. As a consequence of above mentioned assumptions, the concentration of H_2O_2 in the bulk of the solution ($C_{H_2O_2}^{b}$) is expected to change according to equation (1), where $k_{m(O_2)}$ and $k_{m(H_2O_2)}$ are the mass transfer coefficients for O_2 and H_2O_2 respectively, $C_{O_2}^{b}$ is the bulk concentration of oxygen, A_{cath} and A_{an} are the wet surfaces of cathode and anode, respectively, and V is the solution volume.

$$dC_{H_2O_2}^{b}/dt = k_{m(O_2)} C_{O_2}^{b} A_{cath}/V - k_{m(H_2O_2)} C_{H_2O_2}^{b} A_{an}/V \quad (1)$$

Let us introduce the terms $a = k_{m(H_2O_2)} A_{an}/V$, $b = k_{m(O_2)} A_{cath}/V$ and $y = b\, C_{O_2}^{b} - a\, C_{H_2O_2}^{b}$. Assuming that the concentration of oxygen in the solution is fixed at equilibrium value by the continuous feeding of air during the galvanostatic experiments, $dC_{H_2O_2}^{b}/dt = -1/a\, dy/dt$ and Eq. (1) can be written as:

$$dy/dt = -ay \quad (2)$$

As a consequence, $\ln(y/y^{t=0}) = -a\, t$, and the concentration of hydrogen peroxide with the time can be given by the following expression given that $y^{t=0} = b\, C_{O_2}^{b}$ as no hydrogen peroxide was present at the beginning of the electrolyses:

$$C_{H2O2}^{b} = bC_{O2}^{b} \frac{[1-\exp(-at)]}{a} \quad (3)$$

Since we are interested only to evaluate the effect of the pressure on the system, which results mainly on the variation of $C_{O_2}^{b}$, and we performed experiments in such

a way to fix the flow-dynamic regime *a* and *b* are substantially the same for all experiments and they can be simply obtained as fitting parameters for the electrolyses carried out at atmospheric pressure. As shown in figure 4.17, a good fitting was obtained for $a = 2.6\ 10^{-3}\ s^{-1}$ and $b = 3.1\ 10^{-4}\ s^{-1}$ using 8 mg/L for $C_{O_2}^{\ b}$. Please consider that the ratio $b/a = k_{m(O_2)}\ A_{cath}/(k_{m(H_2O_2)}\ A_{an})$ assumed a value of 8.6 in agreement to the fact that a drastically higher area of the cathode was used with respect to that of the anode ($A_{cath}/A_{an} > 10$).

Worth mentioning, when the experiments were repeated at 6 and 11 bar the theoretical predictions based on eq. (3) well predict the experimental data (Fig. 4.18 and 4.19) using the same values of *a* and *b* obtained at 1 bar and changing the $C_{O_2}^{\ b}$ according to the Henry law thus offering confirmation that modification of the flow-dynamic regime can be neglected with adopted experimental set-up.

A2. APPENDIX

In order to better rationalize the results obtained in the micro reactor, a very simple model previously developed by some of the authors for the oxidation of organics in water in micro reactors was here extended to reduction processes.[21] The following assumptions were considered:

- Reduction of the substrate takes place only by cathodic reaction (e.g., no homogeneous reduction processes are considered).

- Amperostatic electrolyses are considered since the galvanostatic mode is general preferred from an applicative point of view. An uniform current density in the reactor is considered for simplicity.

- A parallel plate micro reactor is considered where h is the height of the channel (which coincides with the inter electrodic gap), W and L the width and the length of the channel (and of the electrodes), respectively. Electrolyte solution flows through the reactor in the x-direction with an average velocity u_{av}. We assume that electrodes are both very wide (e.g., $W/h >> 1$), so that the formulation of the problem can be approximated to a two-dimension one, and very long (e.g., $L/h >> 1$). Usually, the flux of the organic at the electrode J as a function of x is expressed by the following equation:

$$J = -D\left(\frac{\partial[RH]}{\partial y}\right)_{y=0,x} = k_m([\overline{RH}]_x - [RH]_{y=0,x}) = -Sh\frac{D([\overline{RH}]_x - [RH]_{y=0,x})}{2h} \qquad (4)$$

- where $[\overline{RH}]_x$ is the average concentration of the organic for a given value of x, k_m is the mass transfer coefficient and $Sh = 2k_m h/D$ the Sherwood number. It is important to observe that the value of Sh depends strongly on several factors. In the absence of bubble gas evolution, the Sh number depends on the geometry of

the channel, the ratio between the length of the entrance zone for the concentration profile and the total length of the reactor and the reaction kinetics at the reactor wall.In particular, by neglecting the entrance zones, *Sh* is expected to assume the limiting values of 5.384 and 4.86 for oxidation reaction control and mass transfer control, respectively. The effect of bubble gas formation on mass transfer was here neglected according to literature.

– The only competitive process to the reduction of the substrate DCAAto MCAA at graphite cathode is assumed to be the reduction of the solvent. Some cyclic voltammograms recorded a compact graphite cathode in the presence of water, Na_2SO_4 (as supporting electrolyte) and increasing amounts of DCAA (0, 5 and 10 mM) at 0.1 V/s showed that the addition of DCAA does not give rise to the formation of well defined peaks but only to an increase of the current due to the water discharge. Furthermore, the electrolyses carried out in the conventional cell under amperostatic mode reported in paragraph 2.1 occurred from the beginning at a cathode potential (measured by the reference electrode) of about 1.35 – 1.40 V which involves the water reduction. Hence, the competition between water reduction to hydrogen and DCAA reduction was here described, in a first approximation approach, considering that the current efficiency for a given value of x CE_x is given by the following expression:

$$CE_x = \frac{i_{RH}}{i_{app}} = \frac{i_{RH}}{i_{RH} + i_{paras}} = \frac{1}{1 + \frac{i_{paras}}{i_{RH}}} = \frac{1}{1 + \frac{[RH]^*}{[RH]_x^{y=0}}} \qquad (5)$$

– where i_{RH} and i_{paras} are the current densities involved in the reduction of the organic and in the cathodic parasitic process, respectively, $i_{app}$is the applied current density, $[RH]_x^{y=0}$ is the concentration of the substrate *RH* at the cathodic surface for a given value of *x* and the term [*RH*]* is the value of $[RH]_x^{y=0}$ which

gives a current density for the *RH* reduction equal to the current density involved for the parasitic cathodic processes, e.g. the value of $[RH]_x^{y=0}$ that gives a current efficiency of 50%.

Let us consider that under pseudo-steady state conditions, during an electrolysis carried out with amperostatic alimentation the following expression should apply for any value of *x*:

$$k_m\,([\overline{RH}]_x - [RH]_{y=0,x}) = i_{app} CE_x / nF \qquad (6)$$

Hence, by combination of Equations (7b) and (8) and elimination of the term $[RH]_{y=0,x}$, one can obtain the expression for the CE_x during an amperostatic electrolysis:

$$CE_x = \frac{1}{1 + \dfrac{2[RH]^*}{[RH]' + ([RH]'^2 + 4[RH]^*[\overline{RH}]_x)^{0.5}}} \qquad (7)$$

where $[RH]' = [\overline{RH}]_x - [RH]^* - c^*$ and $c^* = i_{app}/(nFk_m)$ is the concentration of *RH* that gives rise to a limiting current density $i_{lim} = nFk_m[\overline{RH}]_x$ equal to the applied current density i_{app}.As a consequence the conversion *X* can be obtained by numerical combination of Eqns. (7) and (8).

$$d[RH]_x = -\frac{i_{app}\,dt}{nFh} CE_x \qquad (8)$$

In particular, in the limiting cases of an organic concentration, respectively, strongly higher and strongly lower than c^* the equations reported in table 2 can be easily derived.

Table 2.*Theoretical expressions for current efficiency (CE) and conversion (X)* [a]

Rate determining step	*CE*	*X*
Reduction reaction $i_{lim} >> i_{app} CE^{OC}$ (i.e., if $[\overline{RH}]_x >> c >> c^* CE^{OC}$)	$CE_x = \frac{1}{1+\frac{[RH]^*}{[\overline{RH}]_x}}$ (11)	*X* is obtained by numerical combination of Eqns. (10) and (11) $d[RH]_x = -\frac{i_{app} dt}{nFh} CE_x$ (10)
Mass transfer control $i_{lim} << i_{app} CE^{OC}$ (i.e., if $c^0 << c^* CE^{OC}$)	$CE = \frac{nFc^0 \Phi_V X}{i_{app}}$ (12)	$X = 1 - \exp(-Sh \frac{DA}{2h\Phi_V})$ (13)

[a] CE^{OC} is the local intrinsic current efficiency for a process under the kinetic control of the cathodic reduction reaction, $c^* = i_{app}/(nFk_m)$, V is the reactor volume, $t=V/\Phi_V$ is the average residence time experienced by the electrolytic solution inside the reactor, L is the electrode length and v is the linear velocity of the electrolityc solution, $t^* = \frac{nFV(c^0 - c^*)}{i_{app} A}$ is the time necessary to decrease the concentration of the organic in the reactor to the value c^* by a cathodic process with CE = 1.

CONCLUSIONS

The electrochemical processes offer several advantages over conventional routes, such as a more environmentally sustainable route and milder operating conditions, and in some cases provide the only viable route. They also provide the possibility to influence the reaction directly in real-time, offering both more control and the ability to perform the treatment in a continuous fashion. The utilization of microfluidic electrochemical reactors (i.e. cells with a distance between the cathode and the anode of tens or hundreds of micrometers) can potentially allow to improve the performances of the processes.

The thesis was focused to the investigation of the set-up of different kinds of microfluidic electrochemical devices and of their performances in the frame of some model processes. In particular, the treatment of wastewater polluted by Acid Orange 7 and the synthesis of chloroacetic acid were studied in detail during the PhD thesis, in both conventional and microfluidic cells in order to highlight advantages and disadvantages given by the utilization of such devices.

Electrochemical abatement of Acid Orange 7

The performances of the process, in terms of abatement of colour, AO7, TOC and COD and formation of by-products, depend dramatically on the adopted electro-catalytic route:

– Electrochemical treatment with electro-generated active chlorine (IOAC) gave the faster abatement of colour.
– The higher abatement rate of COD was achieved by the direct electrochemical oxidation (EO) process at BDD that gave rise to a very small generation of by-products, while the lower one was observed for electro-Fenton (EF) process as a result of the formation of quite resistant by-products that remains in the electrolytic medium also after long electrolysis times.

– Intermediate abatement of COD were given by IOAC as a result of the formation of a number of intermediates that are oxidized with higher rate with respect to EF.

Optimization of investigated catalytic routes occurs under very different operative conditions:

– Performances of IOAC, in terms of abatement of both colour and COD, were improved by working with a Ru based electrode (that gives high generation of active chlorine) and higher current densities and residence times but were not significantly affected by the adopted reactor.
– The performances of EO depended obviously on the nature of anode. Higher abatements of both colour and COD were achieved at BDD anode and in the microfluidic cell that enhances the mass transport phenomena. Higher abatements of COD but lower current efficiencies were achieved by increasing the current density and lowering the flow rate.
– The abatement of AO7 by electro-Fenton (EF) strongly benefited by the utilisation of air diffusion electrode or of a microfluidic reactor or working at high pressures. For experiments carried out in the microfluidic reactor in the presence of cheap compact graphite cathodes, higher abatements of both colour and COD were achieved by working at intermediate values of the current density (between 20 and 40 A/m^2). For what concern the experiments performed at moderately high pressures, a dramatic increase of the generation of H_2O_2 and a drastic higher abatement of the TOC were obtained, using cheap bulk planar electrodes that are much easier to manage at the industrial scale with respect to carbon felt or AED.

  A dramatic increase of the generation of H_2O_2 (up to one order of magnitude) was readily achievable simply through a moderate increase of the air pressure contacted with the electrolytic solution in a pressure range (1 – 11 bar) or using microfluidic cells with proper inter-electrodic distances.

Performances of coupled processes (EF-IOAC, EF-EO) were improved using microfluidic devices which furthermore allowed to work in the absence of supporting electrolytes.

The possibility to use more reactors in series for the treatment of wastewater was also evaluated. It was shown that EO process strongly benefited from the utilization of more reactors in series in terms of higher abatements and productivity. Very interesting results in terms of reduced investment and operating costs and high abatements were achieved using EF and EO in two different reactors in series

Electro synthesis of chloroacetic acid

The performances of the process in terms of conversion, selectivity and stability of electrodes strongly depended on the nature of the cathode material. Good results were achieved with graphite electrodes while copper and silver cathodes gave worse results in terms of selectivity and stability. The utilization of both employed microreactors allowed to achieve high conversions and selectivity with a single-pass continuous process with low cell voltages and in the absence of supporting electrolyte. Interestingly, the utilization of micro cells allowed to increase the selectivity of the process by reducing the relevance of follow-up reaction as an effect of low residence times. Experiments in microreactors were carried out for long times (up to one month) without leakages.

A stack of several cells in series allowed a substantial increase of the process productivity and to operate at higher initial substrate concentrations. This was coupled to high yields and selectivity in simple and compact devices. Using micro reactors in series allowed also to modulate the current densities in the series reactors, thus allowing to improve the figures of merit of the process in terms of conversions and selectivity.

The present results offered an excellent proof of concept showing that microreactors may be proposed for operation in the frame of electrochemical synthesis of organics and treatment of wastewaters.

PUBLICATIONS

[1] ELECTROCHEMICAL ABATEMENT OF ORGANIC POLLUTANTS IN CONTINUOUS REACTION SYSTEMS OBTAINED BY ASSEMBLY OF MICROFLUIDIC CELLS IN SERIES. Autori: Simona Sabatino, Onofrio Scialdone, Alessandro Galia. Accepted in ChemElectroChem.

[2] EFFECT OF AIR PRESSURE ON THE ELECTRO-GENERATION OF H2O2 AND THE ABATEMENT OF ORGANIC POLLUTANTS IN WATER BY ELECTRO-FENTON PROCESS. Autori: Onofrio Scialdone, Alessandro Galia, Carolina Gattuso, Simona Sabatino, Benedetto Schiavo. Electrochimica Acta 182 (2015) 775–780.

[3] ELECTROCHEMICAL CONVERSION OF DICHLOROACETIC ACID TO CHLOROACETIC ACID IN A MICROFLUIDIC STACK AND IN A SERIES OF MICROFLUIDIC REACTORS" Autori: Onofrio Scialdone, Alessandro Galia, Simona Sabatino, Domenico Mira, Christian Amatore, ChemElectroChem 2 (2015), 684-690.

[4] ELECTROCHEMICAL PROCESSES AND APPARATUSES FOR THE ABATEMENT OF ACID ORANGE 7 IN WATER. Autori: Scialdone O., D'Angelo A., Pastorella G., Sabatino S., & Galia A., Chemical Engineering Transactions, 41 (2014) 31-36.

[5] ELECTROCHEMICAL CONVERSION OF DICHLOROACETIC ACID TO CHLOROACETIC ACID IN CONVENTIONAL CELL AND IN TWO MICROFLUIDIC REACTORS. Autori: Onofrio Scialdone, Alessandro Galia, Simona Sabatino, Giovanni Marco Vaiana, Diego Agro, Alessandro Busacca, Christian Amatore, ChemElectroChem 2014, 1, 116 – 124

[6] ABATEMENT OF ACID ORANGE 7 IN MACRO AND MICRO REACTORS. EFFECT OF THE ELECTRO - CATALYTIC ROUTE. Autori: Onofrio Scialdone, Alessandro Galia, Simona Sabatino, Applied Catalysis B: Environmental 148– 149 (2014) 473– 483.

[7] ELECTRO-GENERATION OF H_2O_2 AND ABATEMENT OF ORGANIC POLLUTANT IN WATER BY AN ELECTRO-FENTON PROCESS IN A MICROFLUIDIC REACTOR. Autori:Onofrio Scialdone, Alessandro Galia, Simona Sabatino, Electrochemistry Communications 26 (2013) 45–47.

COMMUNICATIONS

[1] ABATEMENT OF POLLUTANTS IN WATER BY DIFFERENT ELECTROCHEMICAL APPROACHES. AUTORI: Onofrio Scialdone Adriana D'Angelo, Alessandro Galia, Simona Sabatino, Fabrizio Vicari. The 66rd Annual Meeting of the International Society of Electrochemistry, 4-9 October 2015, Taipei, Taiwan.

[2] ELECTROCHEMICAL REDUCTION OF CARBON DIOXIDE TO FORMIC ACID AT TIN CATHODE IN DIVIDED AND UNDIVIDED CELLS: EFFECT OF OPERATING PARAMETERS. AUTORI: Onofrio Scialdone, Alessandro Galia, Simona Sabatino. The 66rd Annual Meeting of the International Society of Electrochemistry, 4-9 October 2015, Taipei, Taiwan.

[3] ELECTROCHEMICAL MICROREACTORS FOR THE ABATEMENT OF ORGANIC POLLUTANTS IN WATER SOLUTION Autori: Onofrio Scialdone, Simona Sabatino, Alessandro Galia, EuroMed 2015 – Desalination for Clean Water and Energy 10–14 May 2015, NH Hotel, Palermo, Italy.

[4] ELECTROCHEMICAL PROCESSES AND APPARATUSES FOR THE ABATEMENT OF ACID ORANGE 7 IN WATER. Autori: Scialdone O.; D'Angelo A.; Pastorella G.; Sabatino S.; Galia A. The10th European Symposium on Electrochemical Engineering, Chia, Sardinia, Italy, 28 September-02 October 02, 2014.

[5] ABATEMENT OF ACID ORANGE 7 IN WATER BY DIFFERENT ELECTROCHEMICAL APPROACHES. Autori: Onofrio Scialdone, Adriana D'Angelo, Simona Sabatino, Alessandro Galia, The 65rd Annual Meeting of the International Society of Electrochemistry, Lausanne, Switzerland 31 August - 5 September, 2014.

[6] ELECTROCHEMICAL MICROREACTORS FOR SYNTHESIS OF CHEMICALS AND ABATEMENT OF ORGANIC POLLUTTANTS Autori: Simona Sabatino, Onofrio Scialdone, Alessandro Galia, Domenico Mira, al Convegno XXXV Meeting of the Electrochemistry Group of the Spanish Royal Society of Chemistry and 1st E3 Mediterranean Symposium: Electrochemistry for environment and Energy. Burgos – Spain, 14-16 Luglio, 2014.

[7] NEW ELECTROCHEMICAL MICROFLUIC DEVICES FOR THE SYNTHESIS OF CHEMICALS AND THE TREATMENT OF WASTE WATERS Autori: O. Scialdone, S. Sabatino, M. Vaiana, S. La Mantia, C. Guarisco al Convegno GEI 2013

(Giornate dell'Elettrochimica Italiana e Elettrochimica) presso l'Università degli studi di Pavia, 22-27 Settembre 2013.

[8] ELECTROSYNTHESIS IN MICROFLUIDIC CELLS: PRELIMINARY INVESTIGATIONS Autori: S. Sabatino, A. Galia, P. Librino, G.M. Vaiana, O. Scialdone, al Convegno GEI2013 (Giornate dell'Elettrochimica Italiana e Elettrochimica), Università degli studi di Pavia, 22-27 Settembre 2013.

[9] ELECTROCHEMICAL ABATEMENT OF AZO 7 IN WATER SOLUTION IN MACRO AND MICRO CELLS. Autori: O. Scialdone, S. Sabatino, A. Galia, al Convegno GEI-ERA (Giornate dell'Elettrochimica Italiana e Elettrochimica per Il Recupero Ambientale) presso Santa Marina Salina ME, 17-22 Giugno 2012.

[10] ELECTROCHEMICAL TREATMENT OF WASTE WATERS CONTAMINATED BY ORGANIC POLLUTANTS: A LOOK ON SOME NEW APPROACHES. Autori: Onofrio Scialdone, Simona Sabatino, Chiara Guarisco, Roberta Riccobono, A. D'angelo, A. Galia , A. Busacca , D. Agrò, GEI-ERA (Giornate dell'Elettrochimica Italiana e Elettrochimica per Il Recupero Ambientale, Santa Marina Salina ME, 17-22 Giugno 2012.

[11] ELECTROCHEMICAL ABATEMENT OF ORGANIC POLLUTANTS IN WATER IN MICROFLUIDIC DEVICES. Autori O. Scialdone, A. Galia, C. Guarisco, S. Sabatino, S. La Mantia – The 63rd Annual Meeting of the International Society of Electrochemistry presso Praga 19-24 Agosto 2012.

[12] STUDIO DI PROCESSI ELETTROCHIMICI PER L'ABBATTIMENTO DI INQUINANTI ORGANICI IN ACQUA IN MACRO E MICRO REATTORI. Autori: O. Scialdone, A. Galia, C. Guarisco, S. La Mantia, S. Sabatino - Convegno GRICU 2012, presso Montesilvano PE, 16- 19 settembre 2012.

[13] ELECTROCHEMICAL TREATMENT OF ORGANIC POLLUTANTS IN MACRO AND MICRO REACTORS. In XXIV Congresso Nazionale della Società Chimica Italiana Lecce 11-16 settembre 2011. Lecce, 12/09/2011. Autori: *Scialdone, O; Guarisco, C; Galia, A; Gurreri, L; La Mantia, S; Sabatino, S*.

ACKNOWLEDGEMENTS

Prof. Scialdone Onofrio

Prof. Galia Alessandro

Ing. Sonia Lanzalaco and Dr. Adriana D'Angelo and the others of our laboratory.